Holographic Applications on Quark Stars and Black Holes

KILAR ZHANG
張　弘

Shanghai University

Based on:
Le-Feng Chen, Jing-Yi Wu, Hao Feng, Tian-Shun Chen, KZ, arXiv: 2505.04477
Xian-Hui Ge, Masataka Matsumoto and KZ, arXiv: 2502.15627
Le-Feng Chen, Heng-Yi Yuan, Meng-Hua Zhou, Kun Lu, Jing-Yi Wu, KZ, arXiv: 2501.17121
Wei Li, Jing-Yi Wu and KZ, arXiv: 2403.20240
Xian-Hui Ge, Masataka Matsumoto and KZ, arXiv: 2402.17441
Jing-Yi Wu, Wei Li, Xin-Han Huang and KZ, arXiv: 2309.07971

相关工作

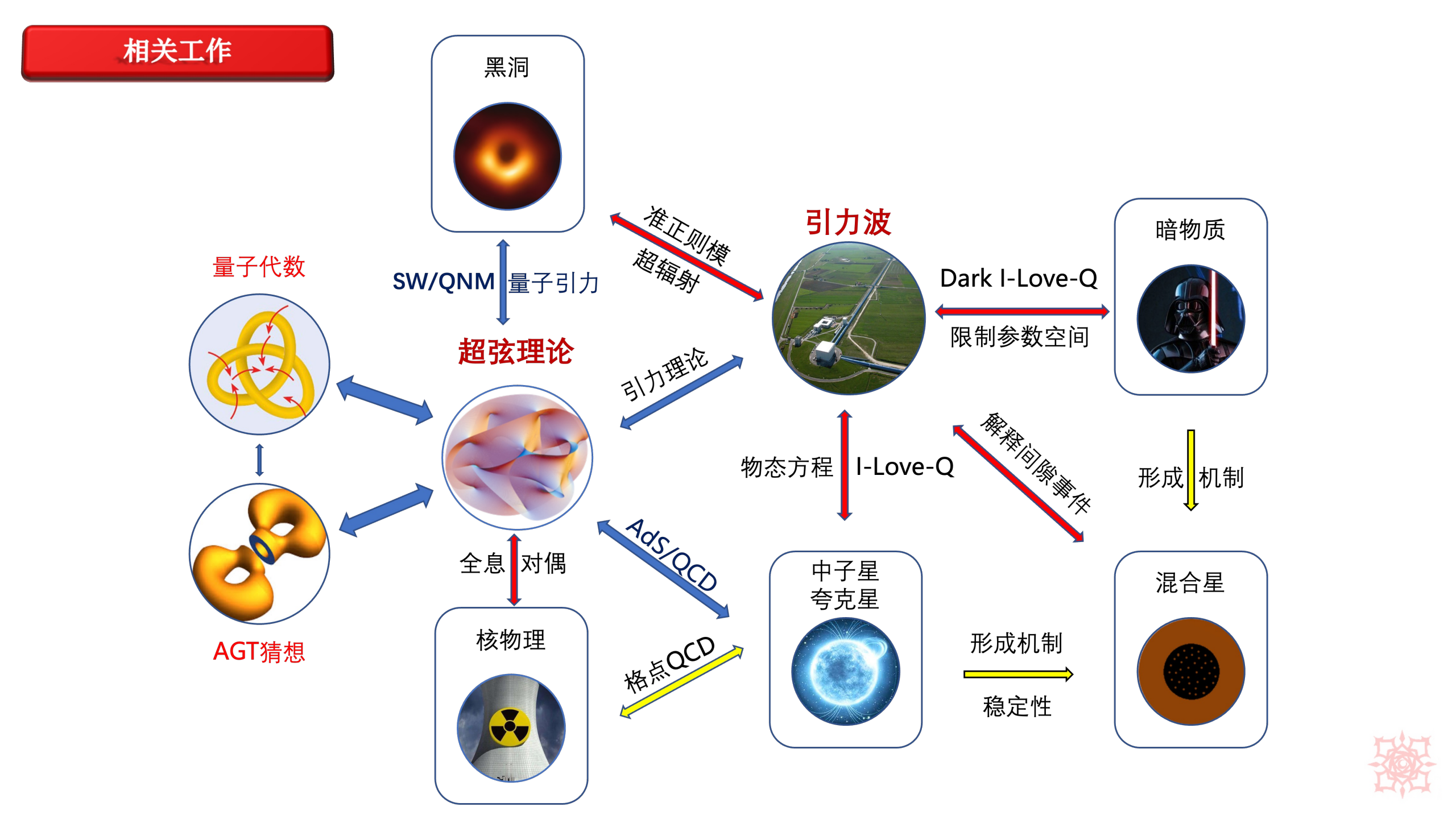
黑洞
准正则模
超辐射
引力波
暗物质
Dark I-Love-Q
限制参数空间
量子代数
SW/QNM
量子引力
超弦理论
引力理论
物态方程
I-Love-Q
解释间隙事件
形成
机制
AdS/QCD
全息
对偶
中子星
夸克星
混合星
形成机制
稳定性
核物理
格点QCD
AGT猜想

演示页

GW

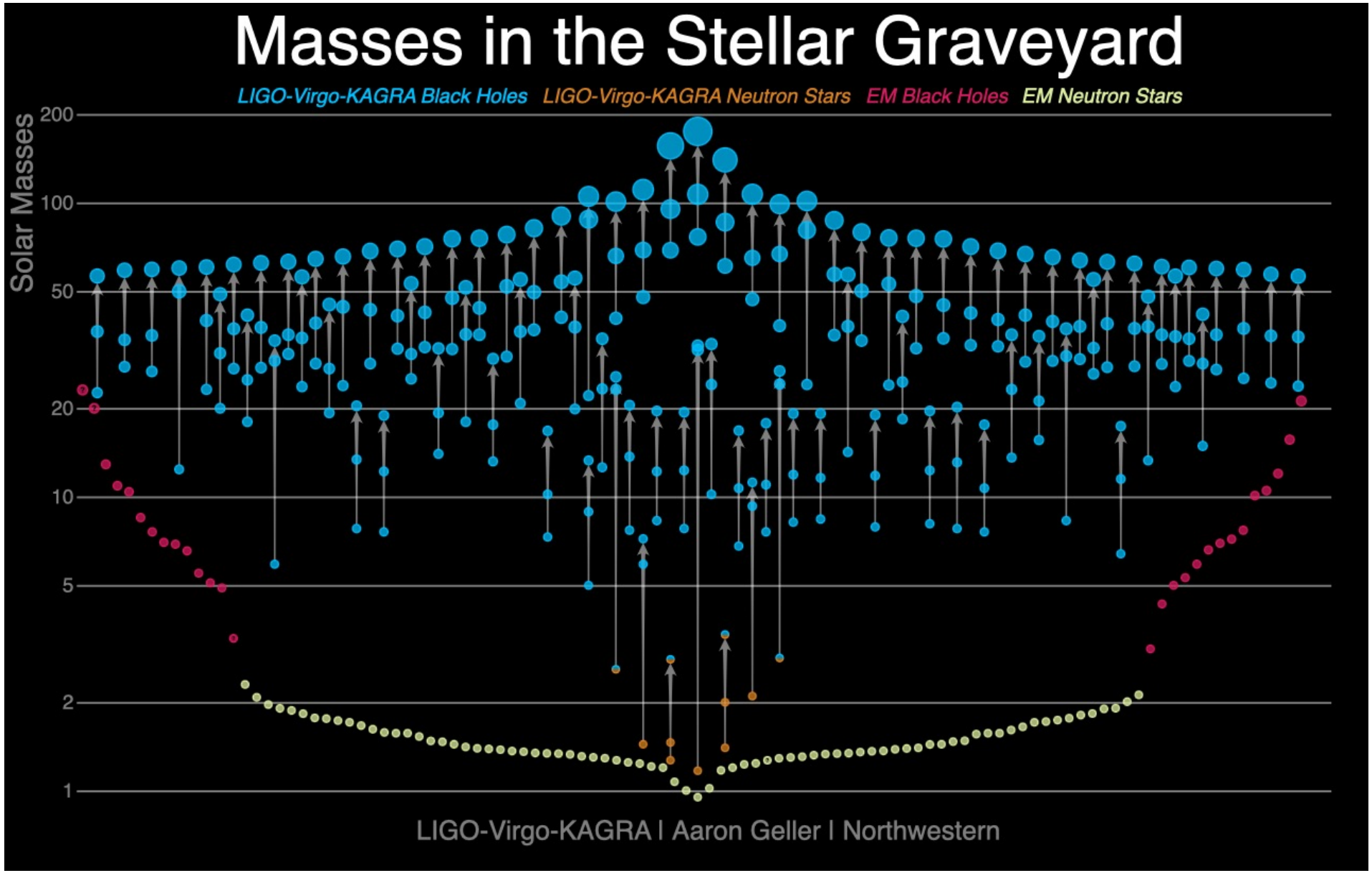
Masses in the Stellar Graveyard
LIGO-Virgo-KAGRA Black Holes
LIGO-Virgo-KAGRA Neutron Stars
EM Black Holes
EM Neutron Stars
Solar Masses
200
100
50
20
10
5
2
1
LIGO-Virgo-KAGRA | Aaron Geller | Northwestern

Neutron Stars

Matters in Neutron stars

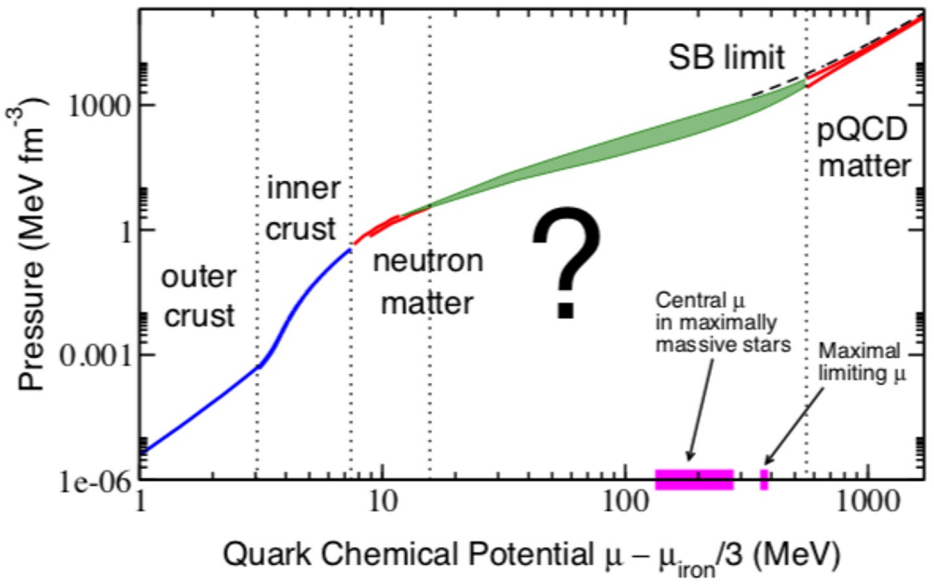

c.f. 1508.05019

The nuclear matter phase depends on non-perturbative QCD vacuum which is uncertain.

There are some phenomenological models, e.g. MIT bag model, NJL model, etc.

中子星

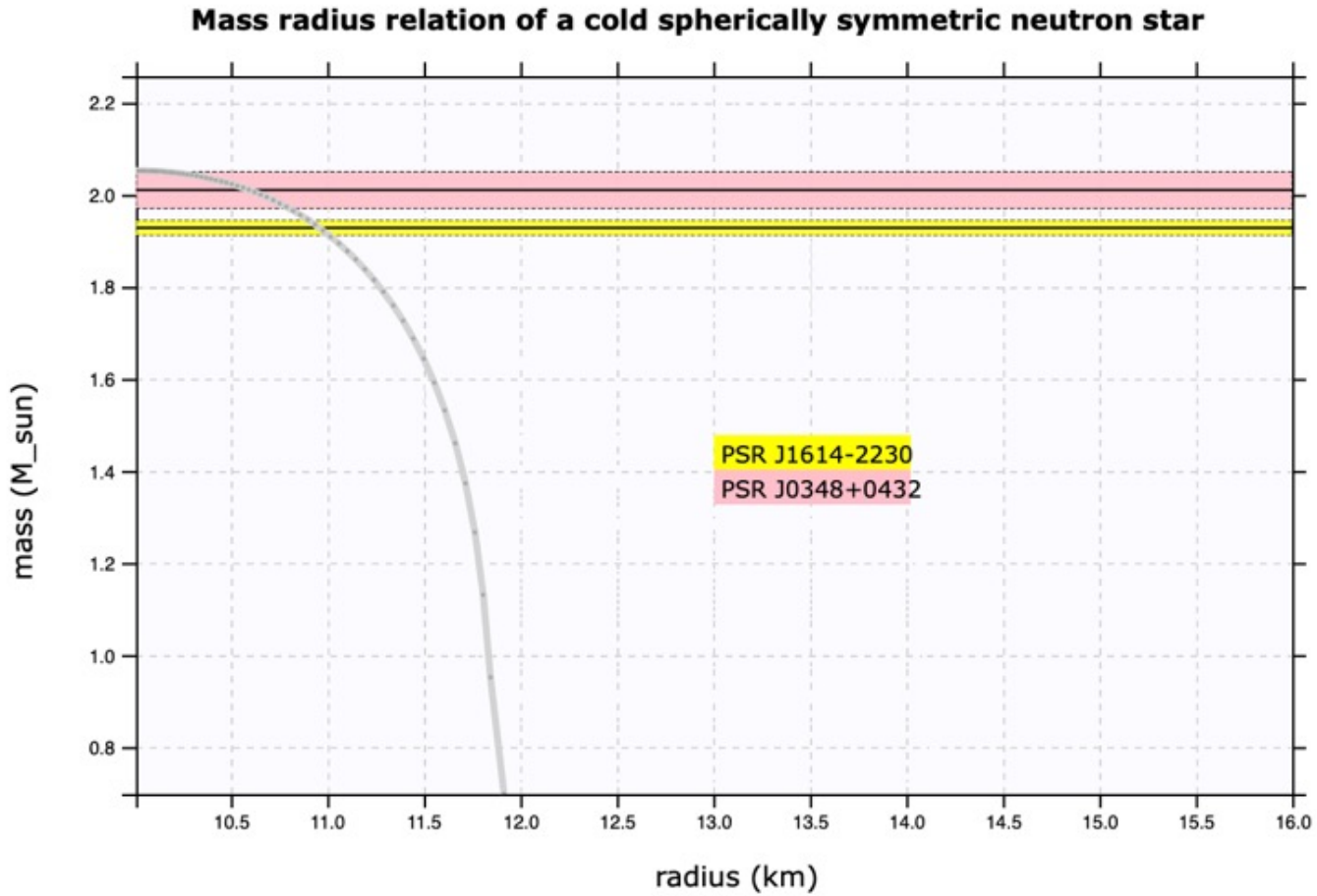
Mass radius relation of a cold spherically symmetric neutron star
mass (M_sun)
radius (km)
2.2
2.0
1.8
1.6
1.4
1.2
1.0
0.8
10.5
11.0
11.5
12.0
12.5
13.0
13.5
14.0
14.5
15.0
15.5
16.0
PSR J1614-2230
PSR J0348+0432

中子星

What are TOV equations?

Neutron stars and, to some extent, also white dwarfs are relativistic objects and computations of their structure should be carried out in a general-relativistic (GR) framework.
Assuming zero space velocity, spherical symmetry, and an ideal fluid model.

The Tolman-Oppenheimer-Volkoff Equations

$$M' = 4\pi r^2 \rho,$$

$$p' = -G_N(\rho + p)\phi',$$

$$\phi' = \frac{M + 4\pi r^3 p}{r(r - 2G_N M)},$$

中子星

在双星合并期间，首先通过引力波频率等信息可以给出星体的总质量与质量比范围。另一方面，因为潮汐变形会使互绕加速，会使引力波波形相比点质量互绕产生相位移动，如图所示。虽然是高阶修正(正比于光速的负5次方，相当于2.5后牛顿展开)，但仍在探测器的灵敏度范围内。

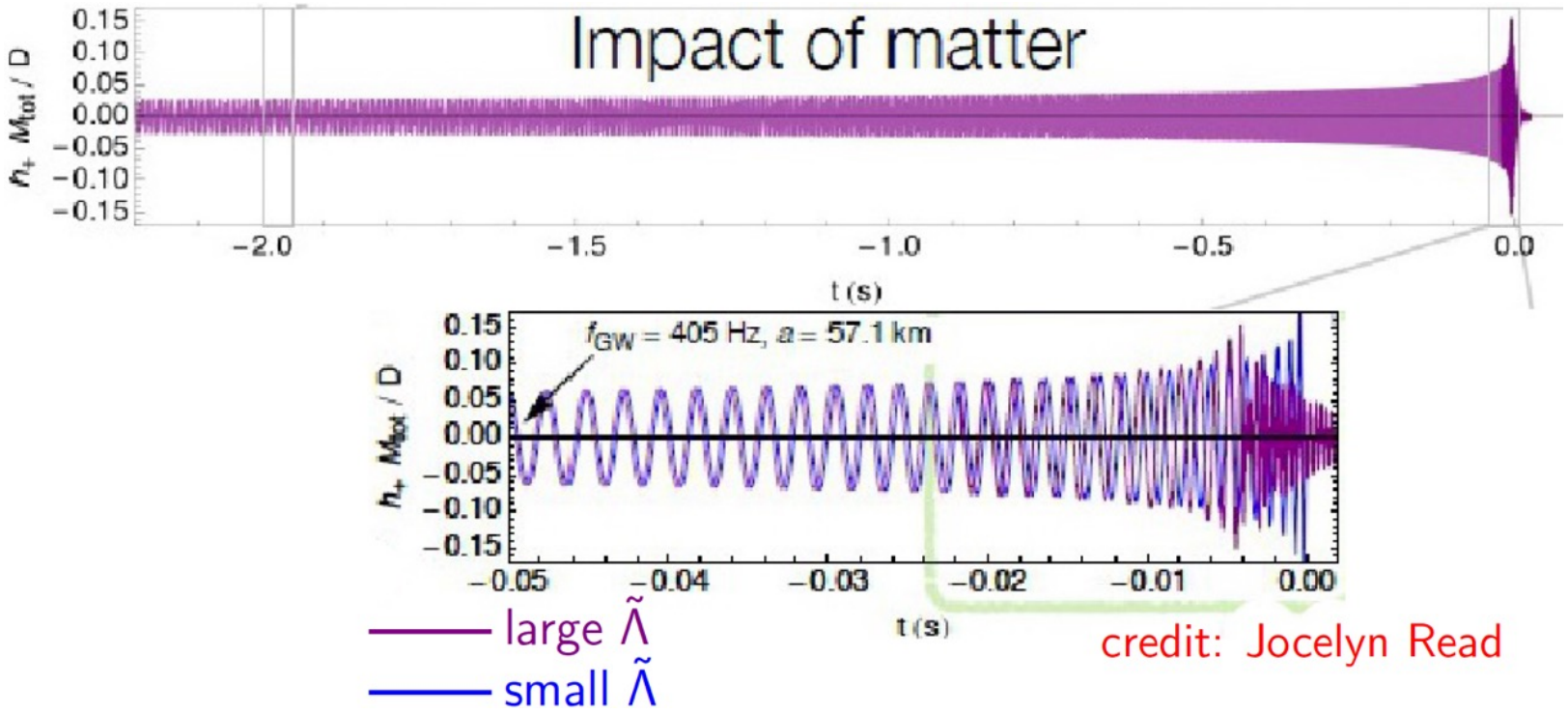

中子星

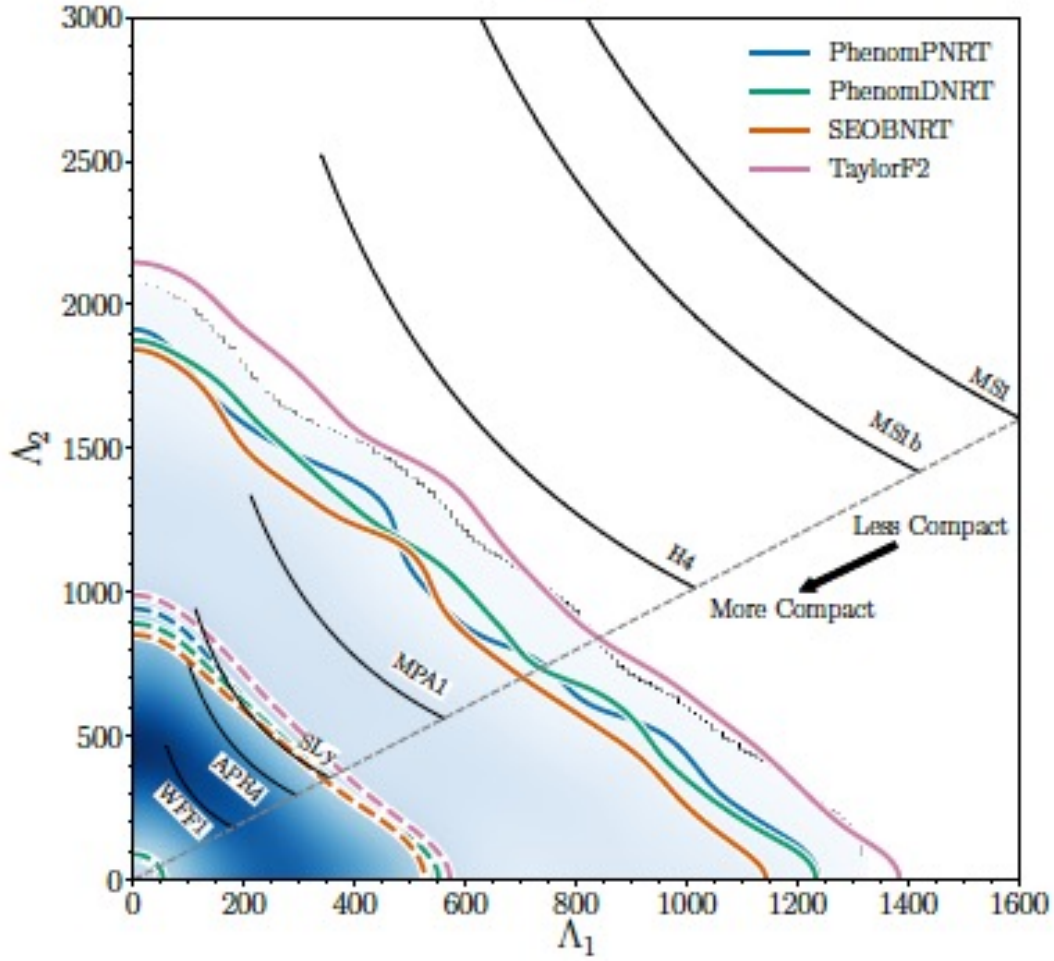

FIG. 10. PDFs for the tidal deformability parameters Λ_1 and Λ_2 using the high-spin (top) and low-spin (bottom) priors. The blue shading is the PDF for the precessing waveform PhenomPNRT. The 50% (dashed) and 90% (solid) credible regions are shown for the four waveform models. The seven black curves are the tidal parameters for the seven representative EOS models using the masses estimated with the PhenomPNRT model, ending at the $\Lambda_1 = \Lambda_2$ boundary.

中子星

Adding quarks --- Sakai-Sugimoto- model

- Weak coupling D-brane picture of SS model

Witten Edward. Anti-de Sitter space, thermal phase transition, and confinement in gauge theories. Adv Theor Math Phys 1998;2:505–32.
Sakai Tadakatsu, Sugimoto Shigeki. More on a holographic dual of QCD. Progr Theoret Phys 2005;114:1083–118.
Sakai Tadakatsu, Sugimoto Shigeki. Low energy hadron physics in holographic QCD. Progr Theoret Phys 2005;113:843–82.

N_c D4	0	1	2	3	(4)					
N_f D8/D8	0	1	2	3		5	6	7	8	9

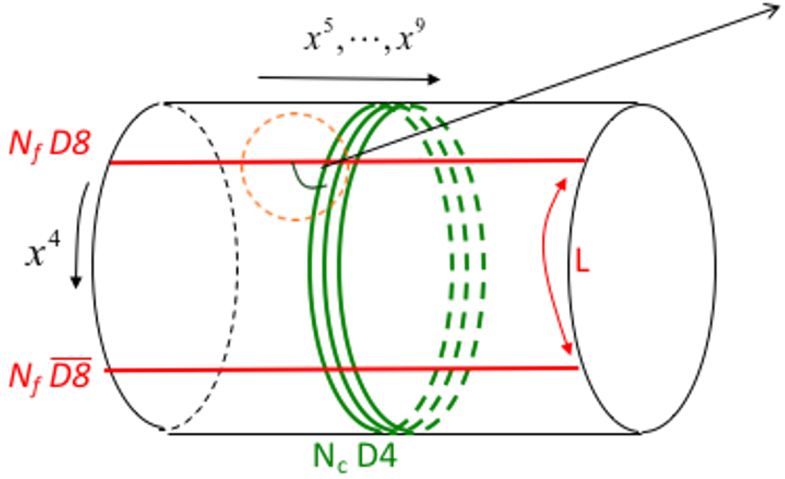

4-8 strings: chiral quark
4-8 strings: anti-chiral quark

Massless U(Nc) QCD with N_f flavors:

$$U(N_c)\times U(N_f)_L \times U(N_f)_R$$

Li Si-wen, Schmitt Andreas, Wang Qun. From holography towards real-world nuclear matter. Phys Rev D 2015;92(2).

中子星

D3/D7 model
additional inputs to break the conformal sound barrier.
explores the static and dynamical properties
of quark star

Hoyos Carlos, Rodríguez Fernández David, Jokela Niko, Vuorinen Aleksi. Holographic quark matter and neutron stars. Phys Rev Lett 2016;117(3):032501.
Hoyos Carlos, Jokela Niko, Rodríguez Fernández David, Vuorinen Aleksi. Breaking the sound barrier in AdS/CFT. Phys Rev D 2016;94(10):106008.
Annala Eemeli, Ecker Christian, Hoyos Carlos, Jokela Niko, Rodríguez Fernández David, Vuorinen Aleksi. Holographic compact stars meet gravitational wave constraints. JHEP 2018;12:078.
Aleixo M, Lenzi CH, de Paula W, da Rocha R. Quark stars in D_3–D_7 holographic model. Eur Phys J C 2024;84(3):253.

homogeneous ansatz case, in the Hard-Wall
model or in the WSS model, including
the proton and lepton fractions as well
as a crust modeled with a phenomenological
surface tension.

Bartolini Lorenzo, Gudnason Sven Bjarke. Symmetry energy in holographic QCD. 2022.
Kovensky Nicolas, Poole Aaron, Schmitt Andreas. Building a realistic neutron star from holography. Phys Rev D 2022;105(3):034022.

the instanton gas shows chiral restoration at high densities but an unrealistic second-order baryon onset

the homogeneous ansatz behaves exactly the other way around

中子星

Thermodynamics

The on-shell D8-brane action is the grand-canonical free energy density.

$$\Omega[T,\mu;n_I,m_i,k] = \frac{T}{V} S|_{\text{on-shell}}$$

$$S[a_0,x_4;A_\mu(m_i)] := \mathcal{N}\frac{V}{T}\int_{u_c}^{\infty} du\, \mathcal{L} = S_{DBI} + S_{CS}$$

$$\text{BC:} \quad \frac{\ell}{2} = \int_{u_c}^{\infty} du\, x_4'(u)\ , \qquad \mu := \hat{a}_0(U=\infty)$$

The derived thermodynamics is

$$\text{pressure } p := -\Omega[\mu,T]\ , \qquad \text{baryon density } n := -\frac{\partial\Omega}{\partial\mu}|_T$$

$$\text{energy density } \epsilon := \Omega + n\mu \quad +Ts \quad \text{with } s := -\frac{\partial\Omega}{\partial T}|_\mu$$

中子星

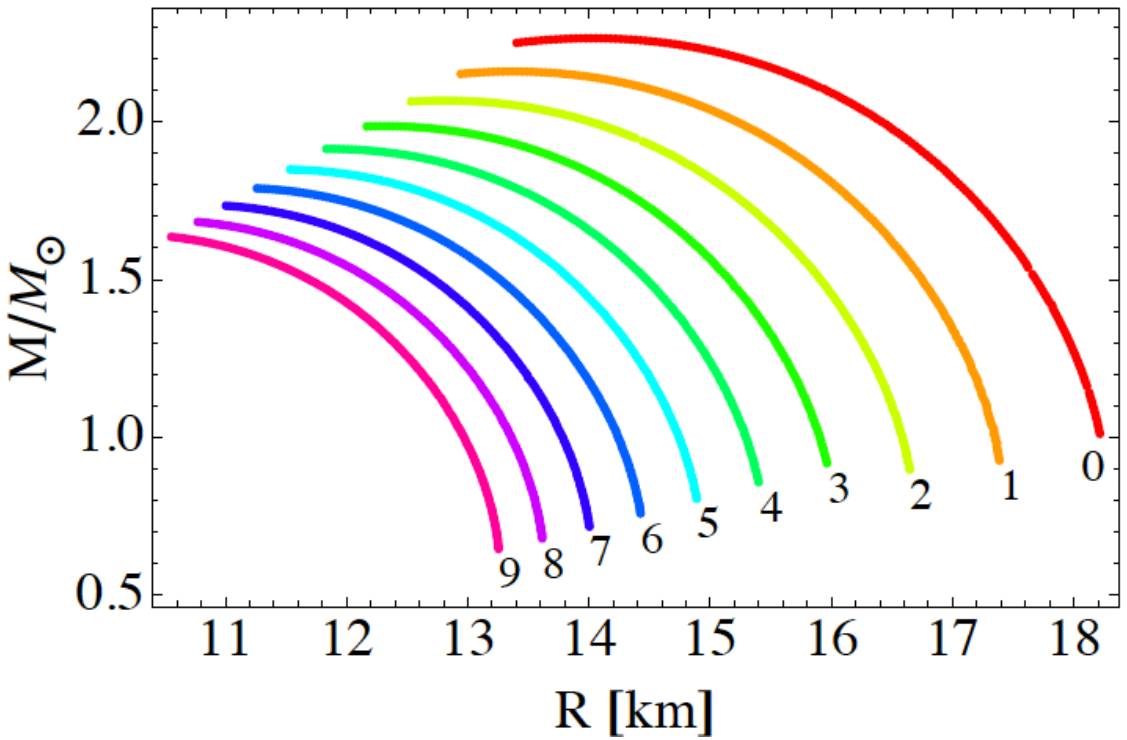
M/M⊙
R [km]
2.0
1.5
1.0
0.5
11
12
13
14
15
16
17
18
0
1
2
3
4
5
6
7
8
9

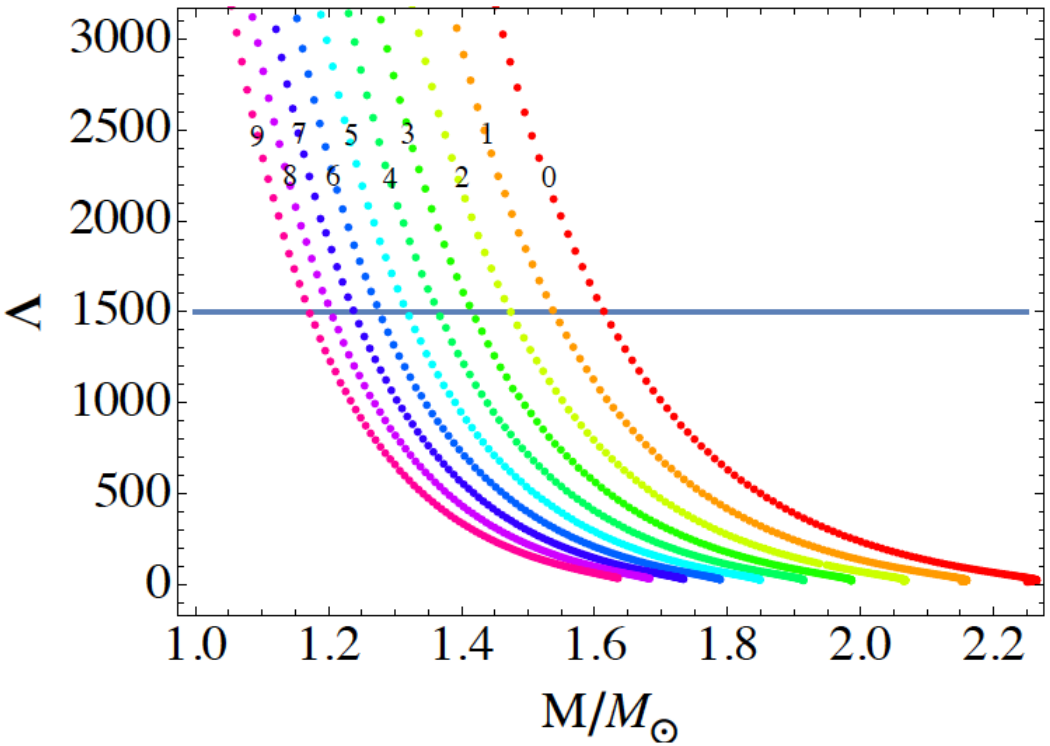
Λ
M/M⊙
3000
2500
2000
1500
1000
500
0
1.0
1.2
1.4
1.6
1.8
2.0
2.2
0
1
2
3
4
5
6
7
8
9

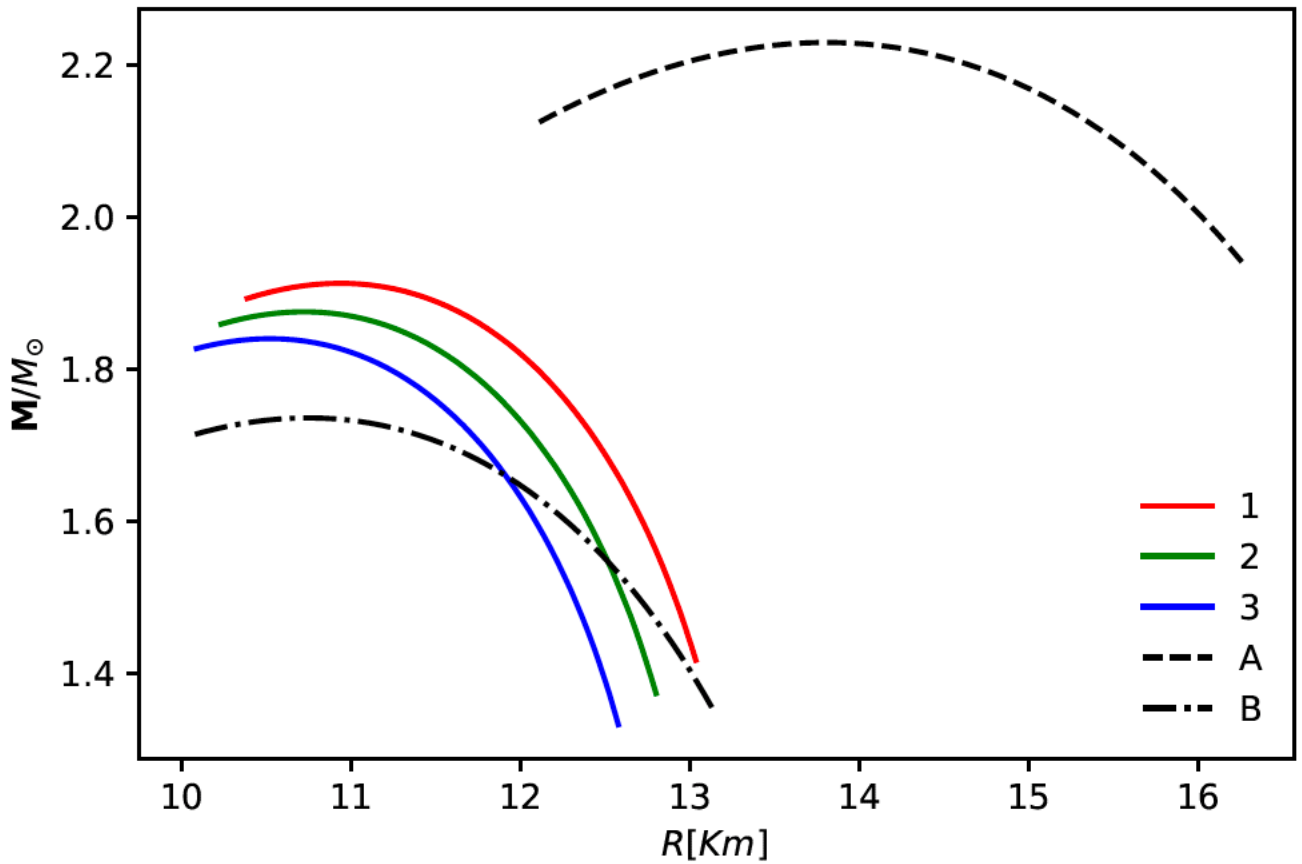

FIG. 1: Mass-Radius relations for different EoS

中子星

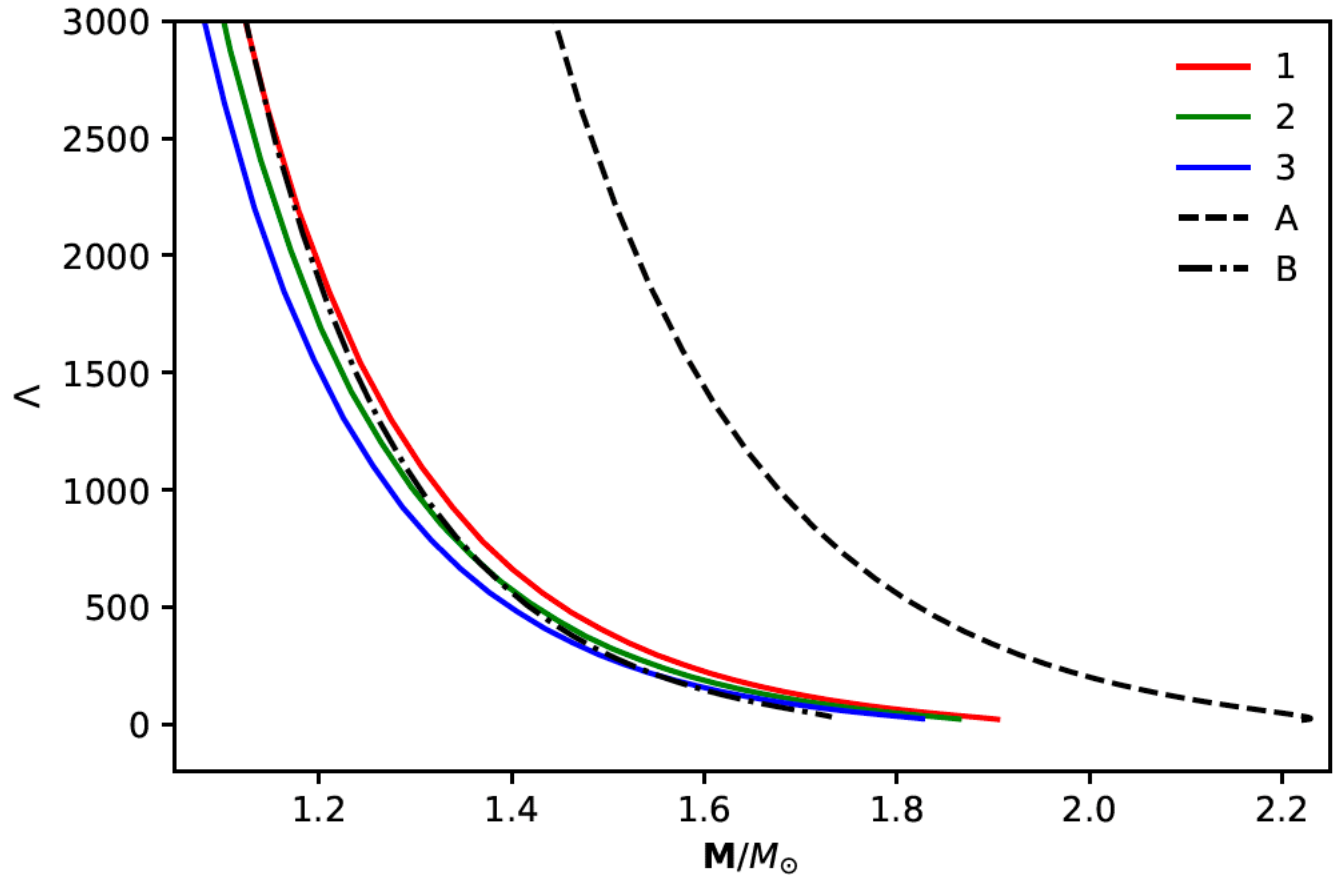

FIG. 2: TLN (Λ) vs Mass (M) for the holographic stars of EoS with the same sets of values and labels for ℓ as in Fig. 1.

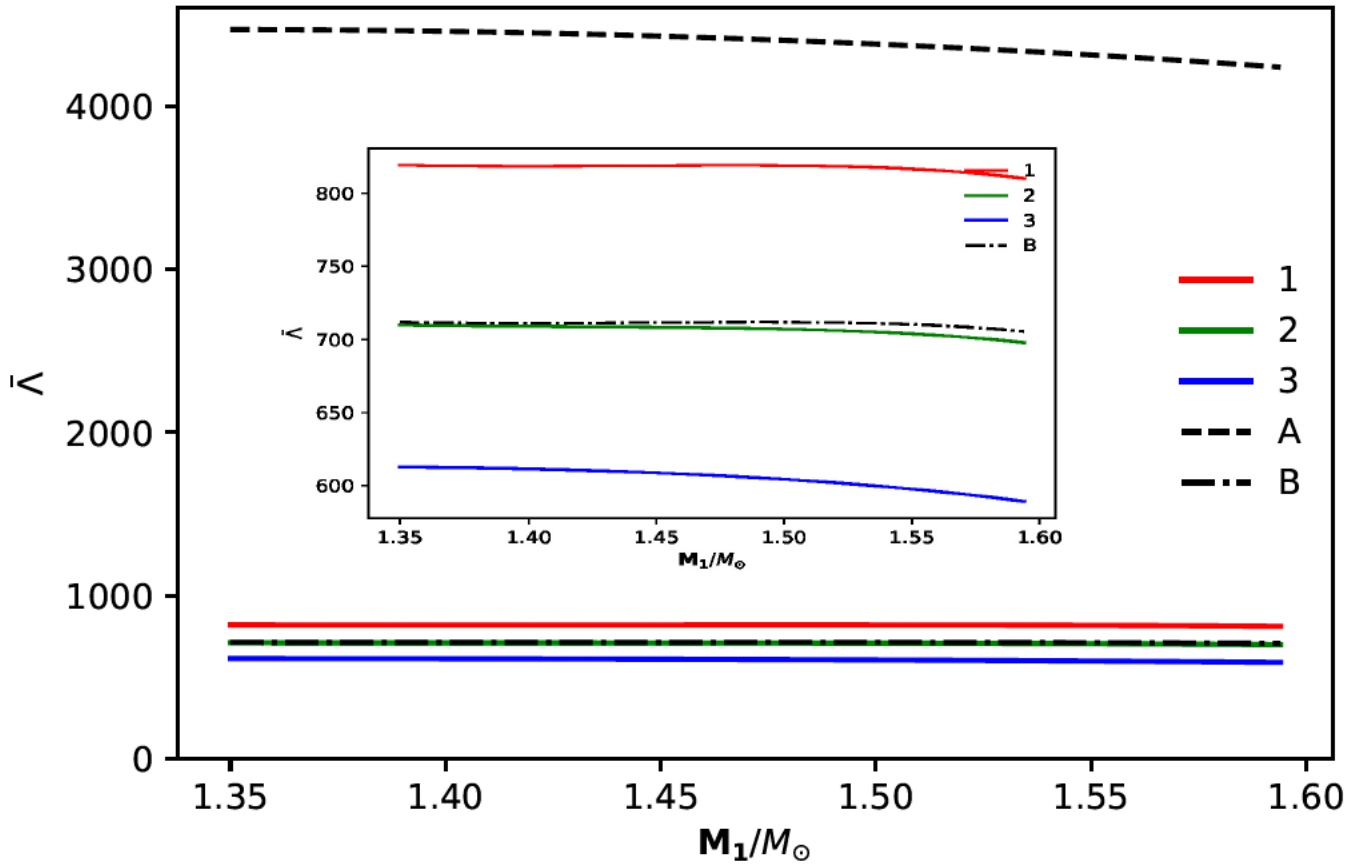

FIG. 3: Tidal deformability of the binary holographic stars of EoS vs one of the masses ($\bar{\Lambda}$ vs M_1) for partial sets of the values for ℓ used in Fig. 1.

演示页

Quark Star

夸克星

Extract the EoS from the holographic model built by
Prof. Rong-Gen Cai, Prof. Song He, Prof. Li Li and Prof. Yuan-Xu Wang

R.-G. Cai, S. He, L. Li and Y.-X. Wang, *Probing QCD critical point and induced gravitational wave by black hole physics*, *Phys. Rev. D* **106** (2022) L121902, [2201.02004].

Y.-Q. Zhao, S. He, D. Hou, L. Li and Z. Li, *Phase structure and critical phenomena in two-flavor QCD by holography*, *Phys. Rev. D* **109** (2024) 086015, [2310.13432].

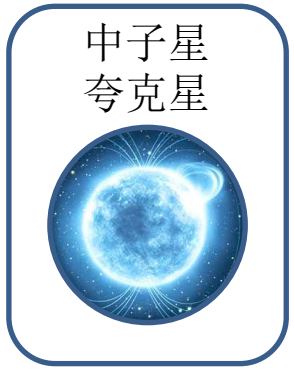

L. Zhang and M. Huang, *Holographic cold dense matter constrained by neutron stars*, *Phys. Rev. D* **106** (2022) 096028, [2209.00766].

We start from the action of the five dimensional EMD theory,

$$S = \frac{1}{2\kappa_N^2}\int d^5x\sqrt{-g} \left[R - \frac{1}{2}\bigtriangledown_\mu \phi \bigtriangledown^\mu \phi - \frac{Z(\phi)}{4}F_{\mu\nu}F^{\mu\nu} - V(\phi)\right], \tag{1}$$

where κ_N is the effective Newton constant, ϕ is the scalar field, $Z(\phi)$ and $V(\phi)$ are the coupling constants determined from the lattice QCD data at $\mu = 0$.

$$V(\phi) = -12\cosh[c_1\phi] + (6c_1^2 - \frac{3}{2})\phi^2 + c_2\phi^6,$$
$$Z(\phi) = \frac{\mathrm{sech}[c_4\phi^3]}{1+c_3} + \frac{c_3}{1+c_3}e^{-c_5\phi}. \tag{2}$$

The parameters κ_N and c_i are fixed [24] with lattice data, that $\kappa_N^2 = 2\pi(1.68)$, $c_1 = 0.7100$, $c_2 = 0.0037$, $c_3 = 1.935$, $c_4 = 0.085$, and $c_5 = 30$.

Quark Star

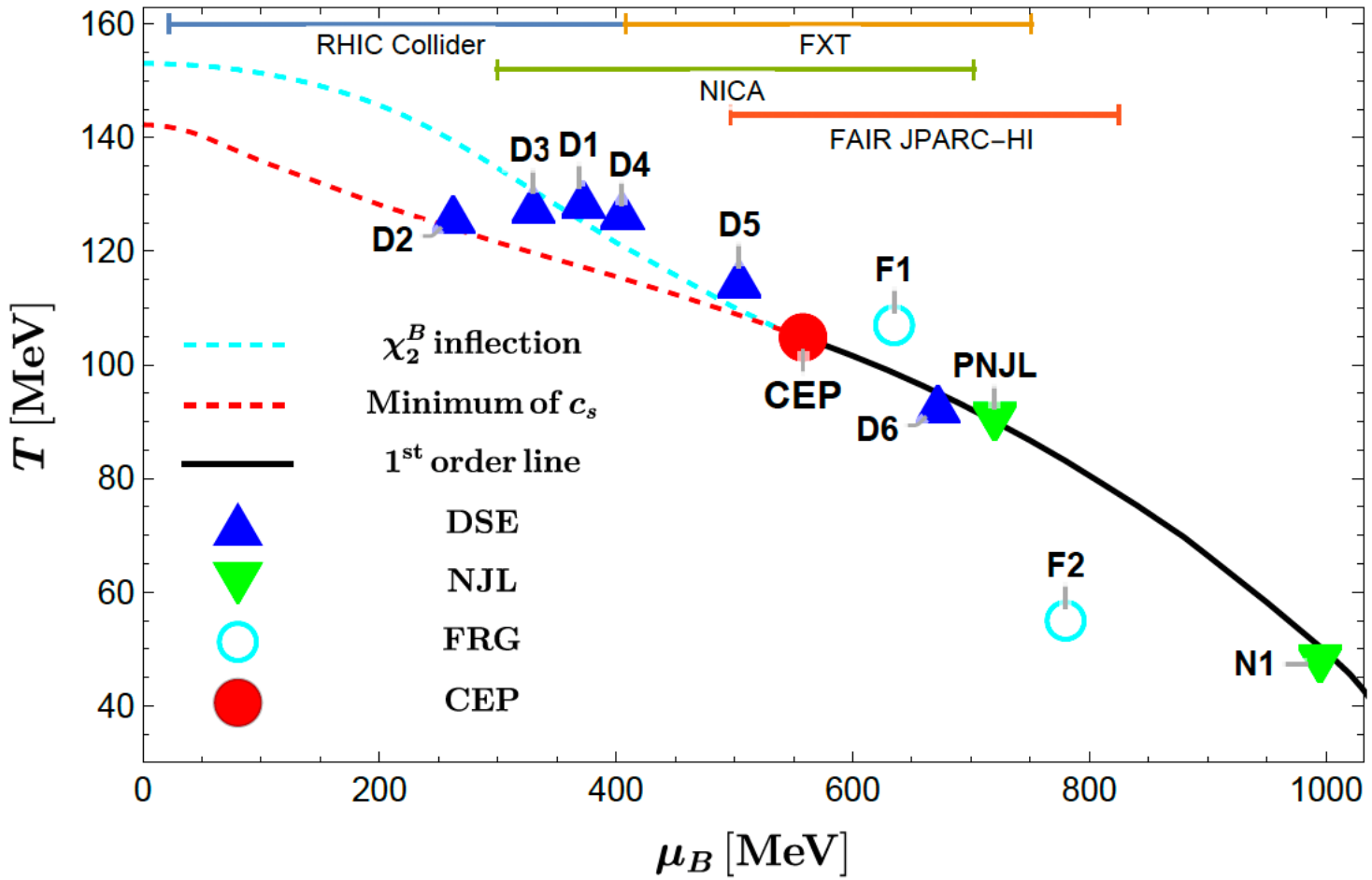

arXiv: 2201.02004

Quark Star

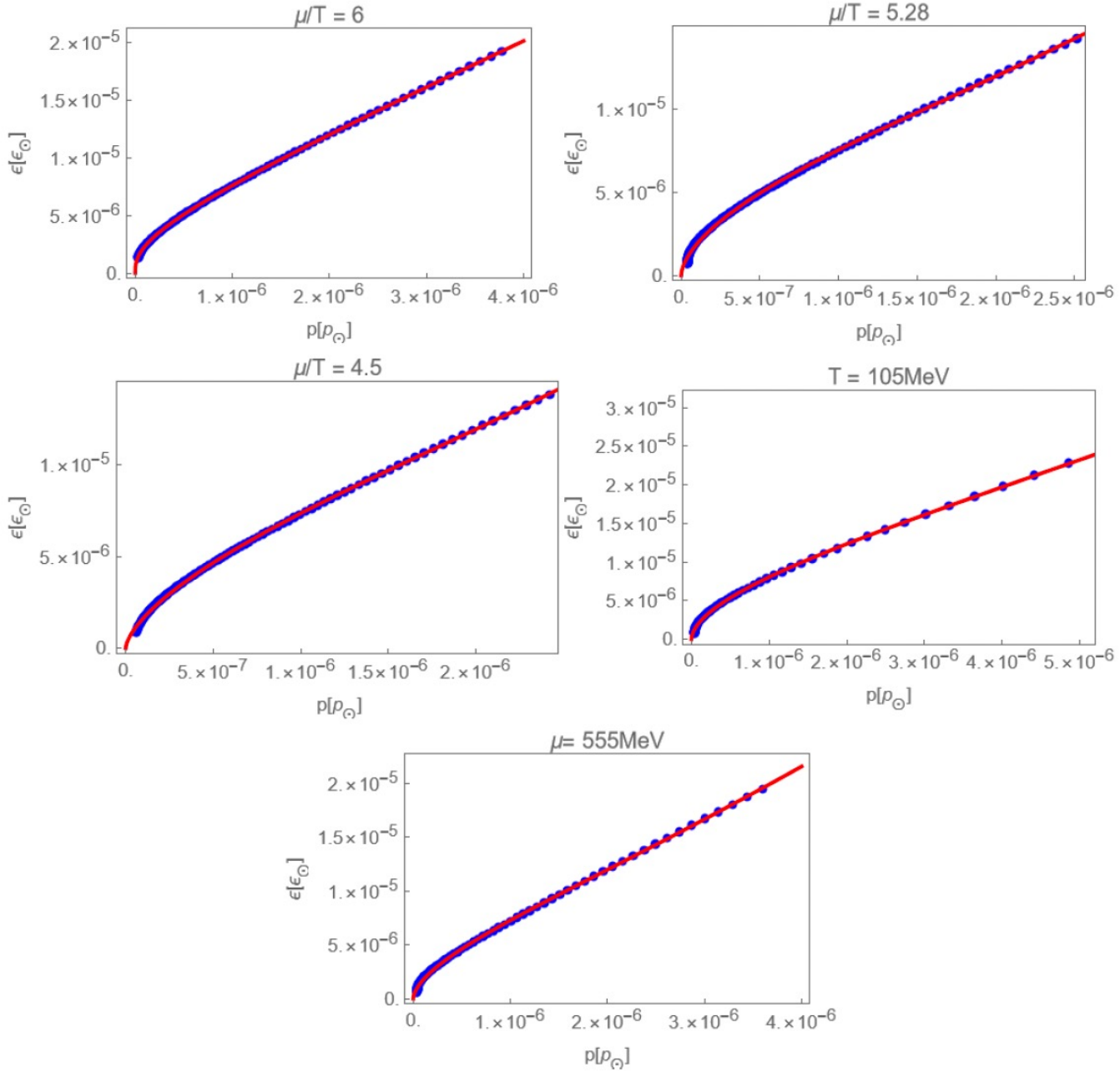

Fig. 1: The energy-pressure data and fitting curves under five different T, μ conditions. The blue dots represent the numerical data, and the red lines are the fitting curves. The data near the origin have small blanks, which indicate reaching the phase transition point.

Their fitting results (p_1, ϵ_1 corresponds to $\mu/T = 4.5$, p_2, ϵ_2 corresponds to $\mu/T = 5.28$, p_3, ϵ_3 corresponds to $\mu/T = 6$, p_4, ϵ_4 corresponds to $T = 105\text{MeV}$, p_5, ϵ_5 corresponds to $\mu = 555\text{MeV}$) are listed respectively:

$$\begin{aligned}
&\epsilon_1 = 0.0592293 p_1^{0.651263} + 1.43266 \times 10^{13} p_1^{3.42233}, \\
&p_1 \in [6.07854 \times 10^{-8}, 2.42143 \times 10^{-6}], \\
&\epsilon_1 \in [8.65502 \times 10^{-7}, 0.000013846],
\end{aligned} \tag{6}$$

$$\begin{aligned}
&\epsilon_2 = 0.027042 p_2^{0.593438} + 1.80685 \times 10^{10} p_2^{2.87626}, \\
&p_2 \in [3.97089 \times 10^{-8}, 2.5162 \times 10^{-6}], \\
&\epsilon_2 \in [7.09555 \times 10^{-7}, 0.0000142],
\end{aligned} \tag{7}$$

$$\begin{aligned}
&\epsilon_3 = 0.000833022 p_3^{0.370279} + 8.72125 p_3^{1.08721}, \\
&p_3 \in [3.03394 \times 10^{-8}, 9.51759 \times 10^{-6}], \\
&\epsilon_3 \in [1.36385 \times 10^{-6}, 0.000019245],
\end{aligned} \tag{8}$$

$$\begin{aligned}
&\epsilon_4 = 0.017254 p_4^{0.557614} + 3330.51 p_4^{1.68025}, \\
&p_4 \in [3.97113 \times 10^{-8}, 7.12588 \times 10^{-6}], \\
&\epsilon_4 \in [7.98295 \times 10^{-7}, 0.0000305948],
\end{aligned} \tag{9}$$

$$\begin{aligned}
&\epsilon_5 = 0.0235768 p_5^{0.590736} + 23025.1 p_5^{1.77162}, \\
&p_5 \in [3.97265 \times 10^{-8}, 3.60026 \times 10^{-6}], \\
&\epsilon_5 \in [6.111821 \times 10^{-7}, 0.00001945].
\end{aligned} \tag{10}$$

混合星

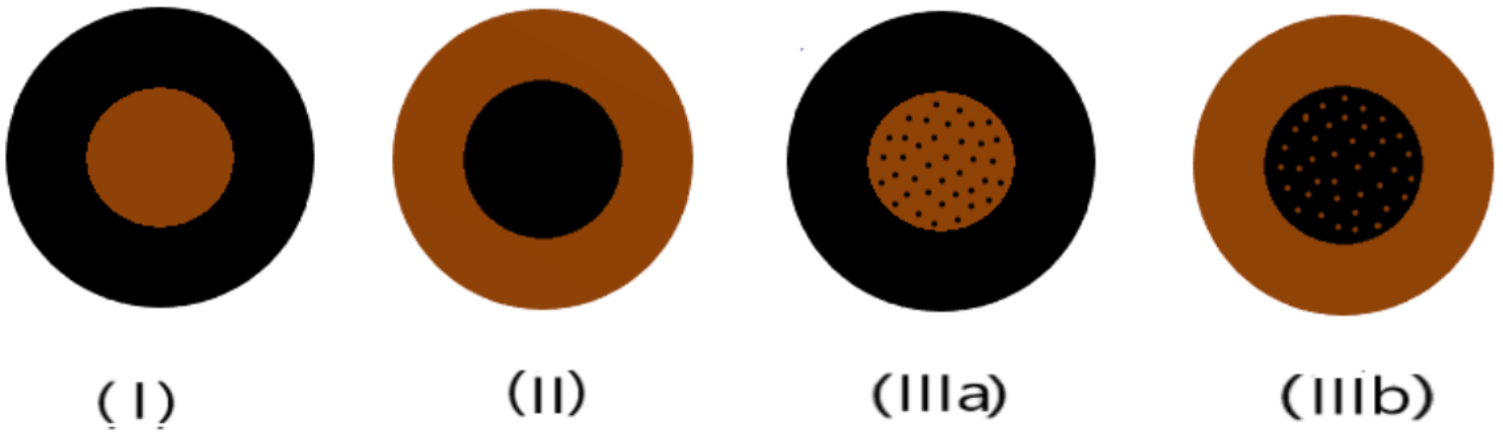

FIG. 1. Three scenarios of hybrid stars. Black color denotes dark matter and brown color denotes nuclear matter. In the first scenario we have a pure nuclear matter core and a pure dark matter crust, and swap the dark and nuclear matter in the second scenario. In the third scenarios, we have a mixed core and either a pure dark matter crust (IIIa) or a nuclear matter one (IIIb). They can form the systems of binary hybrid stars (BHS).

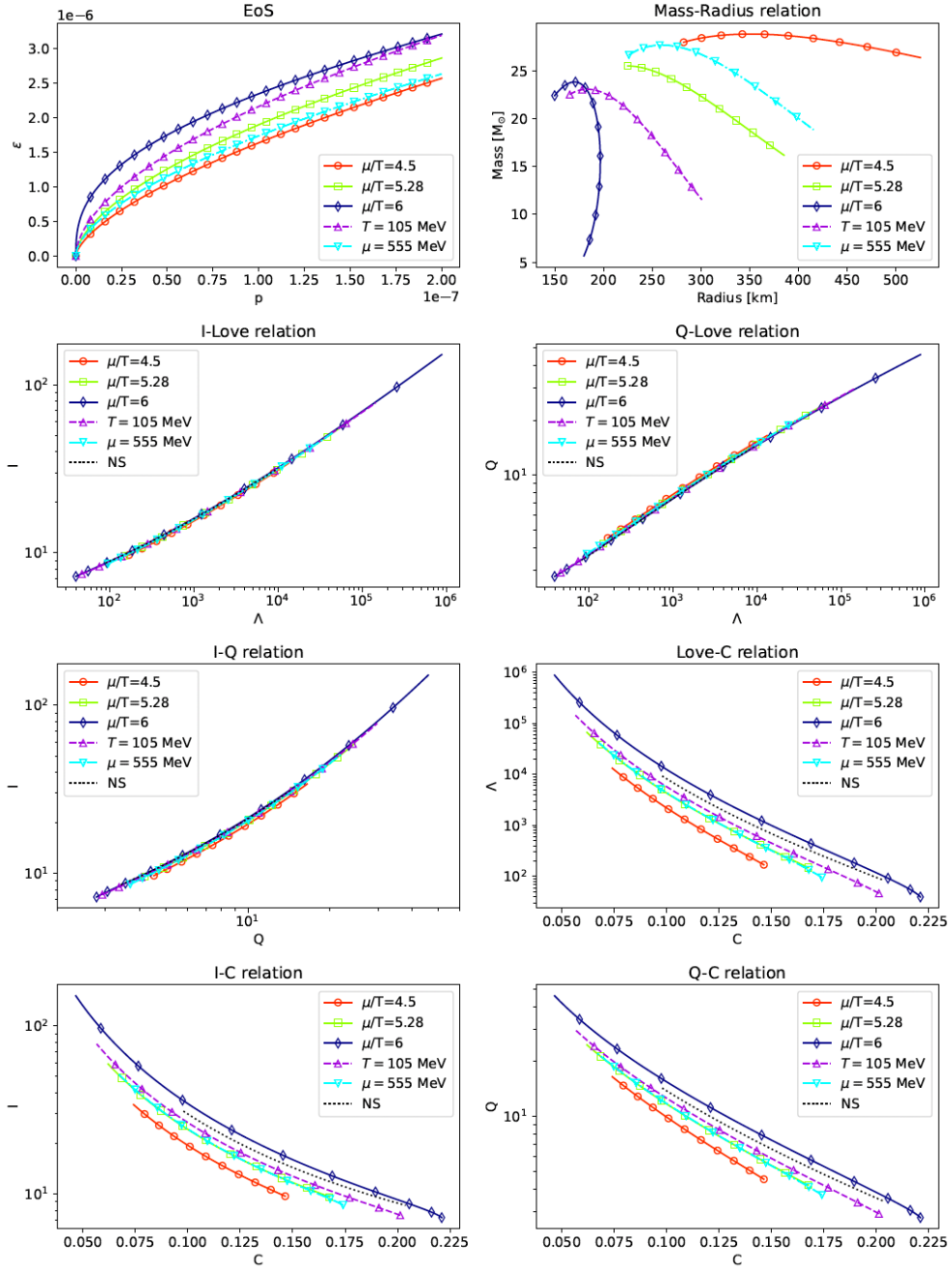

Fig. 4: The EoS, M-R relation and I-Love-Q-C relations for "simple" quark star with different models in eq.(6-10). For reference, the black dotted line representing a polytropic NS $\epsilon = 0.09p^{0.5}$ is plotted in the panels of I-Love-Q-C relations.

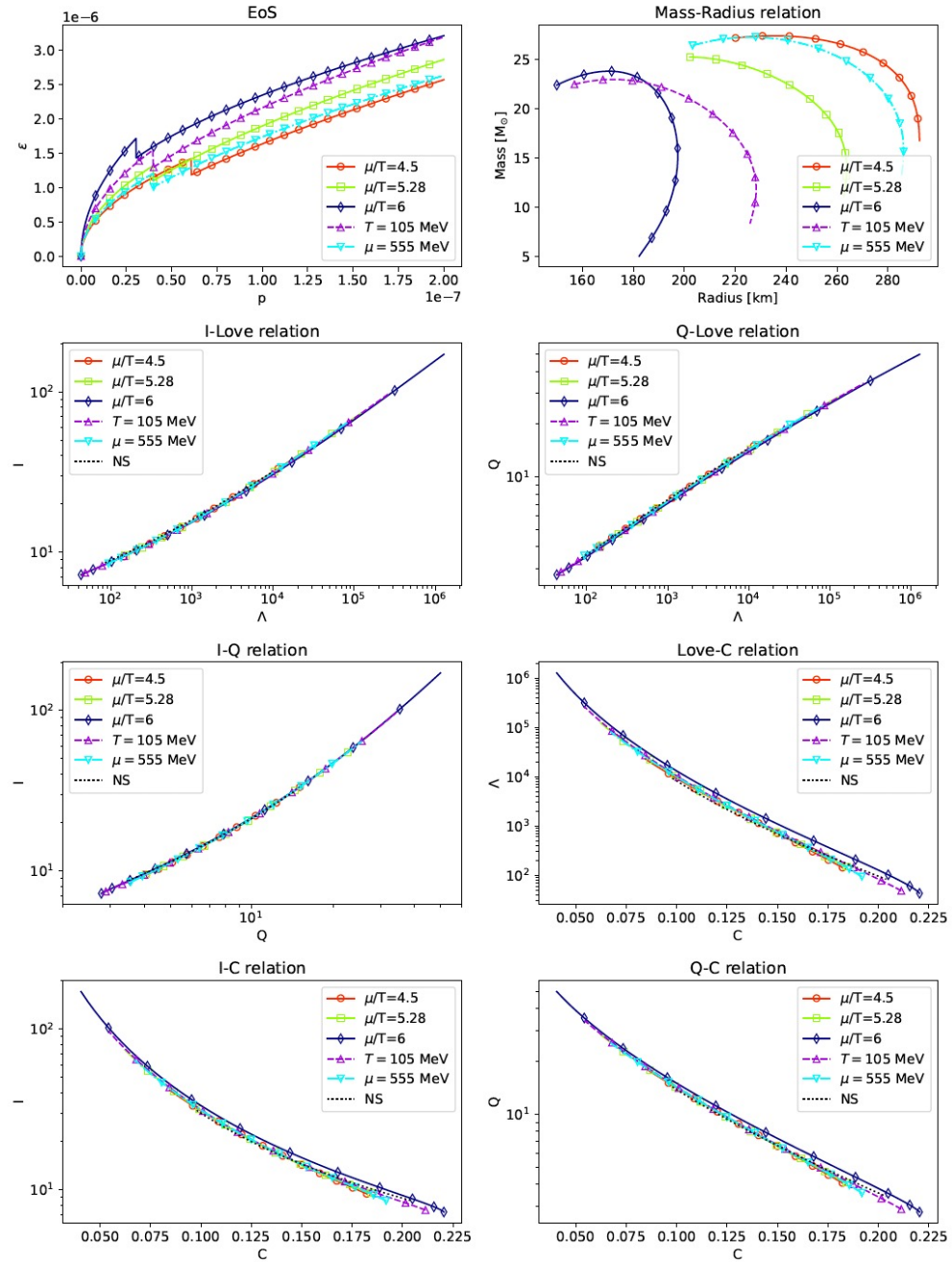

Fig. 6: The EoS, M-R relation and I-Love-Q-C relations of the hybrid stars consist of quark cores and neutron outer layers with $n = 1.2$ in eq.(12). For reference, the black dotted line representing a polytropic NS $\epsilon = 0.09p^{0.5}$ is plotted in the panels of I-Love-Q-C relations.

We conduct research within the EMD theoretical framework in five-dimensional space. The action of the system is represented as:

$$S = \frac{1}{2\kappa_N^2}\int d^5x\sqrt{-g}\left[R - \frac{1}{2}\nabla_\mu\phi\nabla^\mu\phi - \frac{Z(\phi)}{4}F_{\mu\nu}F^{\mu\nu} - U(\phi)\right], \tag{2.1}$$

where κ_N represents the effective Newton constant, ϕ is a scalar field called dilaton, which breaks conformal symmetry, $F_{\mu\nu}$ is the field strength tensor of the U(1) gauge field, and g denotes the determinant of the five-dimensional spacetime metric tensor, R is the Ricci scalar curvature. The scalar potential $U(\phi)$ and the gauge coupling function $Z(\phi)$, are chosen to reproduce key features of 2-flavor lattice QCD at zero chemical potential. Based on the work of [40], we adopt the following forms:

$$\begin{aligned} U(\phi) &= -12\cosh[c_1\phi] + (6c_1^2 - \frac{3}{2})\phi^2 + c_2\phi^6, \\ Z(\phi) &= \frac{\mathrm{sech}[c_4\phi^3]}{1+c_3} + \frac{c_3}{1+c_3}e^{-c_5\phi}. \end{aligned} \tag{2.2}$$

As established by lattice data in [40], the parameters κ_N and c_i are determined as the following values: $\kappa_N^2 = 2\pi(3.72)$, $c_1 = 0.7100$, $c_2 = 0.0002$, $c_3 = 0.530$, $c_4 = 0.085$, and $c_5 = 30$.

The metric form of a five-dimensional AdS black hole with scalar hair is as follows

$$ds^2 = -f(r)e^{-\eta(r)}dt^2 + \frac{dr^2}{f(r)} + r^2(dx^2 + dy^2 + dz^2), \tag{2.3}$$

and

$$\phi = \phi(r), \quad A_t = A_t(r). \tag{2.4}$$

where $f(r)$ and $\eta(r)$ are all functions of r, and A_t is the t-component of the gauge field.

The temperature T and entropy density s can both be obtained from the horizon

$$T = \frac{1}{4\pi}f'(r_h)e^{-\eta(r_h)/2}, s = \frac{2\pi}{\kappa_N^2}r_h^3, \tag{2.5}$$

where r_h is the horizon radius.

Through the calculation method in [23], the specific form of energy density ϵ and pressure p can be obtained

$$\begin{aligned}\epsilon &= \frac{1}{2\kappa_N^2}(-3f_v + \phi_s\phi_v + \frac{1+48b}{48}\phi_s^4),\\ p &= \frac{1}{2\kappa_N^2}(-f_v + \phi_s\phi_v + \frac{3-48b-8c_1^4}{48}\phi_s^4),\end{aligned} \tag{2.6}$$

The fitting results corresponding to different physical conditions are listed below: p_1, ϵ_1 for $\mu/T = 1$, p_2, ϵ_2 for $\mu/T = 1.2033$, p_3, ϵ_3 for $\mu/T = 1.25$, p_4, ϵ_4 for $T = 182$ MeV, p_5, ϵ_5 for $\mu = 219$ MeV.

$$\begin{aligned}
&\epsilon_1 = 0.000501863\, p_1^{0.315468} + 1.15292\, p_1^{0.89651}, \\
&p_1 \in [3.0918 \times 10^{-8},\ 7.3047 \times 10^{-6}], \\
&\epsilon_1 \in [2.1682 \times 10^{-6},\ 4.066 \times 10^{-5}],
\end{aligned} \tag{2.8}$$

$$\begin{aligned}
&\epsilon_2 = 0.00139264\, p_2^{0.375067} + 2.6989\, p_2^{0.982421}, \\
&p_2 \in [2.627 \times 10^{-8},\ 7.3045 \times 10^{-6}], \\
&\epsilon_2 \in [1.7023 \times 10^{-6},\ 4.0658 \times 10^{-5}],
\end{aligned} \tag{2.9}$$

$$\begin{aligned}
&\epsilon_3 = 0.000928211\, p_3^{0.349754} + 2.15744\, p_3^{0.958067}, \\
&p_3 \in [2.3732 \times 10^{-8},\ 7.35366 \times 10^{-6}], \\
&\epsilon_3 \in [1.6962 \times 10^{-6},\ 4.08 \times 10^{-5}],
\end{aligned} \tag{2.10}$$

$$\begin{aligned}
&\epsilon_4 = 0.00117483\, p_4^{0.350591} + 11.3855\, p_4^{1.13679}, \\
&p_4 \in [2.61368 \times 10^{-8},\ 1.1615 \times 10^{-5}], \\
&\epsilon_4 \in [2.1067 \times 10^{-6},\ 4.9673 \times 10^{-5}],
\end{aligned} \tag{2.11}$$

$$\begin{aligned}
&\epsilon_5 = 0.001427\, p_5^{0.378816} + 2.09627\, p_5^{0.958741}, \\
&p_5 \in [2.60394 \times 10^{-8},\ 6.97167 \times 10^{-6}], \\
&\epsilon_5 \in [1.5845 \times 10^{-6},\ 3.967 \times 10^{-5}].
\end{aligned} \tag{2.12}$$

夸克星

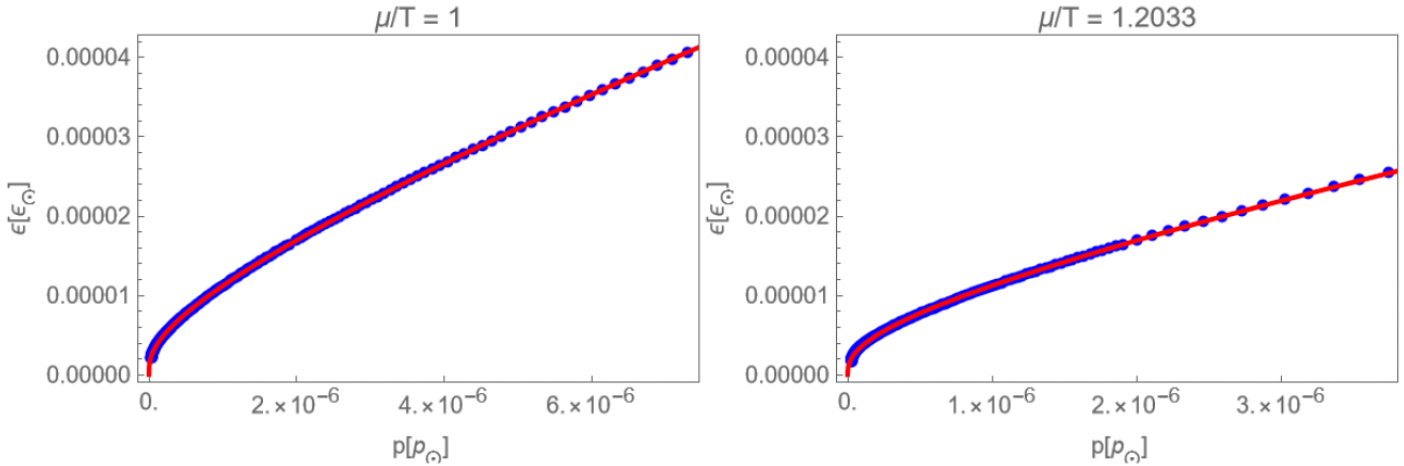
μ/T = 1
0.00004
0.00003
0.00002
0.00001
0.00000
ϵ[ϵ⊙]
0.
2.×10^-6
4.×10^-6
6.×10^-6
p[p⊙]

μ/T = 1.2033
0.00004
0.00003
0.00002
0.00001
0.00000
ϵ[ϵ⊙]
0.
1.×10^-6
2.×10^-6
3.×10^-6
p[p⊙]

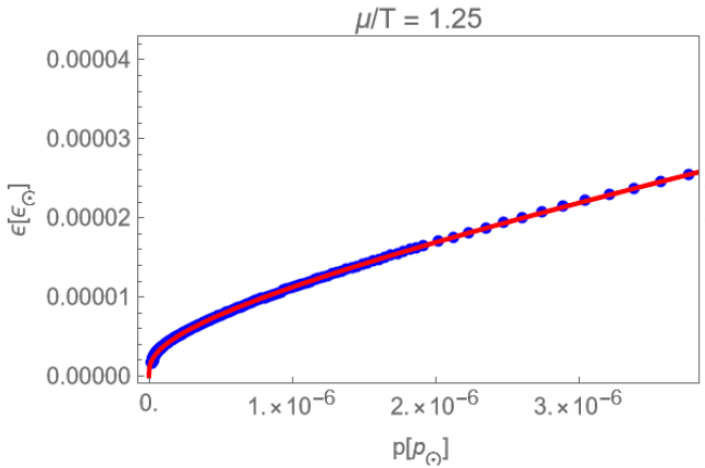
μ/T = 1.25
0.00004
0.00003
0.00002
0.00001
0.00000
ϵ[ϵ⊙]
0.
1.×10^-6
2.×10^-6
3.×10^-6
p[p⊙]

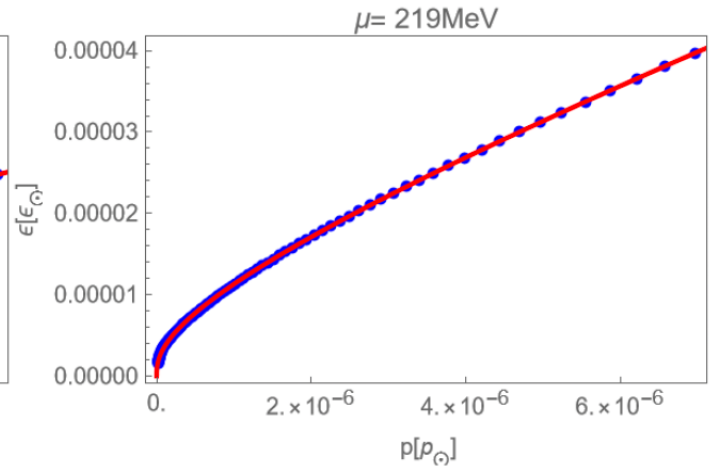
μ= 219MeV
0.00004
0.00003
0.00002
0.00001
0.00000
ϵ[ϵ⊙]
0.
2.×10^-6
4.×10^-6
6.×10^-6
p[p⊙]

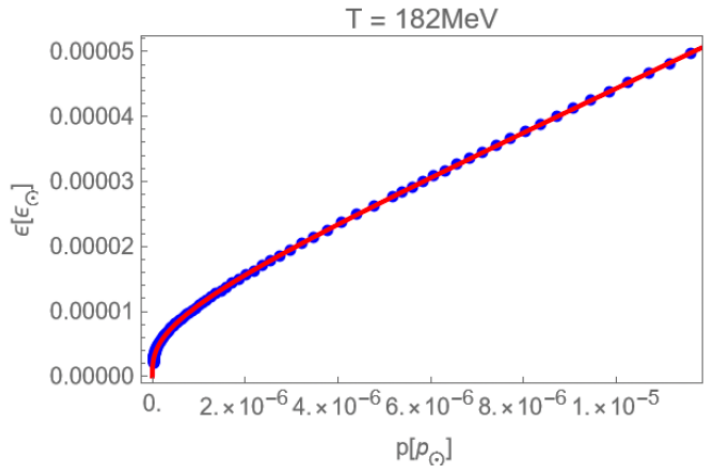
T = 182MeV
0.00005
0.00004
0.00003
0.00002
0.00001
0.00000
ϵ[ϵ⊙]
0.
2.×10^-6
4.×10^-6
6.×10^-6
8.×10^-6
1.×10^-5
p[p⊙]

夸克星

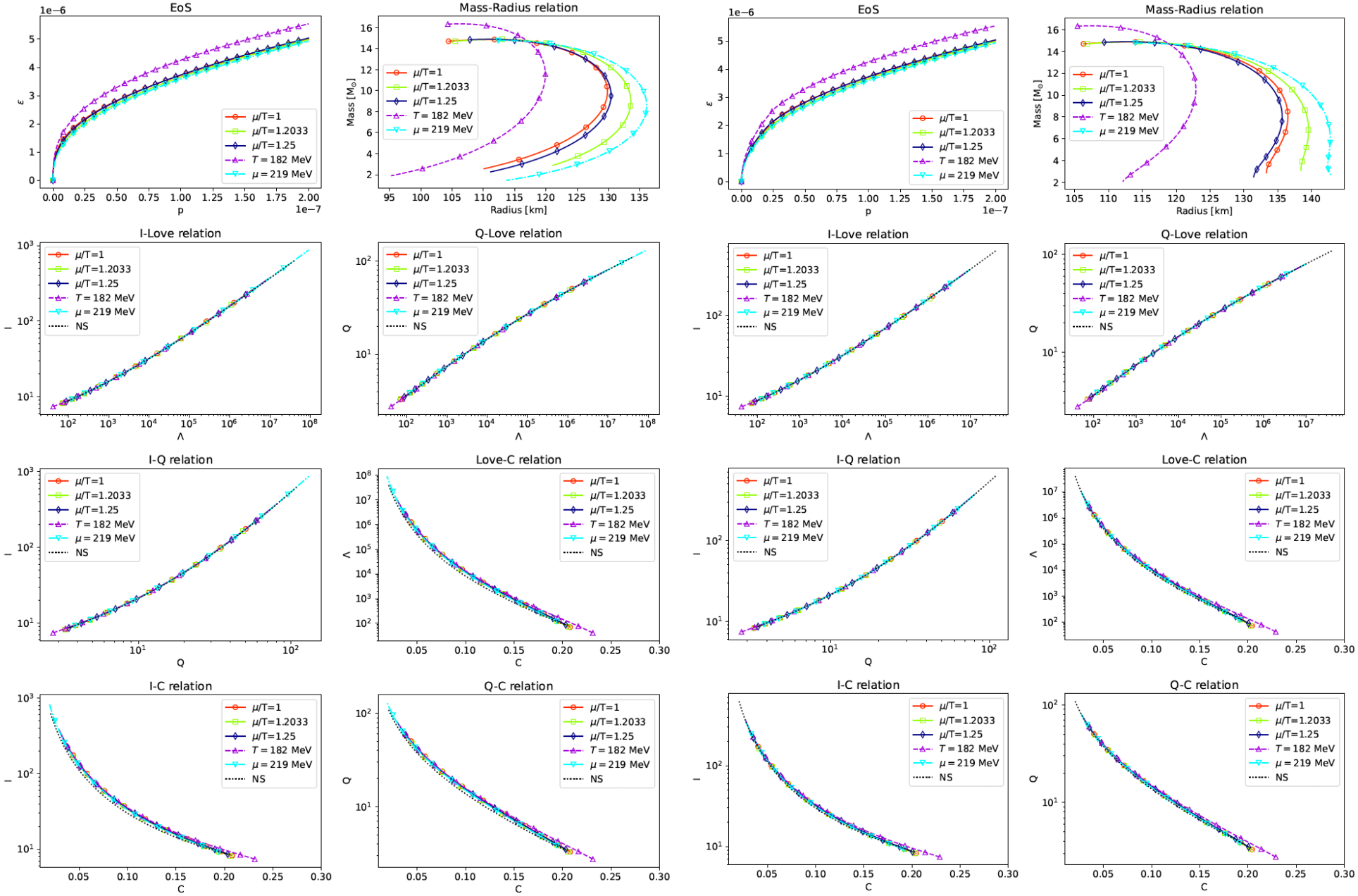

Figure 2: The EoS, M-R relation, and I-Love-Q-C relations for the "simple" QS are presented using various models described in Eq. (2.8–2.12). For comparison, the panels showing the I-Love-Q-C relations of a polytropic NS, given by $\epsilon_n = 0.09 p_n^{0.5}$, is plotted with a black dotted line.

Figure 3: The EoS, M-R relation, and I-Love-Q-C relations for the "combined" QS consisting of quark cores and hadron shells with $m = 1$ in Eq.(3.2). For comparison, the panels showing the I-Love-Q-C relations of a polytropic NS, given by $\epsilon_n = 0.09 p_n^{0.5}$, is plotted with a black dotted line.

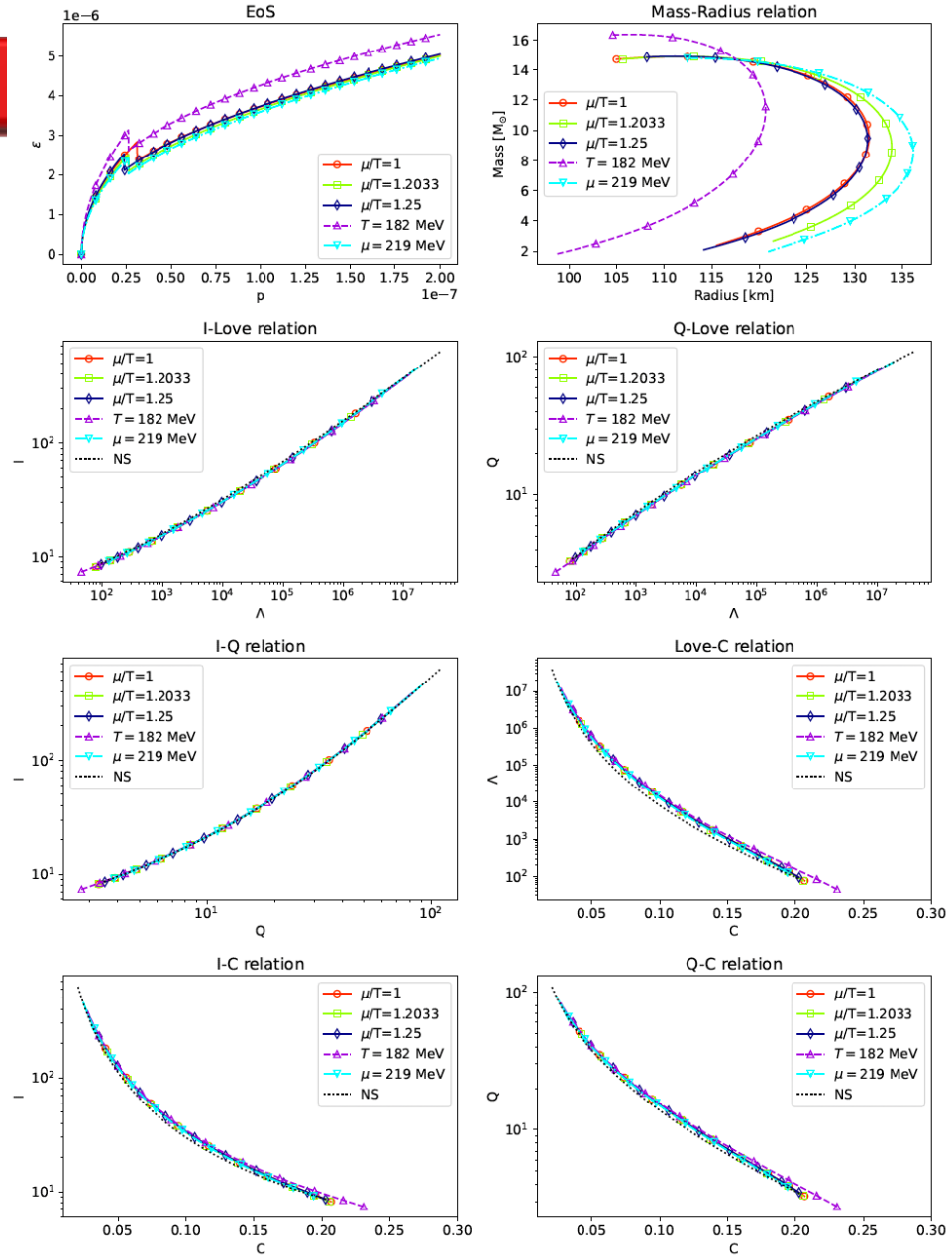

Figure 4: The EoS, M-R relation, and I-Love-Q-C relations for the "combined" QS consisting of quark cores and hadron shells with $m = 1.2$ in Eq.(3.2). For comparison, the panels showing the I-Love-Q-C relations of a polytropic NS, given by $\epsilon_n = 0.09 p_n^{0.5}$, is plotted with a black dotted line.

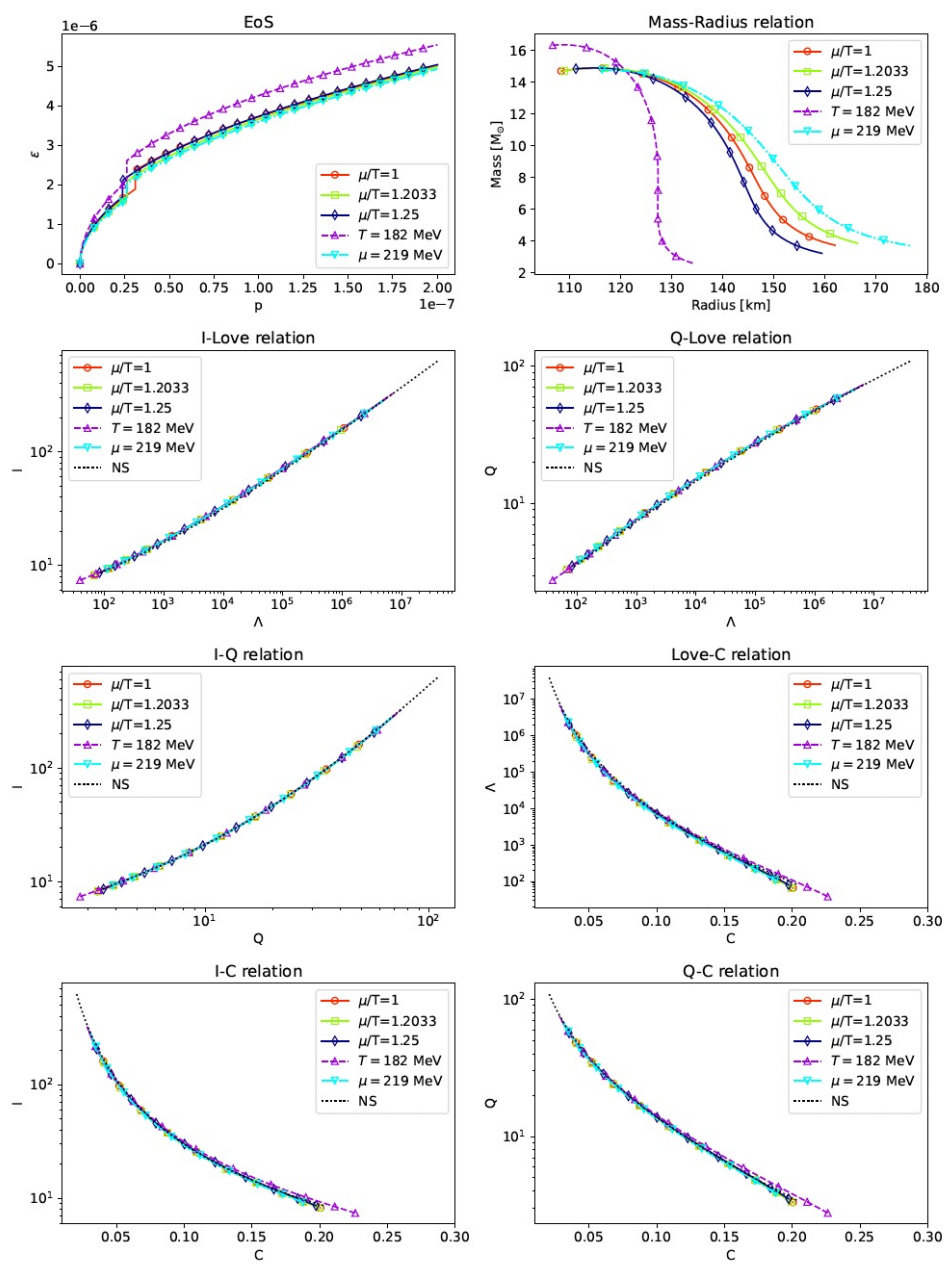

Figure 5: The EoS, M-R relation, and I-Love-Q-C relations for the "combined" QS consisting of quark cores and hadron shells with $m = 0.8$ in Eq.(3.2). For comparison, the panels showing the I-Love-Q-C relations of a polytropic NS, given by $\epsilon_n = 0.09 p_n^{0.5}$, is plotted with a black dotted line.

夸克星

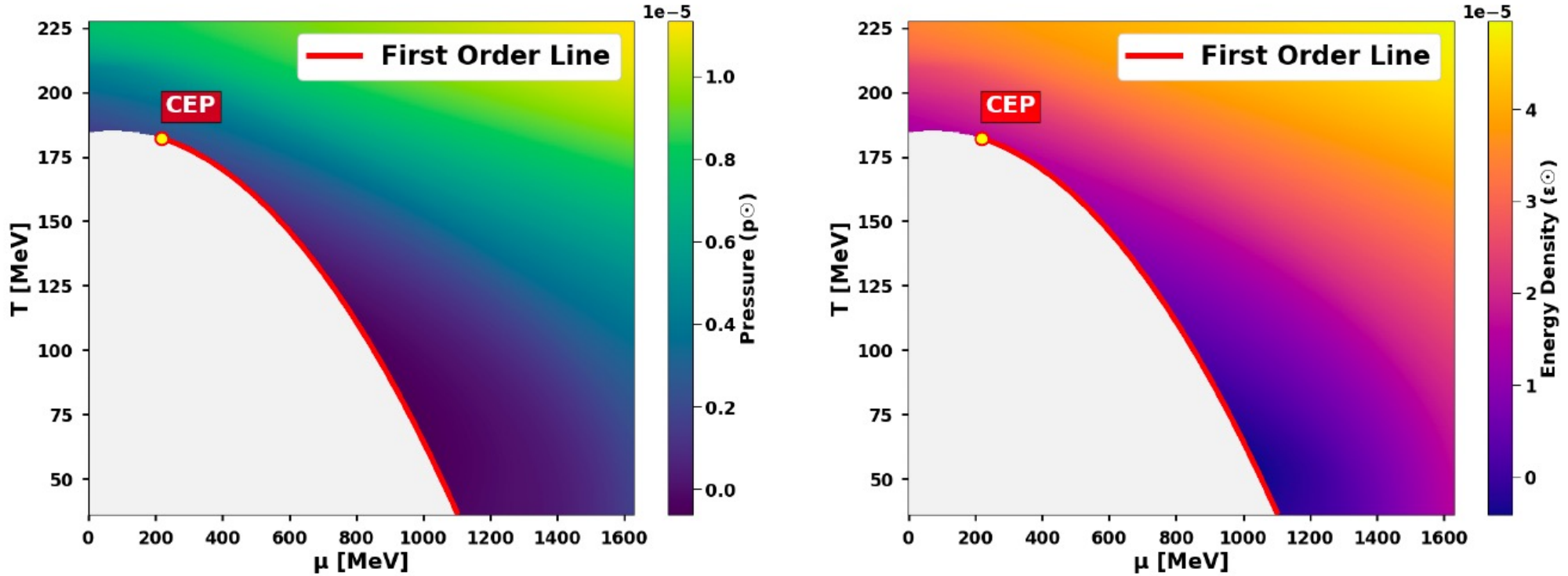

Figure 7: The heatmap presents all the T, μ dependence for p and ϵ of the Holographic 2-flavor QCD Model (Notice that here for p and ϵ we are using astronomical units $p_\odot$ and $\epsilon_\odot$ for later convenience, rather than QCD units): $p = p(\mu, T)$ and $\epsilon = \epsilon(\mu, T)$, where the shading of the background color represents the magnitudes of p and ϵ. The CEP and first order line are taken from reference [40].

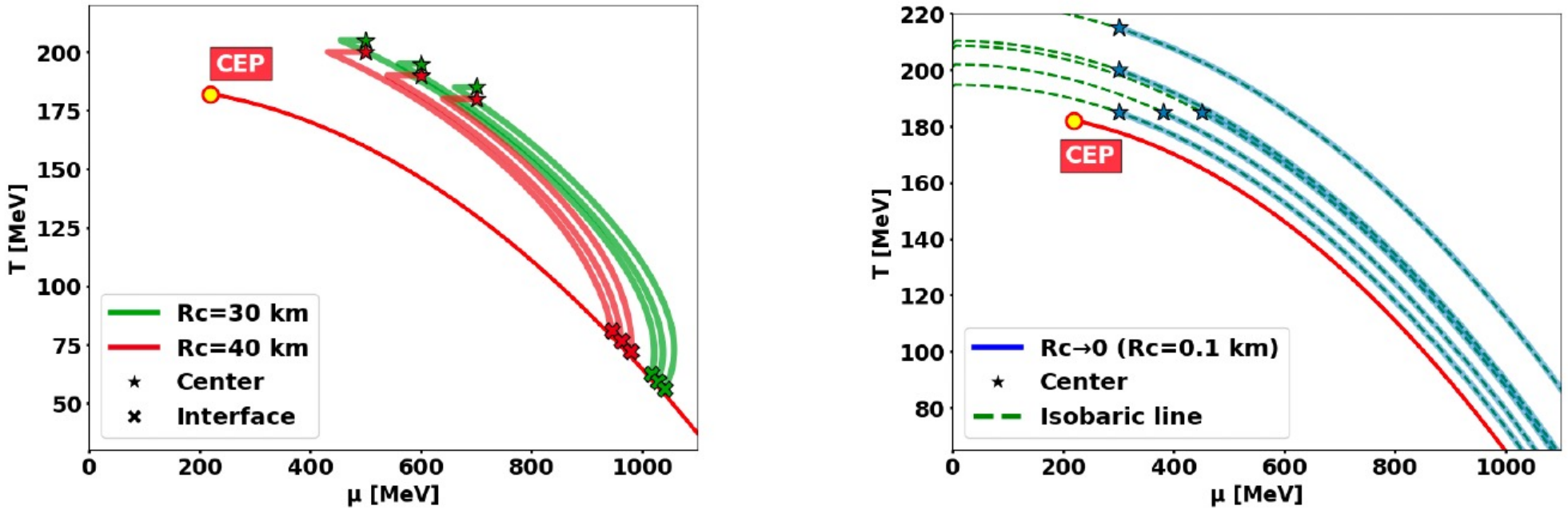

Figure 8: Paths of chemical potential and temperature (μ, T) as functions of radius for different thermal core radius R_c: **(a)** Finite thermal core radius: As radius r increases, the path intersects the phase transition line and terminates at the stellar interface. Different central conditions (μ_0, T_0) correspond to distinct trajectories, reflecting variations in the stellar EoS. **(b)** Infinitesimal core $(R_c \to 0)$: The pressure remains approximately constant during radial expansion, resulting in an isobaric trajectory.

夸克星

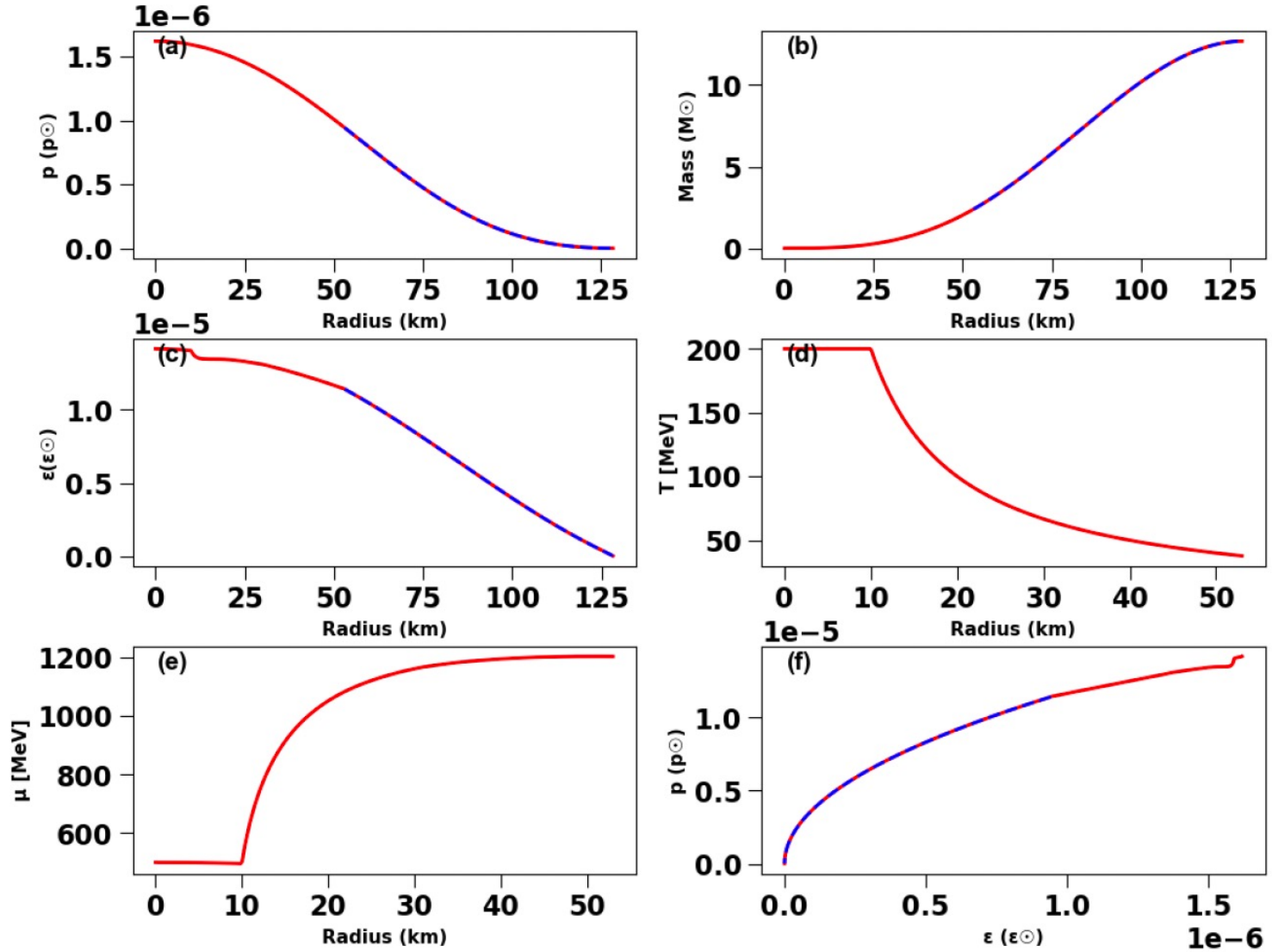

Figure 9: Radial profiles of physical quantities for a complete QS model with R_c = 10 km and central parameters $(T_0, \mu_0) = (200\ \text{MeV}, 500\ \text{MeV})$. **(a)** Pressure, **(b)** Mass accumulation, **(c)** Energy density, **(d)** Temperature, **(e)** Chemical potential, and **(f)** EoS. Blue dashed curves denote contributions from the external single-polytropic hadron matter EoS with $\gamma_n = 0.5$.

夸克星

Mixed Stars

混合星

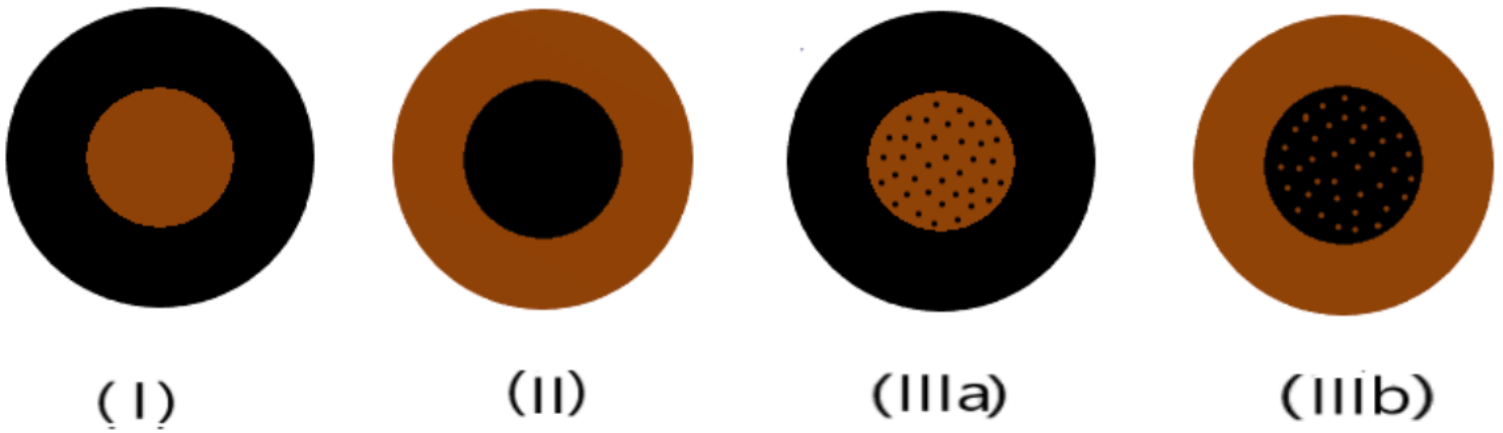

FIG. 1. Three scenarios of hybrid stars. Black color denotes dark matter and brown color denotes nuclear matter. In the first scenario we have a pure nuclear matter core and a pure dark matter crust, and swap the dark and nuclear matter in the second scenario. In the third scenarios, we have a mixed core and either a pure dark matter crust (IIIa) or a nuclear matter one (IIIb). They can form the systems of binary hybrid stars (BHS).

混合星

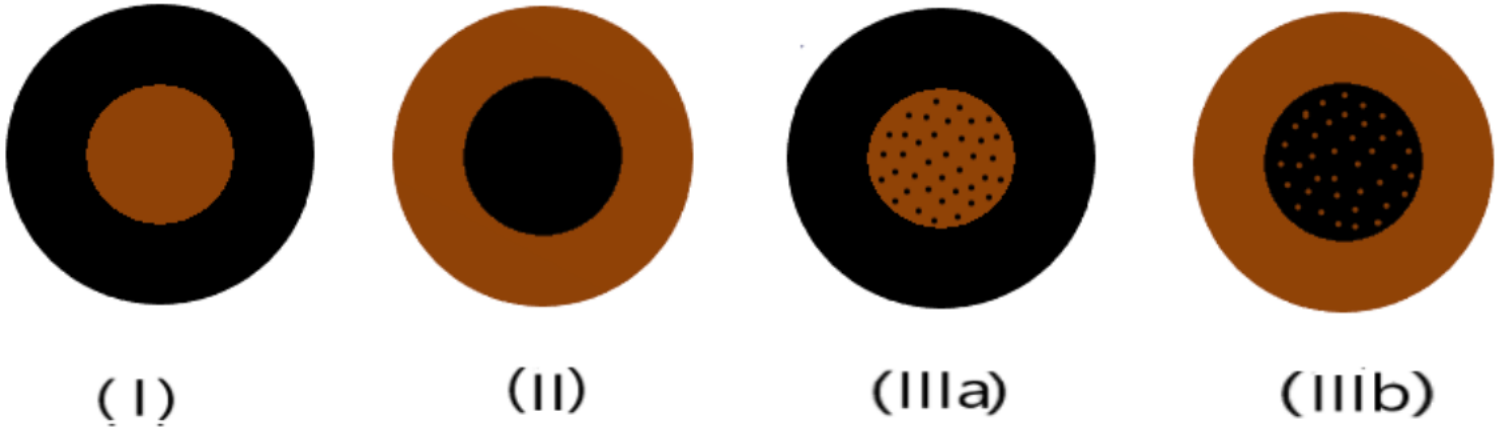

提出了中子与暗物质构成混合星体的三种模型，能够解释中子星合并事件**GW170817**以及**GW190425**。这三种模型考虑了暗物质与中子有相互作用的情况和无相互作用只靠引力耦合的情况。其中首次推导出无相互作用时的混合星体潮汐变形的计算公式。

混合星

Given a set of $(\mathcal{B}, r_W)$ we first obtain the mass–radius relation by solving the Tolman–Oppenheimer–Volkoff (TOV) equations [51,52] for multi-component cases [53,54] using units $G = c = 1$:

$$p_I' = -(\rho_I + p_I)\phi', \quad m_I' = 4\pi r^2 \rho_I, \quad \phi' = \frac{m + 4\pi r^3 p}{r(r-2m)}, \tag{4}$$

where $' := \frac{d}{dr}$, $I = D$ or N, the mass inside radius r is $m(r) = \sum_I m_I$, pressure $p = \sum_I p_I$, energy density $\rho = \sum_I \rho_I$ by summing the contributions from both dark matter ($I = D$) and nuclear matter ($I = N$), and the Newton potential $\phi := \frac{1}{2}\ln(-g_{tt})$ with g_{tt} the tt-component of the metric. The size R of the star is determined by $p(r = R) = 0$, and the mass of the star is given by $m(R)$. For the first scenario strength. To consider the tidal deformability for the hybrid stars of scenario III, we need to generalize the derivation of [56,57] for the single fluid to the multi-fluid cases. We again need to solve the following equation for $y(r) := rH'(r)/H(r)$ with $H(r)$ the linear perturbation of g_{tt} around a TOV configuration:

$$ry' + y^2 + P(r)y + r^2 Q(r) = 0, \tag{6}$$

with the boundary condition $y(0) = 2$ and

$$P = (1 + 4\pi r^2(p - \rho))/(1 - 2m/r), \tag{7}$$

$$Q = 4\pi\left(5\rho + 9p + \sum_I \frac{\rho_I + p_I}{dp_I/d\rho_I} - \frac{6}{4\pi r^2}\right)/(1 - 2m/r) - 4\phi'^2. \tag{8}$$

The above equations are rigorously derived from Einstein equation, and the main difference from the single-fluid case is encoded in the $\sum_I \frac{\rho_I + p_I}{dp_I/d\rho_I}$ term of (8).

Suppose the pressure reads p_W on the domain wall located at $r = r_W$. The sound speed near a density discontinuity is

$$\frac{d\rho}{dp} = \frac{1}{c_s^2} = \left.\frac{d\rho}{dp}\right|_{p\neq p_W} + \Delta\rho_p\,\delta(p - p_W), \tag{9}$$

where $\Delta\rho_p = \rho(p_W + 0) - \rho(p_W - 0)$ is the energy density jump across p_W. Yet since p decreases as r increases, equivalently $\Delta\rho_p = -(\rho(r_W + 0) - \rho(r_W - 0)) \equiv -\Delta\rho$.

to the δ-function can contribute. Therefore, this then results in

$$ry'(r)\Big|_{r=r_W} + r^2 4\pi e^{\lambda(r)}\,(\rho(r) + p(r))\,\left.\frac{d\rho}{dp}\right|_{r=r_W} = 0. \tag{10}$$

Since $\frac{d\rho}{dp} = \frac{d\rho}{dr}\frac{1}{dp/dr}$, where $\frac{dp}{dr}$ can be read off from the first TOV equation (4), and $\frac{d\rho}{dr}|_{r=r_W} = \Delta\rho\,\delta(r - r_W)$, we obtain that[6]

$$\Delta y = \frac{\Delta\rho}{p + m(r_W)/(4\pi r_W^3)}, \tag{11}$$

[6] There are typos in the counterpart of (11) in [57].

混合星

Suppose the pressure reads p_W on the domain wall located at $r = r_W$. The sound speed near a density discontinuity is

$$\frac{d\rho}{dp} = \frac{1}{c_s^2} = \left.\frac{d\rho}{dp}\right|_{p\neq p_W} + \Delta\rho_p\,\delta(p - p_W), \tag{9}$$

where $\Delta\rho_p = \rho(p_W + 0) - \rho(p_W - 0)$ is the energy density jump across p_W. Yet since p decreases as r increases, equivalently $\Delta\rho_p = -(\rho(r_W + 0) - \rho(r_W - 0)) \equiv -\Delta\rho$.

to the δ-function can contribute. Therefore, this then results in

$$ry'(r)\Big|_{r=r_W} + r^2 4\pi e^{\lambda(r)}\,(\rho(r) + p(r))\,\frac{d\rho}{dp}\Big|_{r=r_W} = 0. \tag{10}$$

Since $\frac{d\rho}{dp} = \frac{d\rho}{dr}\frac{1}{dp/dr}$, where $\frac{dp}{dr}$ can be read off from the first TOV equation (4), and $\frac{d\rho}{dr}|_{r=r_W} = \Delta\rho\,\delta(r - r_W)$, we obtain that[6]

$$\Delta y = \frac{\Delta\rho}{p + m(r_W)/(4\pi r_W^3)}, \tag{11}$$

[6] There are typos in the counterpart of (11) in [57].

S. Postnikov, M. Prakash, J.M. Lattimer, Phys. Rev. D 82, 024016(2010). https://doi.org/10.1103/PhysRevD.82.024016

$$\begin{aligned} y(r_d + \epsilon) &= y(r_d - \epsilon) - \frac{\rho(r_d + \epsilon) - \rho(r_d - \epsilon)}{m(r_d)/(4\pi r_d^3)} \\ &= y(h_d - \epsilon) - 3\frac{\Delta\rho}{\tilde{\rho}}, \end{aligned} \tag{14}$$

where $\epsilon \to 0$ and $\tilde{\rho} = m(r_d)/(4\pi r_d^3/3)$ is the average energy density of the inner ($r < r_d$) core.

混合星

GW170817 and GW190425 as hybrid stars of dark and nuclear matter

#12

Kilar Zhang (Taiwan, Natl. Normal U.), Guo-Zhang Huang (Taiwan, Natl. Normal U.), Jie-Shiun Tsao (Taiwan, Natl. Normal U.), Feng-Li Lin (Taiwan, Natl. Normal U.) (Feb 25, 2020)

Published in: *Eur.Phys.J.C* 82 (2022) 4, 366 • e-Print: 2002.10961 [astro-ph.HE]

Suppose the pressure reads p_W on the domain wall located at $r = r_W$. The sound speed near a density discontinuity is

$$\frac{d\rho}{dp} = \frac{1}{c_s^2} = \left.\frac{d\rho}{dp}\right|_{p\neq p_W} + \Delta\rho_p\,\delta(p - p_W), \tag{9}$$

where $\Delta\rho_p = \rho(p_W + 0) - \rho(p_W - 0)$ is the energy density jump across p_W. Yet since p decreases as r increases, equivalently $\Delta\rho_p = -(\rho(r_W + 0) - \rho(r_W - 0)) \equiv -\Delta\rho$.

to the δ-function can contribute. Therefore, this then results in

$$ry'(r)\Big|_{r=r_W} + r^2 4\pi e^{\lambda(r)}\,(\rho(r) + p(r))\,\frac{d\rho}{dp}\Big|_{r=r_W} = 0. \tag{10}$$

Since $\frac{d\rho}{dp} = \frac{d\rho}{dr}\frac{1}{dp/dr}$, where $\frac{dp}{dr}$ can be read off from the first TOV equation (4), and $\frac{d\rho}{dr}|_{r=r_W} = \Delta\rho\,\delta(r - r_W)$, we obtain that[6]

$$\Delta y = \frac{\Delta\rho}{p + m(r_W)/(4\pi r_W^3)}, \tag{11}$$

[6] There are typos in the counterpart of (11) in [57].

混合星

Comment on "Tidal Love numbers of neutron and self-bound quark stars"

#1

János Takátsy (Wigner RCP, Budapest and Eotvos Lorand U., Budapest, Inst. Theor. Phys.), Péter Kovács (Wigner RCP, Budapest and Eotvos Lorand U., Budapest, Inst. Theor. Phys.) (Jun 30, 2020)

Published in: *Phys.Rev.D* 102 (2020) 2, 028501 • e-Print: 2007.01139 [astro-ph.HE]

pdf DOI cite claim reference search 33 citations

dividual tidal deformabilities. The corrected fits – as it was claimed by the authors of Ref. [1] – are negligibly different from the reported fits in Ref. [2]. We also add that the correct formula appears in Ref. [6] as well.

[6] K. Zhang, G. Z. Huang, F. L. Lin, arXiv:2002.10961.

混合星

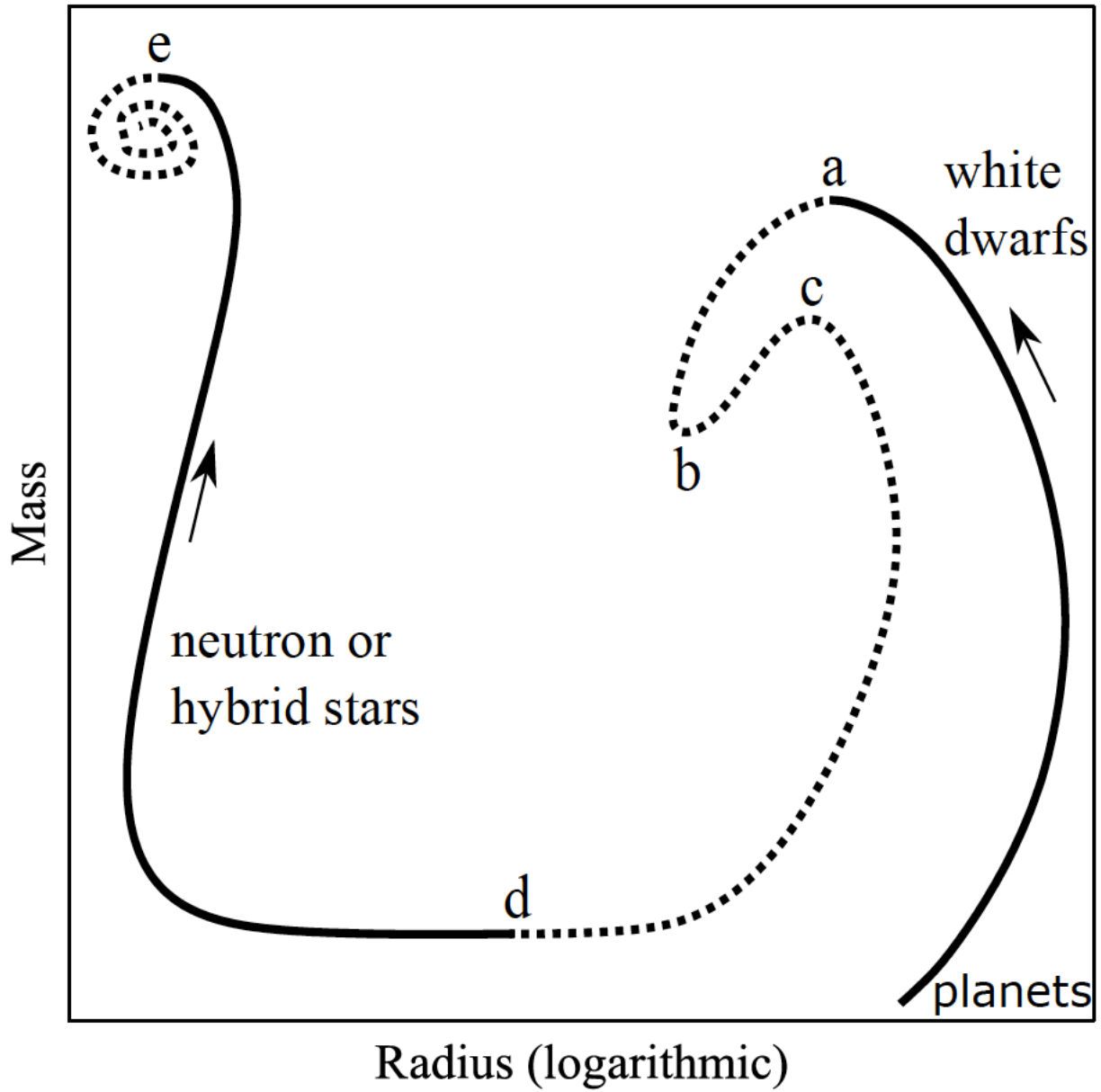

稳定性 BTM准则
压强增大 逆时针

混合星

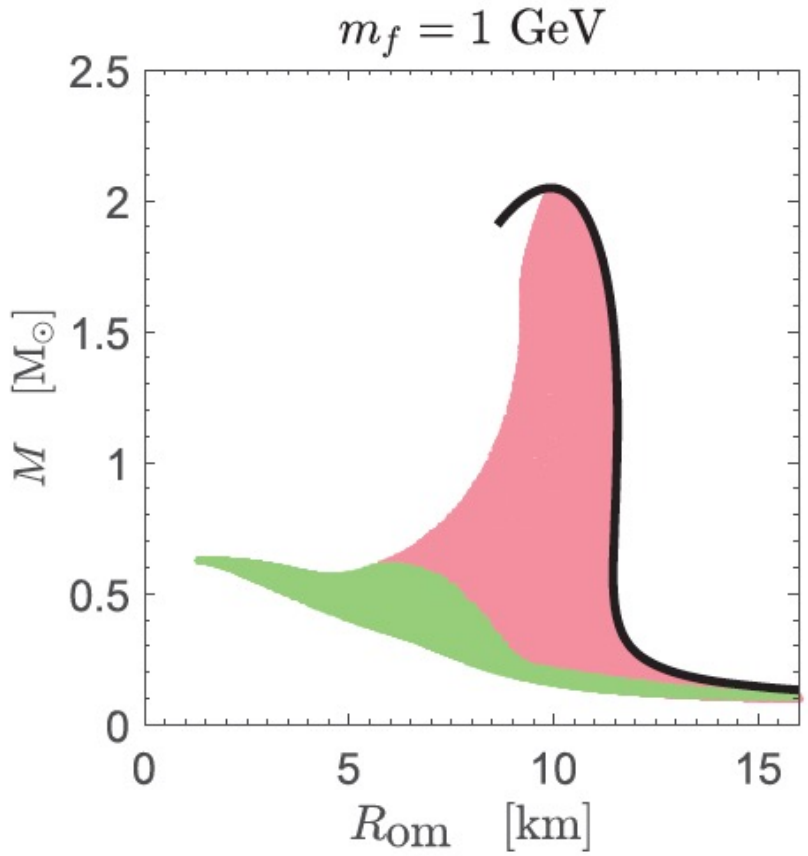

FIG. 4. The mass as a function of the visible radius, which is the radius of ordinary matter, for the stable static solutions shown in Fig. 1 (dark matter is a free Fermi gas with fermion mass $m_f = 1$ GeV). The thick black curve is for the single-fluid star with only ordinary matter, i.e., for a neutron star without dark matter. The color scheme is the same as in Fig. 1, with green indicating a dark matter halo and red a dark matter core.

稳定性 BTM准则

混合星?

演示页

Dark Stars

暗星

$$\rho = \frac{m_{\mathrm{X}}^4 c^3}{\hbar^3}\left[\xi(x) + \frac{2}{9\pi^3}\frac{\alpha_{\mathrm{X}}}{\hbar c}\frac{m_{\mathrm{X}}^2}{m_\phi^2}x^6\right],$$

$$P = \frac{m_{\mathrm{X}}^4 c^5}{\hbar^3}\left[\chi(x) + \frac{2}{9\pi^3}\frac{\alpha_{\mathrm{X}}}{\hbar c}\frac{m_{\mathrm{X}}^2}{m_\phi^2}x^6\right],$$

$$\xi(x) = \frac{1}{8\pi^2}\left[x\sqrt{1+x^2}(2x^2+1) - \ln\left(x+\sqrt{1+x^2}\right)\right],$$

$$\chi(x) = \frac{1}{8\pi^2}\left[x\sqrt{1+x^2}(2x^2/3-1) + \ln\left(x+\sqrt{1+x^2}\right)\right].$$

Maselli Andrea, Pnigouras Pantelis, Nielsen Niklas Gronlund, Kouvaris Chris, Kokkotas Kostas D. Dark stars: Gravitational and electromagnetic observables. Phys Rev D 2017;96(2).

$$\frac{\rho}{\rho_\odot} = \frac{3p}{\rho_\odot} + \mathcal{B}_4\sqrt{\frac{p}{\rho_\odot}}$$

Colpi M, Shapiro SL, Wasserman I. Boson stars: Gravitational equilibria of selfinteracting scalar fields. Phys Rev Lett 1986;57:2485–8.

暗星

$$\mathcal{L} = -\frac{1}{2} g^{\mu\nu} \partial_\mu \phi^* \partial_\nu \phi - V(|\phi|),$$

where

$$V(\phi) = \frac{1}{2} m^2 |\phi|^2 + U(|\phi|)$$

$$V(\phi) = \frac{m^2}{2} |\phi|^2 + \frac{\lambda_4}{4} |\phi|^4$$

$$\frac{\rho}{\rho_\odot} = \frac{3p}{\rho_\odot} + \mathcal{B}_4 \sqrt{\frac{p}{\rho_\odot}}$$

Colpi M, Shapiro SL, Wasserman I. Boson stars: Gravitational equilibria of selfinteracting scalar fields. Phys Rev Lett 1986;57:2485–8.

isotropic limit method

$$\frac{\rho}{\rho_\odot} = \frac{n+2}{n-2} \frac{p}{\rho_\odot} + \mathcal{B}_n \left(\frac{p}{\rho_\odot}\right)^{\frac{2}{n}}$$

暗星

Appendix A. Derivation of isotropic equations of state

In this paper, we study the canonical (massive) complex scalar for boson stars with the following Lagrangian

$$\mathcal{L} = -\frac{1}{2} g^{\mu\nu} \partial_\mu \phi^* \partial_\nu \phi - V(|\phi|), \tag{A.1}$$

where

$$V(\phi) = \frac{1}{2} m^2 |\phi|^2 + U(|\phi|) \tag{A.2}$$

where U is the potential for the self-interactions.

Under spherical symmetry, we consider the following the metric ansatz form

$$ds^2 = -B(r)dt^2 + A(r)dr^2 + r^2 d\Omega \,. \tag{A.3}$$

In such a background, we assume the following stationary and spherical symmetric ansatz for the scalar field,

$$\phi(t, r) = e^{-i\omega t} \Phi(r) \,. \tag{A.4}$$

The field equations for the boson star configurations contain two parts: The first part is the Einstein equation with anisotropic stress tensor given by $T^\mu_\nu = \mathrm{diag}(-\rho, p, p_\perp, p_\perp)$ with

$$\rho = m^2 M_{\rm pl}^2 \Big[\frac{1}{2} (\frac{\Omega^2}{B} + 1)\sigma^2 + \frac{|\partial_x \sigma|^2}{2A} + \frac{U(M_{\rm pl}\sigma)}{m^2 M_{\rm pl}^2} \Big] \tag{A.5}$$

$$p = m^2 M_{\rm pl}^2 \Big[\frac{1}{2} (\frac{\Omega^2}{B} - 1)\sigma^2 + \frac{|\partial_x \sigma|^2}{2A} - \frac{U(M_{\rm pl}\sigma)}{m^2 M_{\rm pl}^2} \Big] \tag{A.6}$$

$$p_\perp = p - \frac{m^2 M_{\rm pl}^2 |\partial_x \sigma|^2}{A} \,, \tag{A.7}$$

where we have introduced the following dimensionless scaled quantities

$$x = mr \,, \qquad \Omega = \frac{\omega}{m} \,, \qquad \sigma = \frac{\Phi}{M_{\rm pl}} \tag{A.8}$$

with the Planckian mass $M_{\rm pl} = 1/\sqrt{4\pi G_N}$. Note that the anisotropy of the pressures is due to the gradient term $|\partial_x \sigma|^2$. The second part of the field equations is the one for Φ (or now σ),

$$\partial_x (x^2 \sqrt{\frac{B}{A}} \partial_x \sigma) + x^2 \sqrt{AB} \Big[(\frac{\Omega^2}{B} - 1)\sigma - \frac{U'(M_{\rm pl}\sigma)}{m^2 M_{\rm pl}} \Big] = 0 \,, \tag{A.9}$$

where $U'(M_{\rm pl}\sigma) := \frac{\delta U(X)}{\delta X}|_{X = M_{\rm pl}\sigma}$.

Due to the anisotropic stress tensor, the Einstein equation cannot be further reduced to TOV equations. The only way to solve the boson star configuration is to solve the coupled field equations by the shooting method, which is numerically difficult to obtain the full mass–radius or even mass-TLN relations. One simplification is to assume the scalar field profile is almost flat inside the boson stars so that the gradient term $\partial_x \sigma|^2$ in (A.5)–(A.6) and (A.9) can be dropped. However, the gradient term cannot always be small unless for some particular self-interaction regime. To see this, let us assume that for some proper choice of a dimensionless parameter Λ, which is the combination of m, σ, and coupling constants in U, one can have

$$\frac{U(M_{\rm pl}\sigma)}{m^2 M_{\rm pl}^2} \longrightarrow \frac{U_*(\sigma_*)}{\Lambda} \qquad \text{where} \quad \sigma_* = \sqrt{\Lambda}\sigma \tag{A.10}$$

with U_* being in a universal form involving none of the model parameters in V. Note that this above implies

$$\frac{U'(M_{pl}\sigma)}{m^2 M_{\rm pl}} \to \frac{U'_*(\sigma_*)}{\sqrt{\Lambda}} \qquad \text{with} \quad U'_*(X) = \frac{\delta U_*(X)}{\delta X}. \tag{A.11}$$

If we further scale x by $x_* = x/\sqrt{\Lambda}$ and assume that A and B are not affected by this scaling, then it is straightforward to see that the terms involving the gradient $\partial_x \sigma$ in (A.5)–(A.6) and (A.9) are suppressed by $1/\Lambda$ factor than the other non-gradient terms in the corresponding equations. Therefore, the gradient terms can be neglected in the large Λ limit. In this case, scalar field equation (A.9) is reduced to the algebraic one

$$(\frac{\Omega^2}{B} - 1)\sigma_* = U'_*(\sigma_*) \,. \tag{A.12}$$

Then we obtain that, (A.5) and (A.6) reduce to

$$\rho = \rho_0 \Big[\frac{1}{2} \sigma_* U'_*(\sigma_*) + U_*(\sigma_*) + \sigma_*^2 \Big] \,, \tag{A.13}$$

$$p = p_\perp = \rho_0 \Big[\frac{1}{2} \sigma_* U'_*(\sigma_*) - U_*(\sigma_*) \Big] \,, \tag{A.14}$$

and the overall energy density scale

$$\rho_0 = \frac{m^2 M_{\rm pl}^2}{\Lambda} \,. \tag{A.15}$$

Then, for specific EoS, we can insert the corresponding potential U_* and find the results listed in the main text.

暗星

Liouville field

$$\frac{m^2}{2\beta^2}\left[e^{\beta^2|\phi|^2}-1\right]$$

$$\frac{\rho}{\rho_\odot} = \mathcal{B}\left(\sigma_*^2 e^{\sigma_*^2}+e^{\sigma_*^2}-1\right),$$
$$\frac{p}{\rho_\odot} = \mathcal{B}\left(\sigma_*^2 e^{\sigma_*^2}-e^{\sigma_*^2}-1\right),$$

cosh-Gordon field

$$\frac{m^2}{\beta^2}\left[\cosh(\beta\sqrt{|\phi|^2})-1\right]$$

$$\frac{\rho}{\rho_\odot} = \mathcal{B}\left(\frac{1}{2}\sigma_*\sinh\sigma_*+\cosh\sigma_*-1\right),$$
$$\frac{p}{\rho_\odot} = \mathcal{B}\left(\frac{1}{2}\sigma_*\sinh\sigma_*-\cosh\sigma_*+1\right).$$

sine-Gordon field

$$\frac{m^2}{\beta^2}\left[1-\cos(\beta\sqrt{|\phi|^2})\right]$$

$$\frac{\rho}{\rho_\odot} = \mathcal{B}\left(\frac{1}{2}\sigma_*\sin\sigma_*-\cos\sigma_*+1\right)$$
$$\frac{p}{\rho_\odot} = \mathcal{B}\left(\frac{1}{2}\sigma_*\sin\sigma_*+\cos\sigma_*-1\right)$$

non-topological soliton stars

$$\frac{1}{2}m^2|\phi|^2(1-\beta^2|\phi|^2)^2$$

$$\frac{\rho}{\rho_\odot} = \mathcal{B}\sigma_*^2(1-\sigma_*^2)(1-2\sigma_*^2),$$
$$\frac{p}{\rho_\odot} = \mathcal{B}\sigma_*^4(\sigma_*^2-1).$$

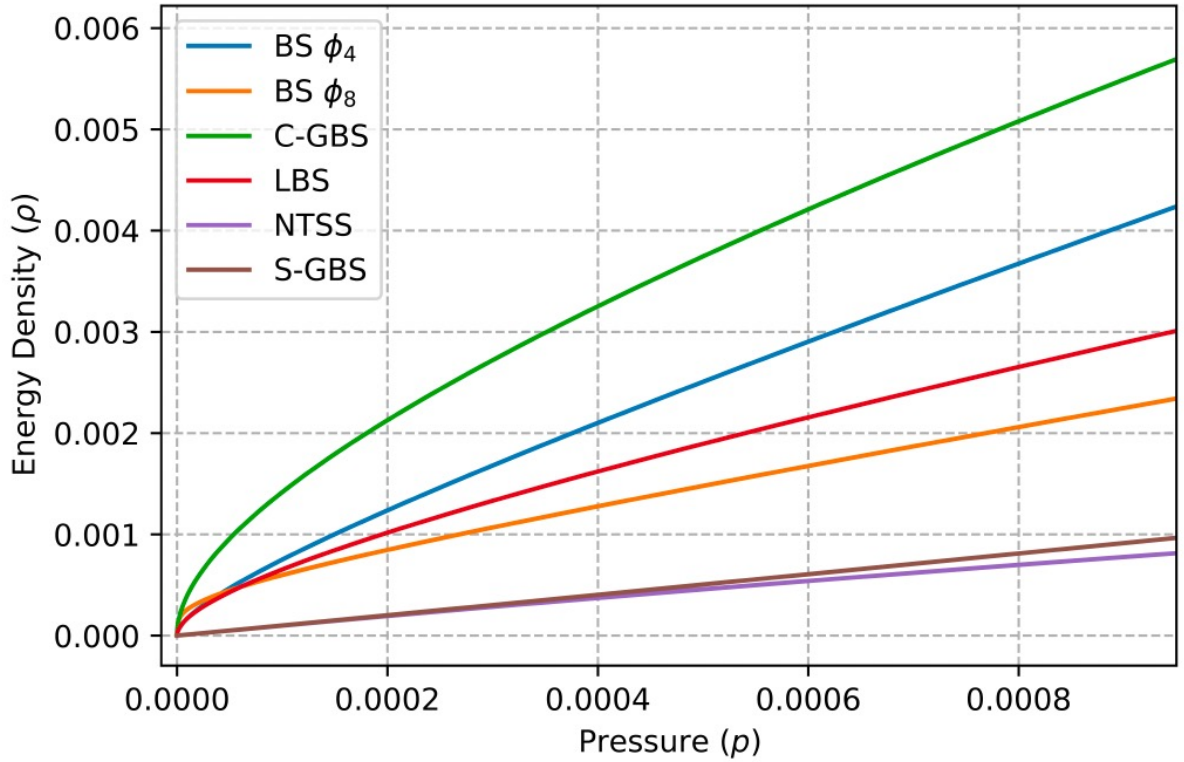

FIG. 1: An illustration of the EoSs discussed above, showing their relative behaviors. The adjusting parameter $\mathcal{B}_n$ and $\mathcal{B}$ are chosen to make the maximal masses of the boson stars have several solar masses. We consider p up to 10^{-3} since the typical range of the corresponding central pressure is between 10^{-6} to 10^{-2} as a reference. Here ρ and p are measured in the unit of $\rho_\odot$.

暗星

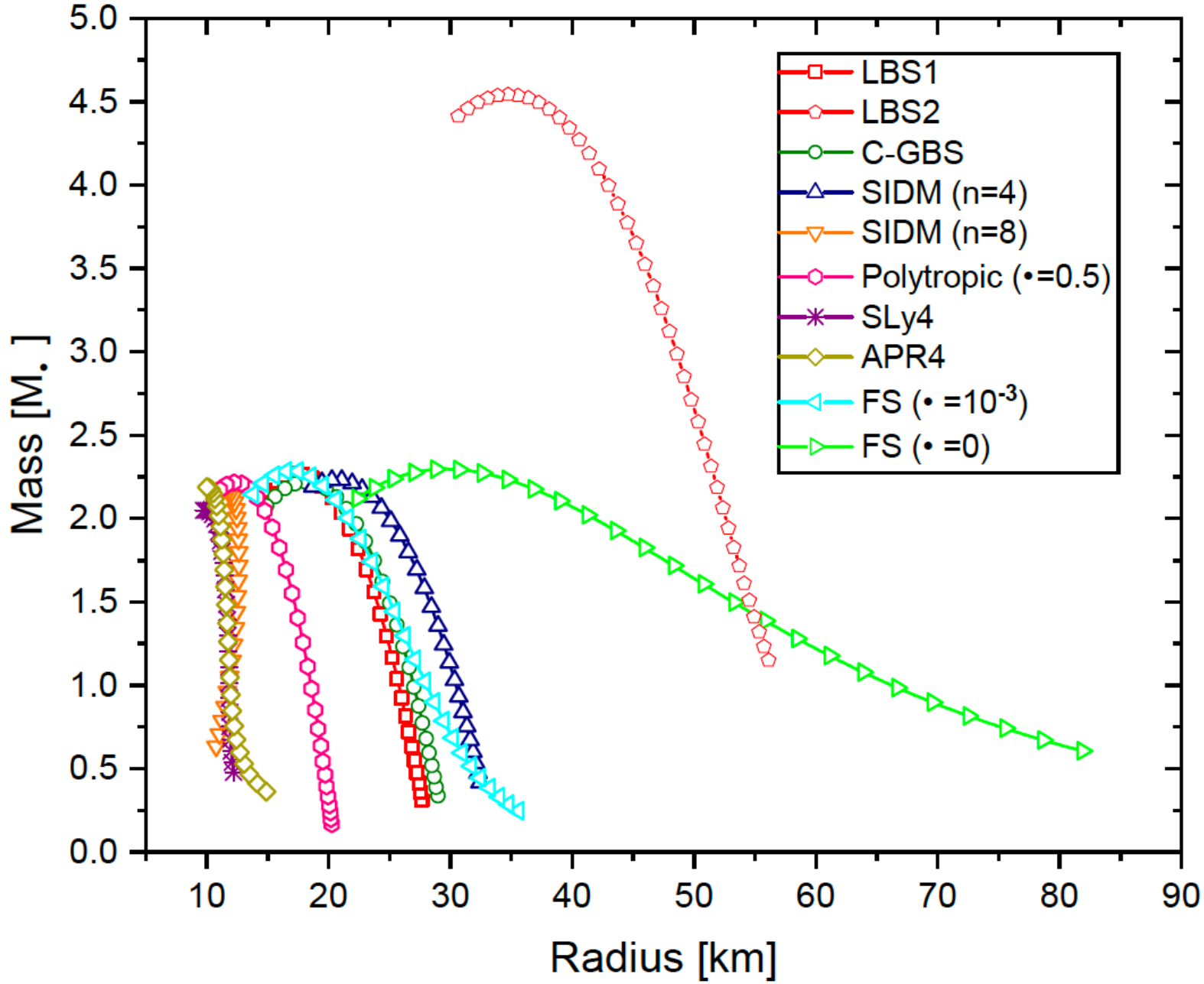
Mass [M.]
Radius [km]
LBS1
LBS2
C-GBS
SIDM (n=4)
SIDM (n=8)
Polytropic (•=0.5)
SLy4
APR4
FS (• =10-3)
FS (• =0)
5.0
4.5
4.0
3.5
3.0
2.5
2.0
1.5
1.0
0.5
0.0
10
20
30
40
50
60
70
80
90

暗星

Scaling Symmetry

The EoS can usually be described by a pair of parameter functions in the form of

$$\frac{\rho}{\rho_\odot} = \mathcal{B}\, f(\sigma_*)\,, \tag{52}$$

$$\frac{p}{\rho_\odot} = \mathcal{B}\, g(\sigma_*)\,, \tag{53}$$

where f and g are some arbitrary functions, and $\mathcal{B}$ is a control parameter. Then we can confirm that, if $\mathcal{B} \to k\mathcal{B}$, then $p \to kp$ is consitent with $\rho \to k\rho$.

And it is easy to check that the TOV condition is invariant under the symmetric transformation:

$$\rho \to k\rho\,, \tag{54}$$

$$p \to kp\,, \tag{55}$$

$$m \to \frac{1}{\sqrt{k}} m\,, \tag{56}$$

$$r \to \frac{1}{\sqrt{k}} r\,. \tag{57}$$

That is to say, if we set $\mathcal{B} \to k\mathcal{B}$, then the variables change according to the above, while the "compactness" $C = M/R$ remains the same.

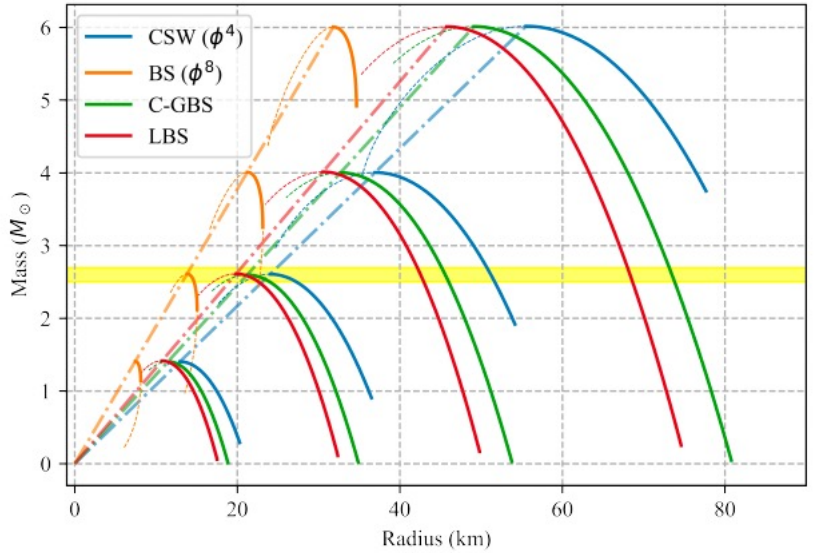

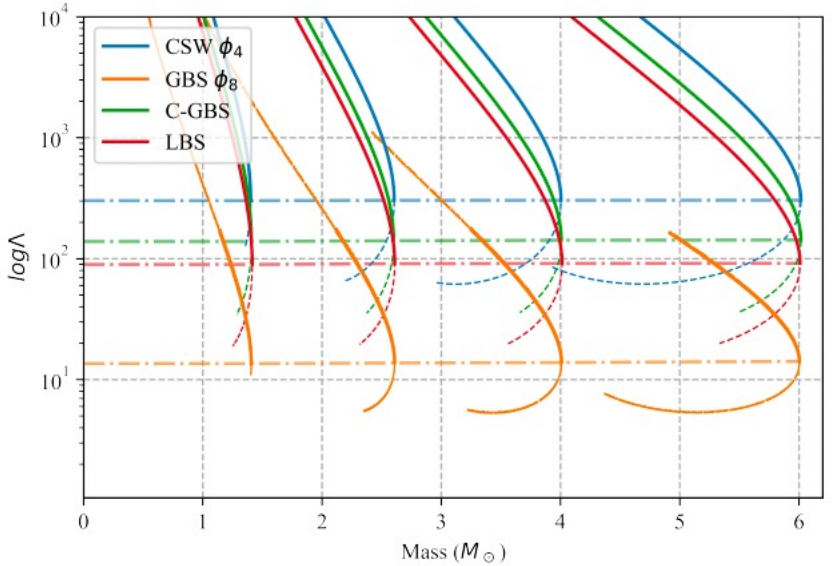

暗星

Scaling Symmetry

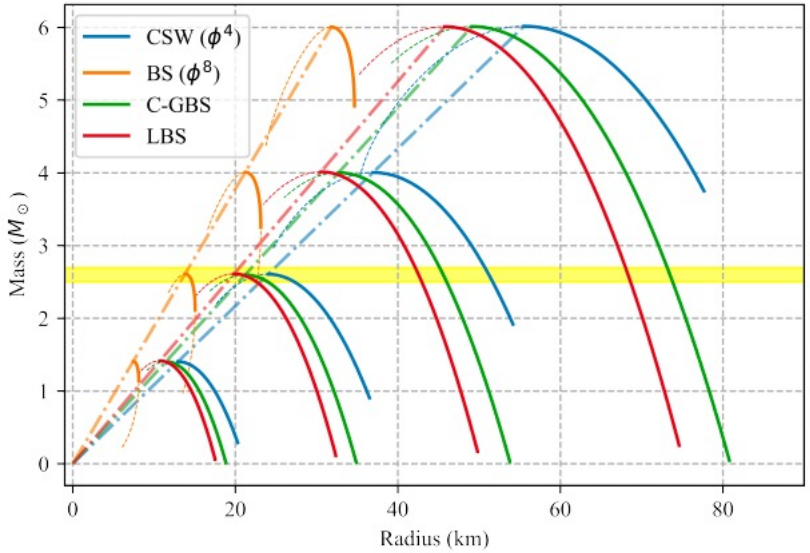

Maselli Andrea, Pnigouras Pantelis, Nielsen Niklas Gronlund, Kouvaris Chris, Kokkotas Kostas D. Dark stars: Gravitational and electromagnetic observables. Phys Rev D 2017;96(2).

暗星

I-Love-Q

Kent Yagi and Nicolas Yunes. I-Love-Q. Science, 341:365–368, 2013.

Kent Yagi and Nicolas Yunes. I-Love-Q Relations in Neutron Stars and their Applications to Astrophysics, Gravitational Waves and Fundamental Physics. Phys. Rev. D, 88(2):023009, 2013.

$$\ln y_i = a_i + b_i \ln x_i + c_i (\ln x_i)^2 + d_i (\ln x_i)^3 + e_i (\ln x_i)^4 .$$

y_i	x_i	a_i	b_i	c_i	d_i	e_i
$\bar{I}$	$\bar{\lambda}^{(\mathrm{tid})}$	1.47	0.0817	0.0149	2.87×10^{-4}	-3.64×10^{-5}
$\bar{I}$	$\bar{Q}$	1.35	0.697	-0.143	9.94×10^{-2}	-1.24×10^{-2}
$\bar{Q}$	$\bar{\lambda}^{(\mathrm{tid})}$	0.194	0.0936	0.0474	-4.21×10^{-3}	1.23×10^{-4}

TABLE I. Estimated numerical coefficients for the fitting formulas of the NS and QS I-Love, I-Q and Love-Q relations.

暗星

I-Love-Q

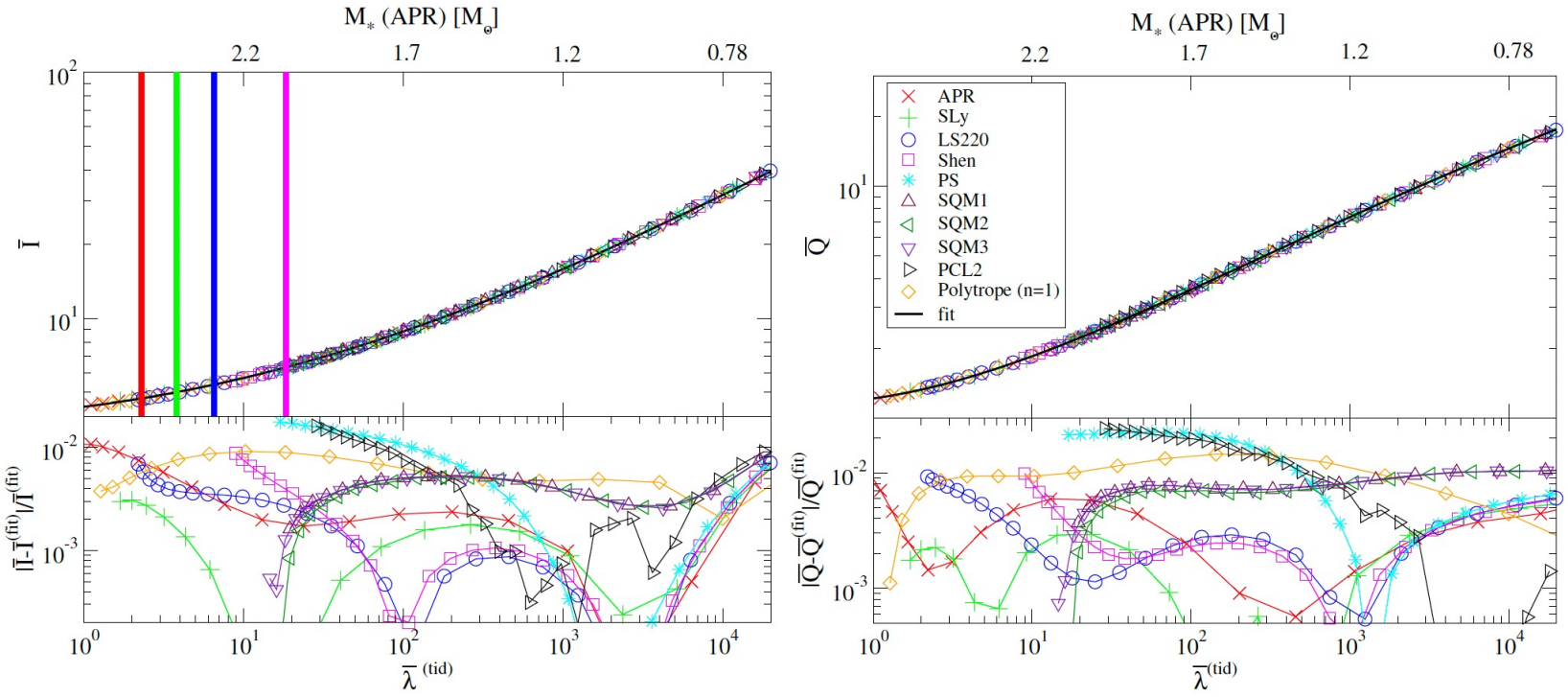

FIG. 1. (Top Left and Right) The neutron star (NS) and quark star (QS) universal I-Love and Love-Q relations for various EoSs, together with fitting curves (solid). On the top axis, we show the corresponding NS mass with an APR EoS. The thick vertical lines show the stability boundary for the APS, SLy, LS220 and Shen EoSs from left to right. The parameter varied along each curve is the NS or QS central density, or equivalently the star's compactness, with the latter increasing to the left of the plots. (Bottom Left and Right) Fractional errors between the fitting curve and numerical results.

暗星

I-Love-Q

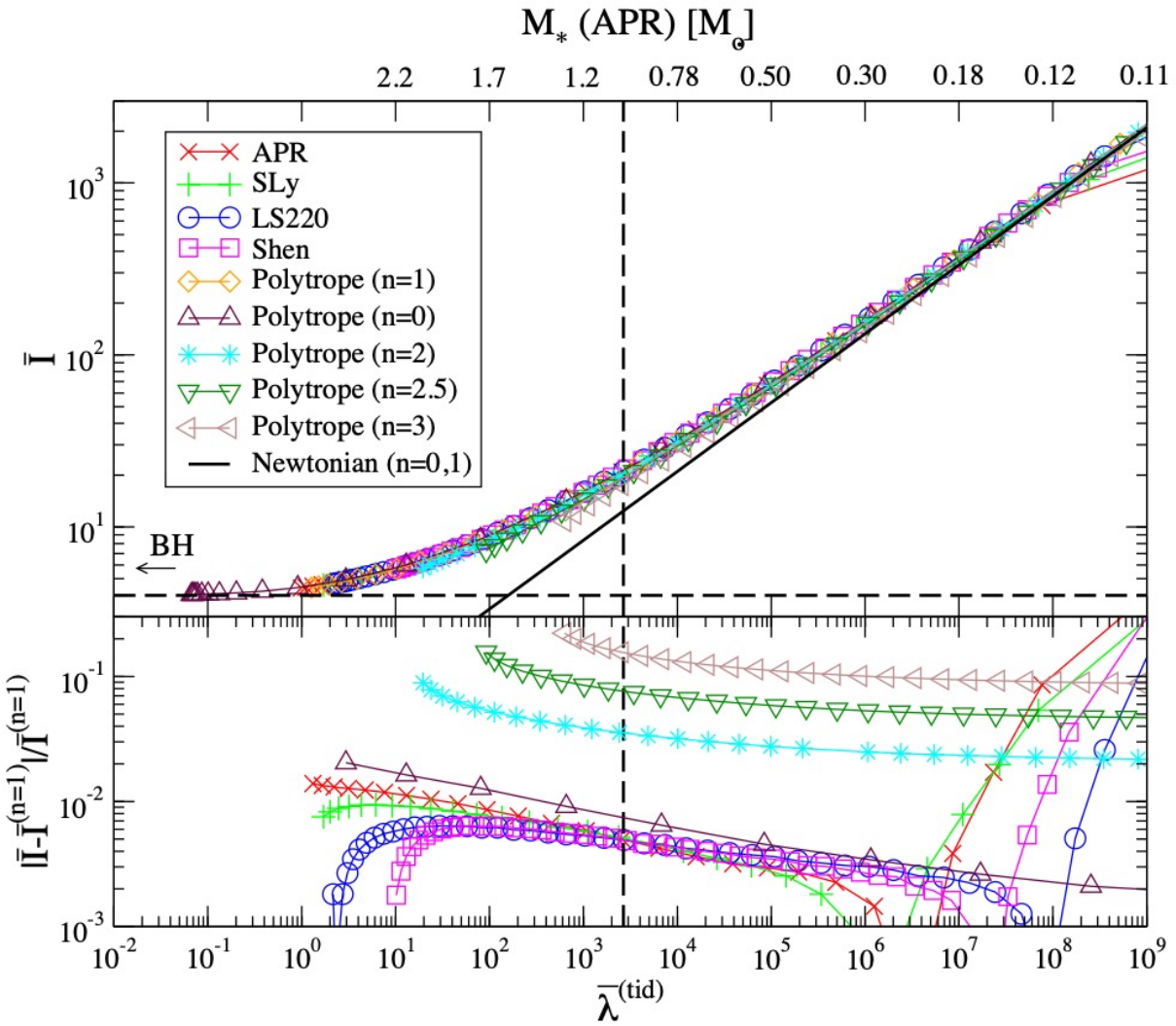

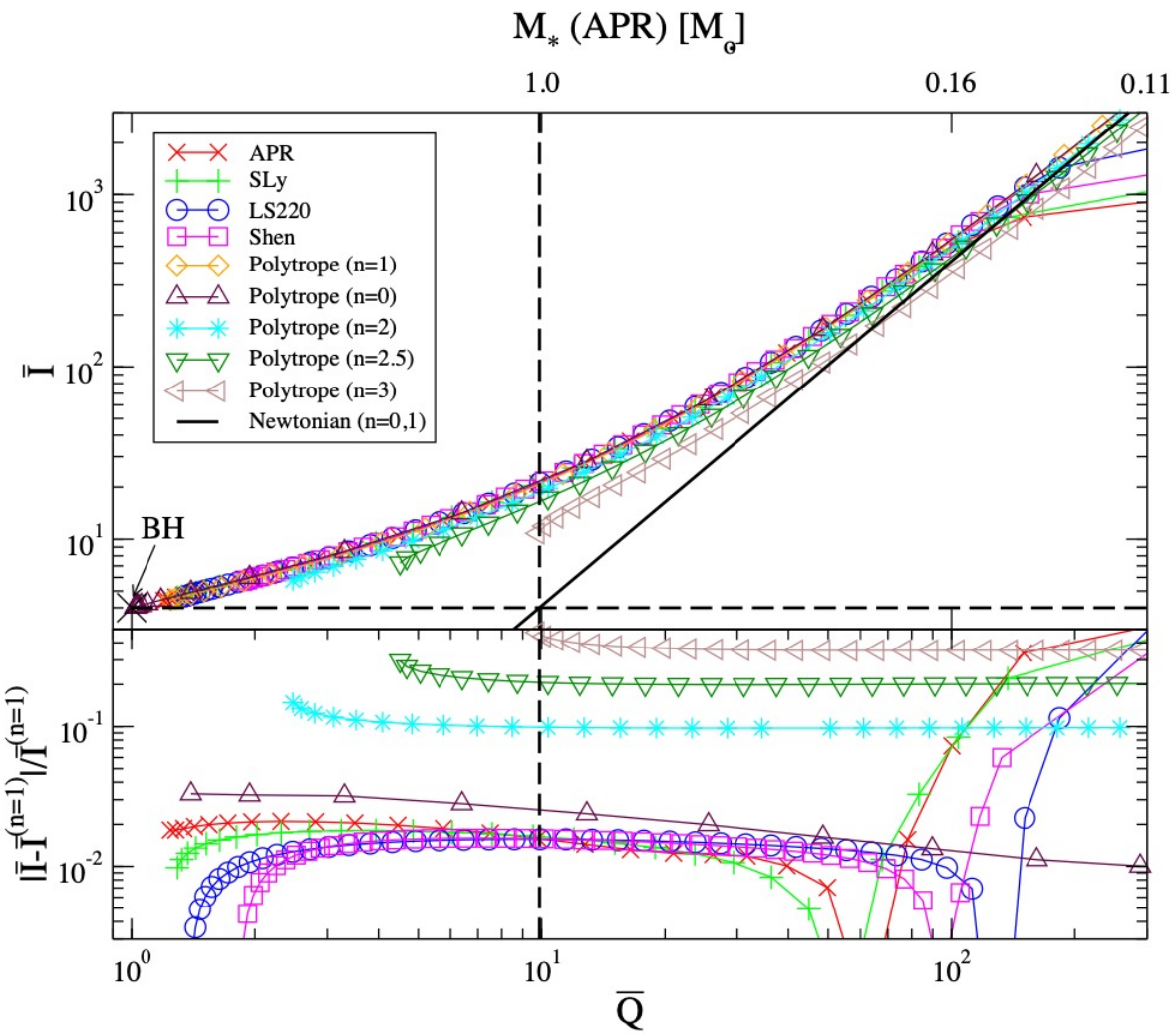

$$p = \kappa\rho^{\gamma} \text{ or } p = \kappa\rho^{1+1/n}$$

暗星

Dark I-Love-Q

Although the I-Love-Q relations have been verified for many continuous EoS [32–38], there is no insurance that any continuous EoS will give the same results. Recently there seems to be an opinion that any smooth EoS (without strong discontinuity) satisfies the universal relation. But as is already pointed out in the original paper [13], that even for a ploytropic EoS with gamma=0.75 (or equivalently n=3 [1]), there is an obvious violation of I-Q relation by 20% while 10% for I-Love and Q-Love relations. Also, deviations will occur when applying some extreme models, and this conclusion is verified in [39, 40]. Therefore, it is worthy and necessary to check whether a new EoS (continuous or not) will obey the I-Love-Q relations.

$$p = \kappa\rho^{\gamma} \text{ or } p = \kappa\rho^{1+1/n}$$

暗星

Dark I-Love-Q

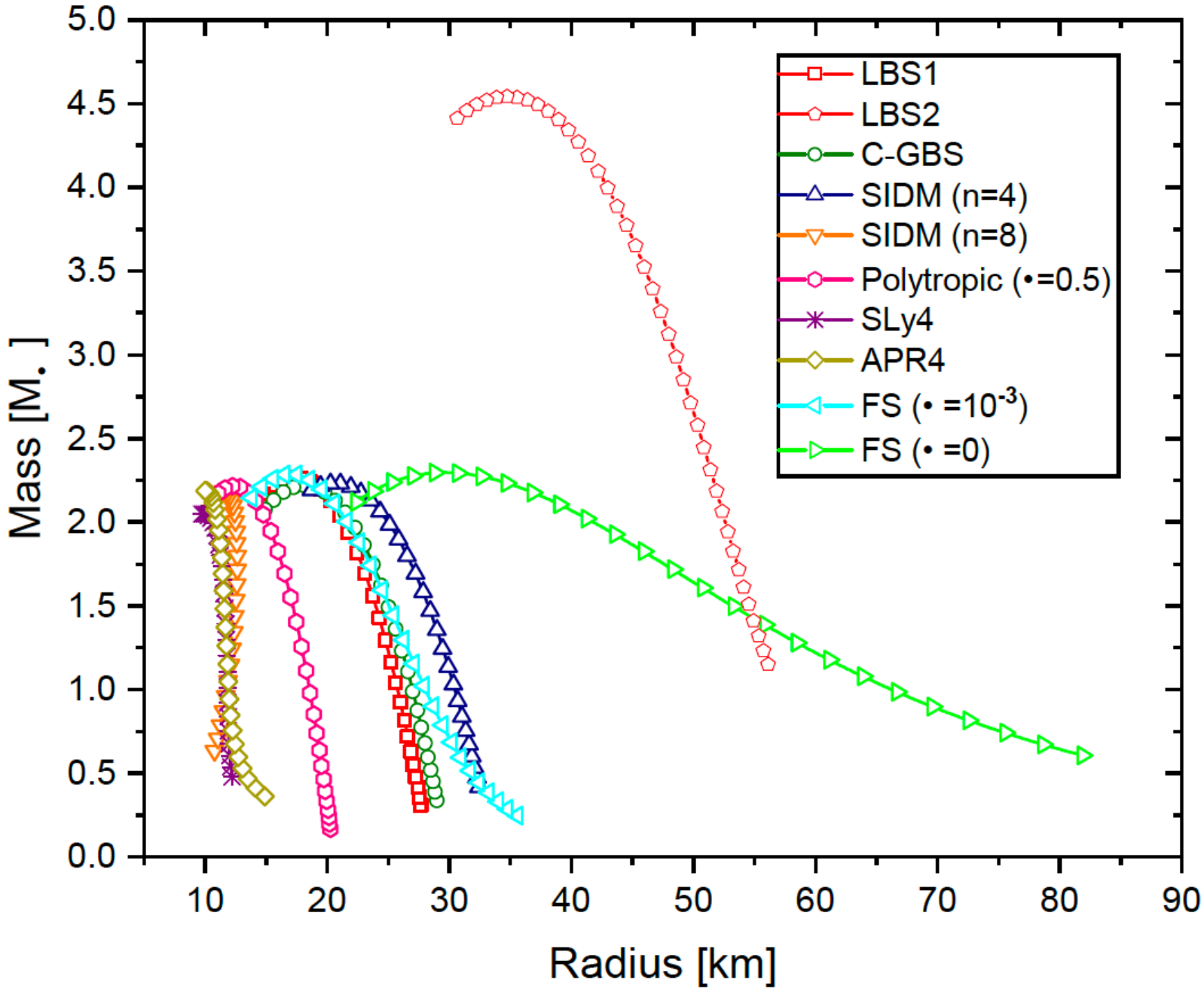

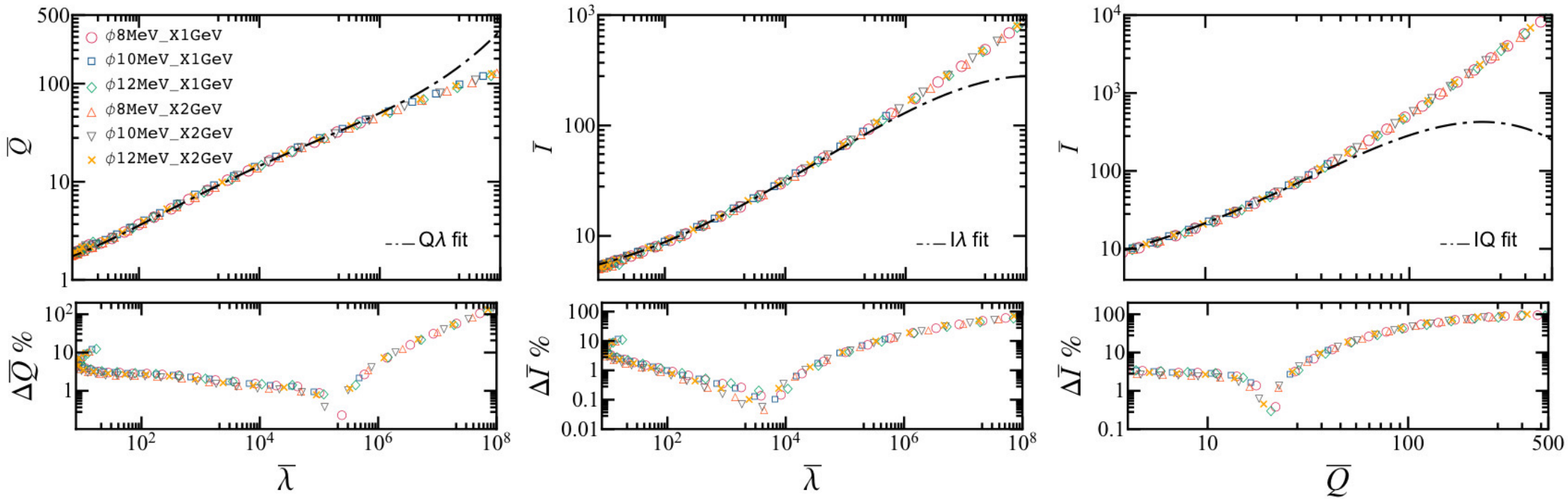

FIG. 6. I-Love-Q relations for fermion stars with a fixed coupling constant $\alpha = 10^{-3}$ and different values for m_ϕ and $m_{\rm X}$. The bottom panels show the relative percentage errors between the numerical data and the universal relation (11) (dashed black curve).

暗星

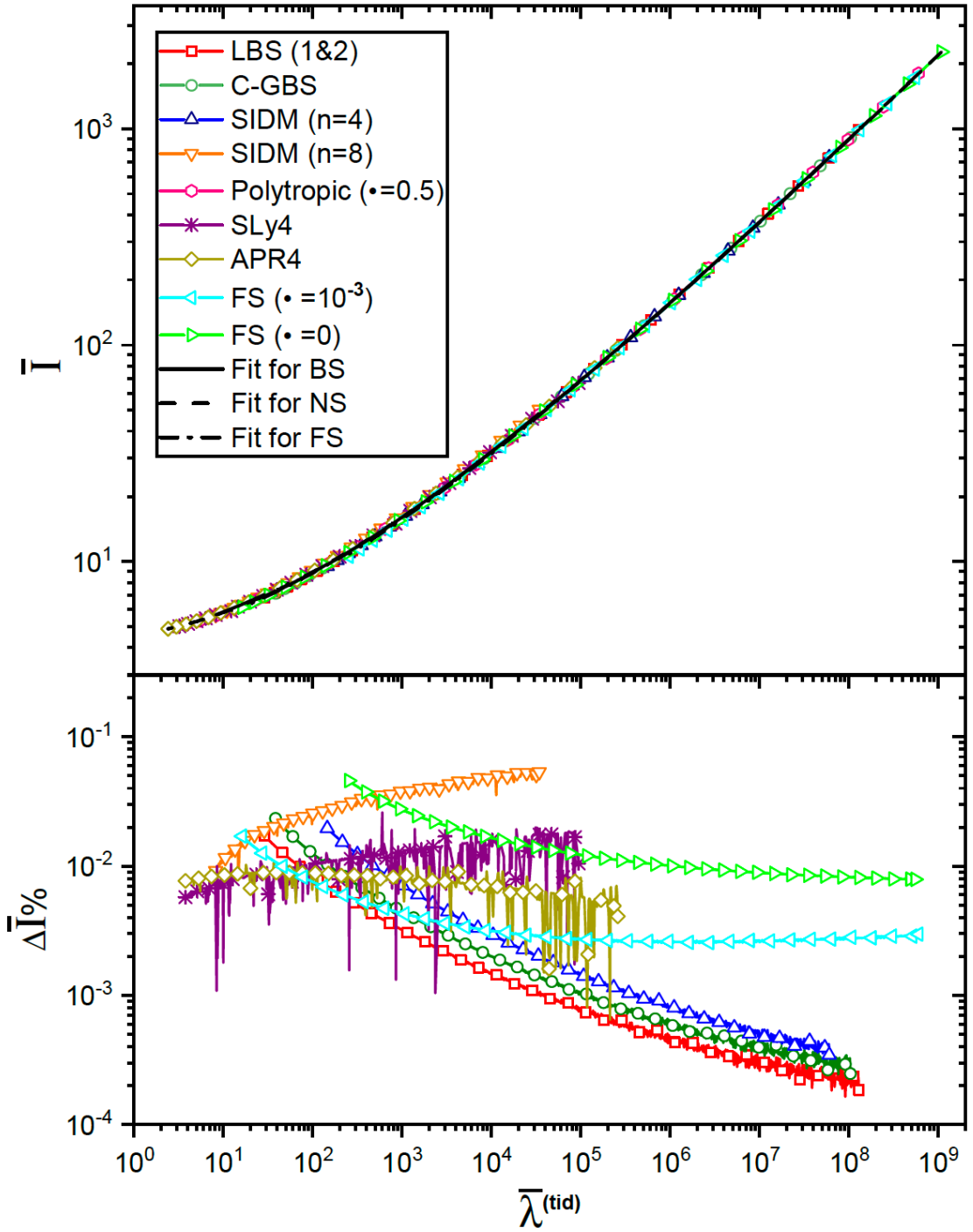
LBS (1&2)
C-GBS
SIDM (n=4)
SIDM (n=8)
Polytropic (•=0.5)
SLy4
APR4
FS (• =10-3)
FS (• =0)
Fit for BS
Fit for NS
Fit for FS
Ī
ΔĪ%
λ̄(tid)

暗星

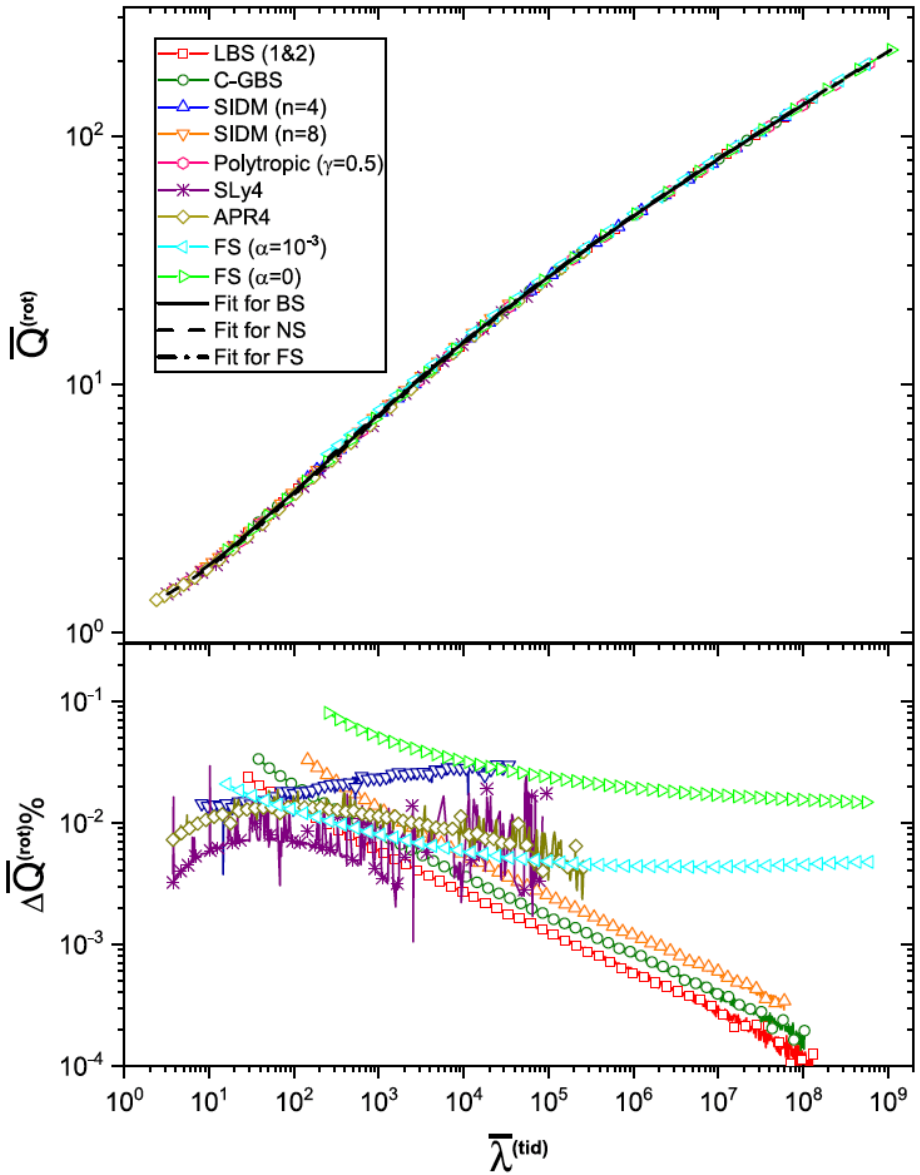

Fig. 3 Top: Q-Love relations of 5 BS models, 2 FS models and 3 NS models. The two LBS curves coincide. The meanings of different lines are the same as those in Fig. 2. Bottom: The relative fractional errors for Q-Love relations whose referenced line is polytropic NS model with index $\gamma = 0.5$

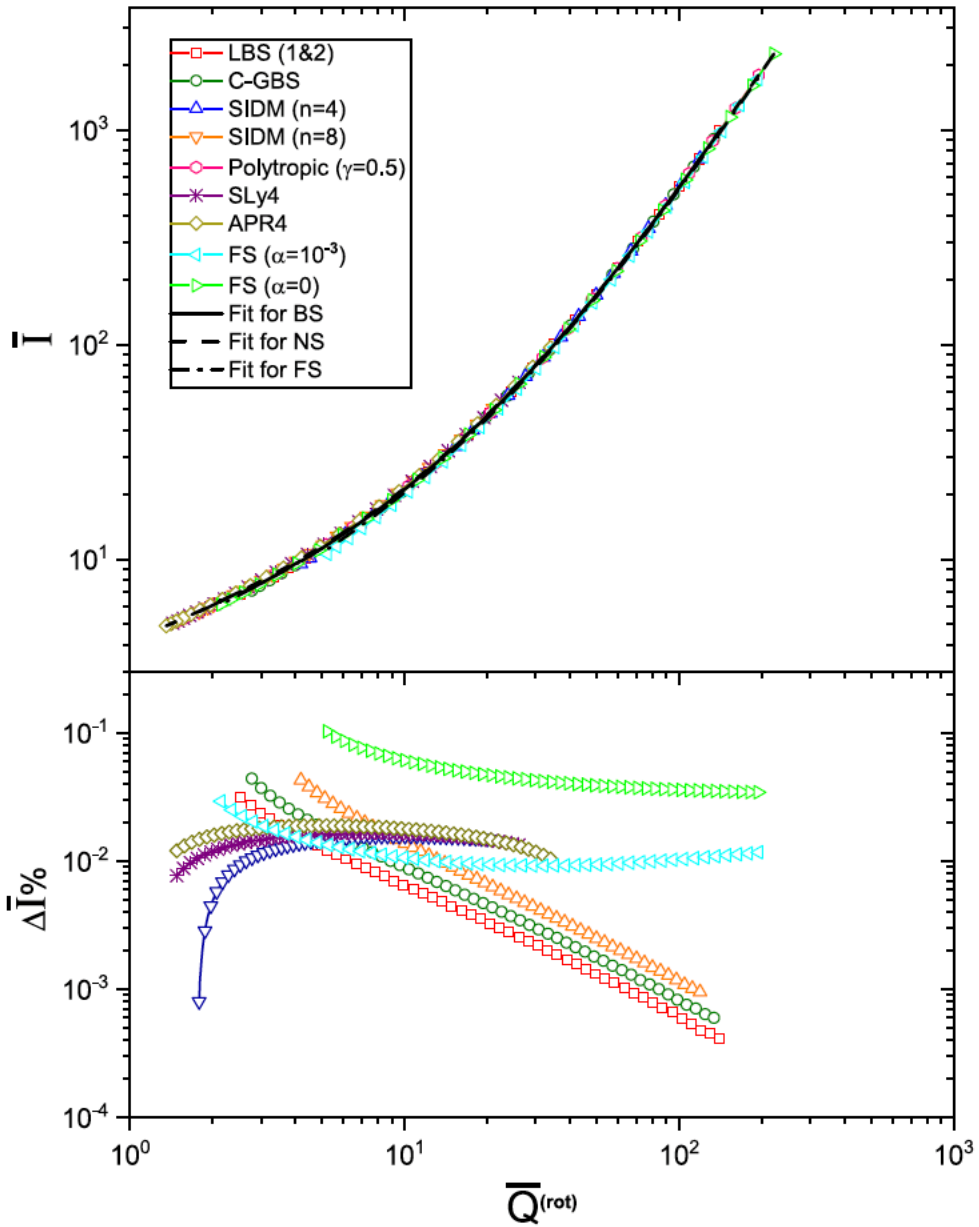

Fig. 4 Top: I-Q relations of 5 BS models, 2 FS models and 3 NS models. The two LBS curves coincide. The meanings of different lines are the same as those in Fig. 2. Bottom: The relative fractional errors for Q-Love relations whose referenced line is polytropic NS model with index $\gamma = 0.5$

夸克星

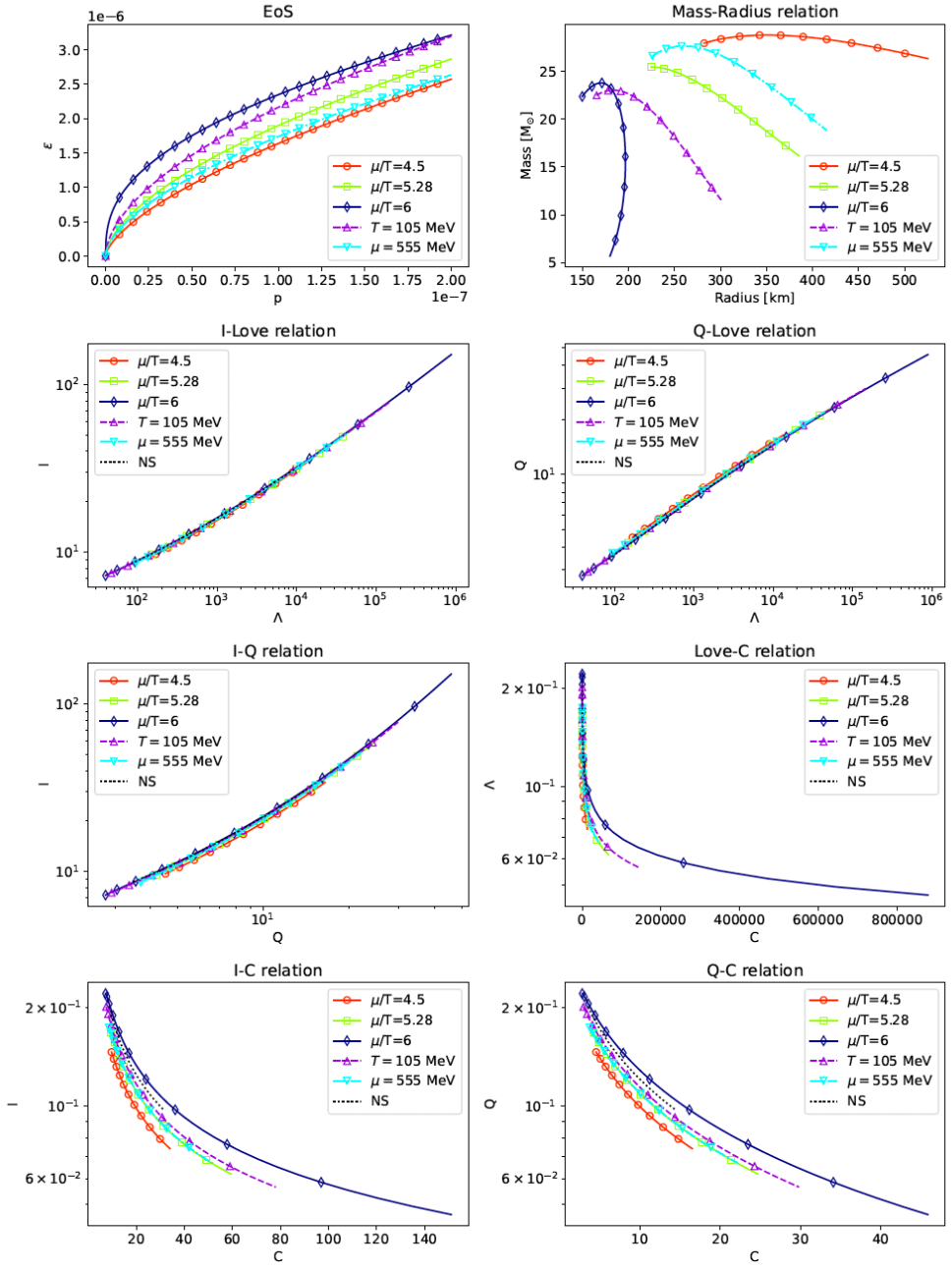

Fig. 4: The EoS, M-R relation and I-Love-Q-C relations for "simple" quark star with different models in eq.(6-10). For reference, the black dotted line representing a polytropic NS $\epsilon = 0.09p^{0.5}$ is plotted in the panels of I-Love-Q-C relations.

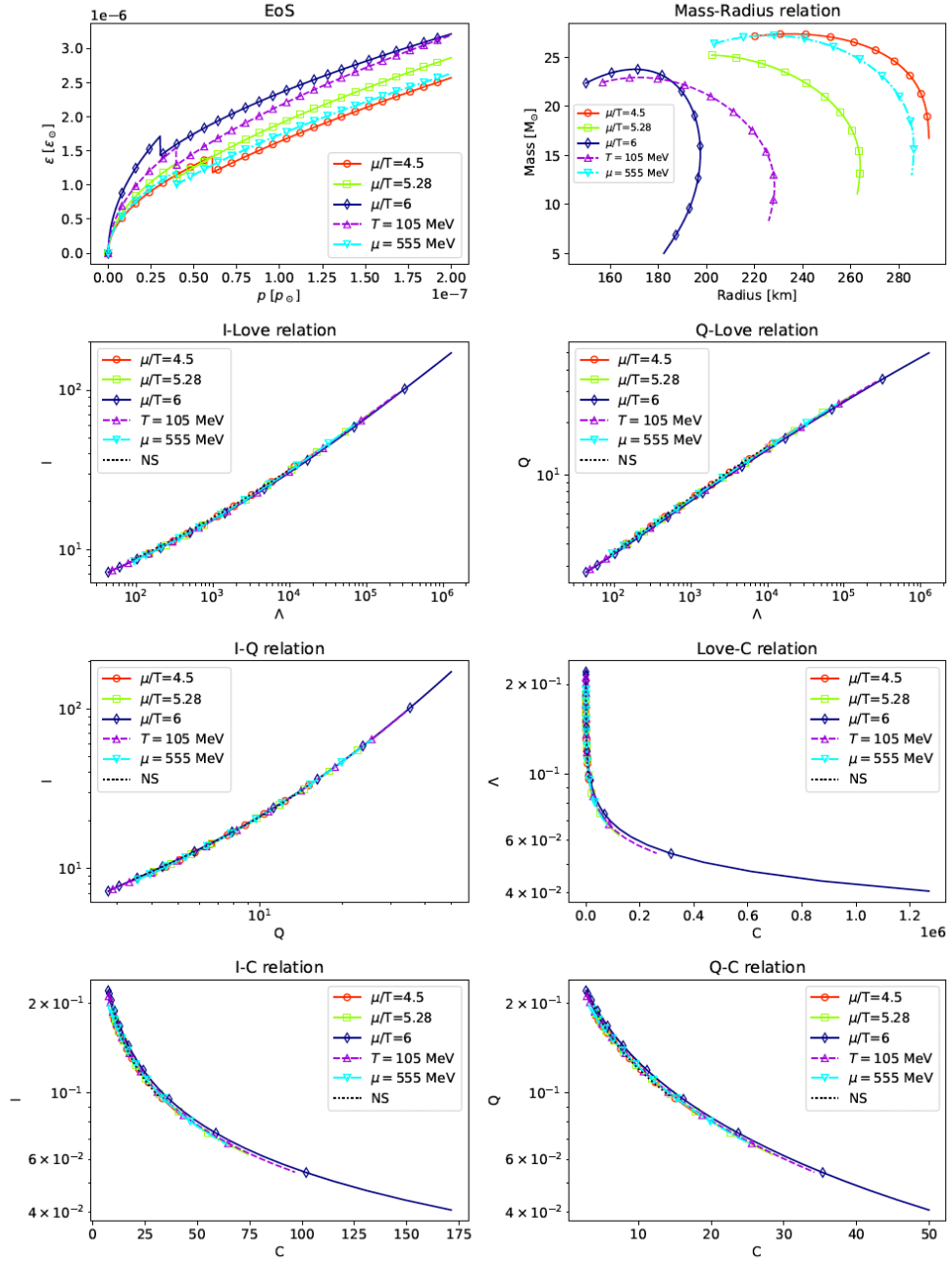

Fig. 6: The EoS, M-R relation and I-Love-Q-C relations of the hybrid stars consist of quark cores and neutron outer layers with $n = 1.2$ in eq.(12). For reference, the black dotted line representing a polytropic NS $\epsilon = 0.09p^{0.5}$ is plotted in the panels of I-Love-Q-C relations.

演示页

Black Holes

黑洞

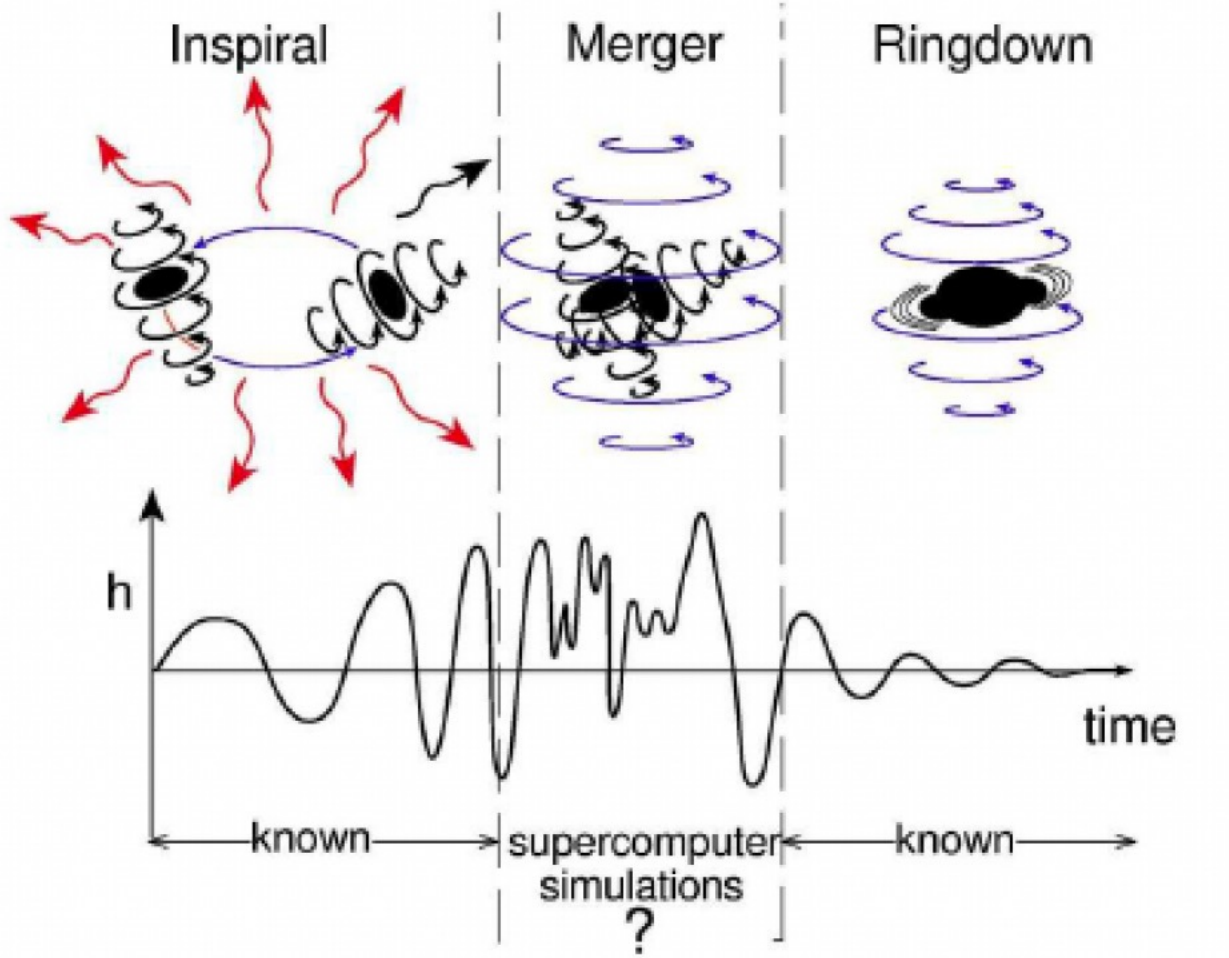

Figure: Credit: Kip Thorne

黑洞

Black Hole Quasinormal Modes and Seiberg-Witten Theory

Gleb Aminov,[a,b] **Alba Grassi**[c,d] **and Yasuyuki Hatsuda**[e]

[a] *Department of Physics and Astronomy, Stony Brook University, Stony Brook, NY 11794, USA*
[b] *ITEP NRC KI, Moscow 117218, Russia*
[c] *Simons Center for Geometry and Physics, SUNY, Stony Brook, NY, 1194-3636, USA*
[d] *Institut für Theoretische Physik, ETH Zürich, CH-8093 Zürich, Switzerland*
[e] *Department of Physics, Rikkyo University, Toshima, Tokyo 171-8501, Japan*

E-mail: gleb.aminov@stonybrook.edu, agrassi@scgp.stonybrook.edu, yhatsuda@rikkyo.ac.jp

Abstract: We present new analytic results on black hole perturbation theory. Our results are based on a novel relation to four-dimensional $\mathcal{N} = 2$ supersymmetric gauge theories. We propose an exact version of Bohr-Sommerfeld quantization conditions on quasinormal mode frequencies in terms of the Nekrasov partition function in a particular phase of the Ω-background. Our quantization conditions also enable us to find exact expressions of eigenvalues of spin-weighted spheroidal harmonics. We test the validity of our conjecture by comparing against known numerical results for Kerr black holes as well as for Schwarzschild black holes. Some extensions are also discussed.

黑洞

SW/QNM correspondence

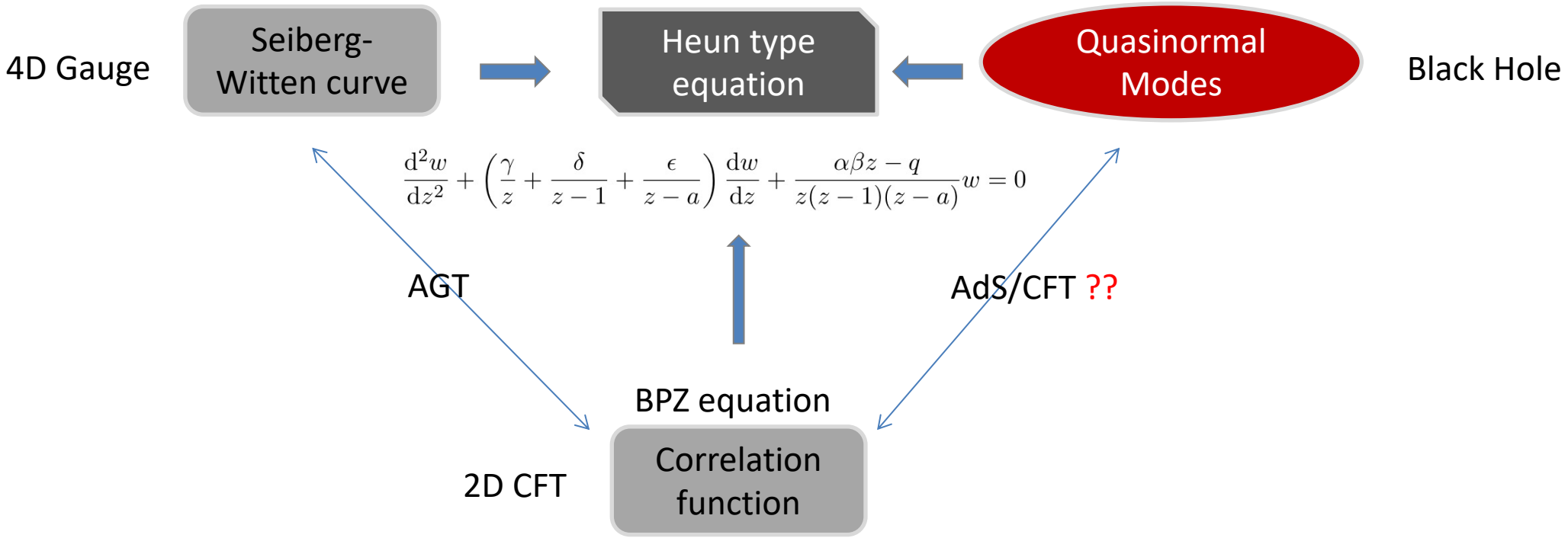

黑洞

from Daniele Gregori

- Schwarschild BH: $SU(2)$ $N_f = 3$
- Kerr BH: $SU(2)$ $N_f = 3$
- Extremal limit Kerr BH: $SU(2)$ $N_f = 2$
- (A)dS Schwarschild BH: $SU(2)$ $N_f = 4$ & $SU(2) \times SU(2)$
- Higher dim. (A)dS BH: $SU(2)^{D-2}$ & $SU(2)^{D-3}$
- D3 brane BH: $SU(2)$ $N_f = 0$

from Daniele Gregori

Schwarzschild BH / $SU(2)$ $N_f = 3$ $\mathcal{N} = 2$ SYM - I

- Schwarzschild metric for **static and spherically symmetric solutions** to the Einstein equation in the vacuum

$$ds^2 = -\left(1 - \frac{2M}{r}\right) dt^2 + \left(1 - \frac{2M}{r}\right)^{-1} dr^2 + r^2(d\theta^2 + \sin^2\theta d\varphi^2) \tag{12}$$

- Scalar ($s = 0$), electromagnetic ($s = 1$) and odd-parity gravitational ($s = 2$) **linear perturbations of the metric** are governed by the **Regge-Wheeler type equation**

$$\left[f(r)\frac{d}{dr}f(r)\frac{d}{dr} + \omega^2 - V(r)\right]\phi(r) = 0\,, \tag{13}$$

$$f(r) = \left(1 - \frac{2M}{r}\right)\,, \qquad V(r) = f(r)\left[\frac{l(l+1)}{r^2} + (1 - s^2)\frac{2M}{r^3}\right]\,, \tag{14}$$

$$\text{boundary conditions} \qquad \phi(r) \sim \begin{cases} e^{-i\omega(r+2M\ln(r-2M))} & r \to 2M \\ e^{+i\omega(r+2M\ln(r-2M))} & r \to \infty \end{cases}\,. \tag{15}$$

Schwarzschild BH / $SU(2)$ $N_f = 3$ $\mathcal{N} = 2$ SYM - II

- By the change of variable [1]

$$r = 2Mz\,, \qquad \phi(r) = \sqrt{\frac{z}{z-1}}\Phi(z)\,, \tag{16}$$

(13) becomes the equation

$$\Phi''(z) + \tilde{Q}(z)\Phi(z) = 0 \qquad \tilde{Q}(z) = \frac{1}{z^2(z-1)^2}\sum_{i=0}^{4}\tilde{A}_i z^i \tag{17}$$

$$\tilde{A}_0 = -s^2 + \frac{1}{4}\,, \quad \tilde{A}_1 = l(l+1) + s^2\,, \quad \tilde{A}_2 = -l(l+1)\,, \quad \tilde{A}_3 = 0\,, \quad \tilde{A}_4 = (2M\omega)^2\,. \tag{18}$$

- Equation (17) has two regular singularities at $z = 0, 1$ and one irregular singularity (of Poincaré rank 1) at $z = \infty$. It corresponds to the **Confluent Heun** equation.

AGH 20'

We refer to appendix A for a definition of these quantities. More precisely the quantum A period is given by

$$\Pi_A^{(N_f)}(E, \mathbf{m}, \Lambda_{N_f}, \hbar) = a(E, \mathbf{m}, \Lambda_{N_f}, \hbar) \tag{2.17}$$

while the quantum period B is

$$\Pi_B^{(N_f)}(E, \mathbf{m}, \Lambda_{N_f}, \hbar) = \partial_a \mathcal{F}^{(N_f)}(a, \mathbf{m}, \Lambda_{N_f}, \hbar)\Big|_{a=a(E,\mathbf{m},\Lambda_{N_f},\hbar)}. \tag{2.18}$$

The very important fact is that we have a combinatorial formula of the Nekrasov partition function [15]. It directly computes the NS free energy exactly in $\hbar$. The quantum mirror map is also exactly related to the NS free energy. As a consequence, the quantum periods can be exactly reconstructed by only the NS free energy. This is a main reason why the geometric/gauge theoretical approach is so powerful in analyzing spectral theory.

According to general expectations coming from the Bethe/gauge correspondence, the discrete part of the spectrum of $\mathrm{H}_{\mathrm{N_f}}$ is captured by the following quantization condition

$$\Pi_I^{(N_f)}(E, \mathbf{m}, \Lambda_{N_f}, \hbar) = \mathcal{N}_I \left(n + \frac{1}{2}\right), \quad I = A, B, \quad n = 0, 1, 2, \ldots, \tag{2.19}$$

黑洞

- Accelerating black holes [Griffiths et.al. '06]

$$ds^2 = \frac{1}{(1-\alpha r\cos\theta)^2}\Big(-f(r)dt^2 + \frac{dr^2}{f(r)} + \frac{r^2 d\theta^2}{P(\theta)} + P(\theta)r^2\sin^2\theta d\phi^2\Big)$$

$$f(r) = (1 - \tfrac{2M}{r} + \tfrac{Q^2}{r^2})(1-\alpha^2 r^2).$$

- $\alpha \to 0$: Reissner-Nordstrom BH, $Q, \alpha \to 0$: Schwarzchild BH.

- BH ODE at radial direction

$$\Big(f(r)\frac{d}{dr}f(r)\frac{d}{dr} + \omega^2 - V(r)\Big)\psi(r) = 0,$$

黑洞

$$V_r = f(r)\left(\frac{\lambda}{r^2} - \frac{f(r)}{3r^2} + \frac{f'(r)}{3r} - \frac{f''}{6}\right)$$

- $\phi(r) = \frac{1}{\sqrt{f(r)}}\tilde{\psi}(r)$:

$$\left(\partial_r^2 + Q_r(r)\right)\tilde{\psi}(r) = 0$$

- Four regular singular points at

$$r_i = \{-\frac{1}{\alpha}, r_-, r_+, \frac{1}{\alpha}\}, \quad r_\pm = M \pm \sqrt{M^2 - Q^2}$$

- Heun equation!

黑洞

- The low energy effective theory of 4D $\mathcal{N} = 2$ SYM can be solved exactly via the Seiberg-Witten theory [Seiberg-Witten '94]

$$H(x, p) = E, \quad \lambda_{\mathrm{SW}} = p dx$$

- One can use the localization to compute the exact partition functions of the gauge theory, where two deformation parameters (ϵ_1, ϵ_2) are turned on [Nekrasov '02].

- In the classical limit ($\epsilon_1 = \epsilon_2 = 0$), one obtains the partition function of SW theory.

- In the Nekrasov-Shatashvili limit ($\epsilon_1 \neq 0, \epsilon_2 = 0$), the SW curve is quantized, where ϵ_1 plays the role of Planck constant ($\hat{p} = \epsilon \partial_x$):

$$\text{Quantum SW curve}: \quad \hat{H}(x, \hat{p})\psi = E\psi \quad \text{[Nekrasov et.al '09]}$$

黑洞

- $SU(2)$ gauge theory with $N_f = 4$ flavor: $\left(\hbar^2\partial_z^2 + Q_{\rm SW}(z)\right)\psi(z) = 0$

  $Q_{\rm SW}(z) = \frac{\frac{1}{4}-a_0^2}{z^2} + \frac{\frac{1}{4}-a_1^2}{(z-1)^2} + \frac{\frac{1}{4}-a_t^2}{(z-t)^2} - \frac{\frac{1}{2}-a_0^2-a_1^2-a_t^2+a_\infty^2+u}{z(z-1)} + \frac{u}{z(z-t)}$.
- Four regular points at $z = (0, 1, t, \infty)$.

- BH data $(r, \omega, M, \cdots) \leftrightarrow$ SW data $(z, t, a_i, \cdots)$

$$r = \frac{1}{\alpha} \leftrightarrow z = 1, \quad r = r_+ \leftrightarrow z = t, \quad t = \frac{2\alpha(r_- - r_+)}{(\alpha r_- - 1)(\alpha r_+ + 1)}, \cdots$$

$$\text{Bdy condition:} \quad \psi(z) \sim \begin{cases} (t-z)^{\frac{1}{2}-a_t} & z \to t \\ (1-z)^{\frac{1}{2}-a_1} & z \to 1 \end{cases}.$$

Need connection formula!

$$\psi^{(t),\rm in} = A\psi_+^{(1)} + B\psi_-^{(1)}, \quad \psi_-^{(1)} \sim (1-z)^{\frac{1}{2}-a_1},$$
$$A(\text{SW data}) = 0 \to A(\omega) = 0.$$

	Connection formula	Numeric data (Destounis et.al '20)
ω_α	$-0.0505984i$	$-0.00506i$
$\omega_{\rm PS}$	$0.11131 - 0.102548i$	$0.1112 - 0.1042i$

Table: $\alpha M = 0.05, Q = 0.3M, \lambda = 0.3317$, # instanton =3

	Connection formula	Numeric data (Destounis et.al '20)
$\omega_{\rm NE}$	$-0.0412141i$	$-0.0412i$
$\omega_{\rm PS}$	$0.11194 - 0.080626i$	$0.117 - 0.0814i$

Table: $\alpha M = 0.3, Q = 0.999M, \lambda = 0.3033$, # instanton =3

超辐射

Seiberg-Witten theory is introduced to solve four dimensional $\mathcal{N}=2$ asymmetric gauge theory by evaluating the singularities and asymptotic behaviors. We leave the details to the references [1, 2], and here focus on SU(2) theory with flavor number $N_f=3$, which is our main concern in this paper. The quantum SW curve in this case can be rewritten in the following form after some reparameterizations:

$$\hbar^2\psi''(z)+\left(\frac{1}{z^2(z-1)^2}\sum_{i=0}^{4}\widehat{A}_i z^i\right)\psi(z)=0, \tag{2.1}$$

which is in the normal form of the so-called confluent Heun equation (A.7) [32]. The coefficients are expressed in gauge parameters by

$$\begin{aligned}
\widehat{A}_0 &= -\frac{(m_1-m_2)^2}{4}+\frac{\hbar^2}{4},\\
\widehat{A}_1 &= -E-m_1m_2-\frac{m_3\Lambda_3}{8}-\frac{\hbar^2}{4},\\
\widehat{A}_2 &= E+\frac{3m_3\Lambda_3}{8}-\frac{\Lambda_3^2}{64}+\frac{\hbar^2}{4},\\
\widehat{A}_3 &= -\frac{m_3\Lambda_3}{4}+\frac{\Lambda_3^2}{32},\\
\widehat{A}_4 &= -\frac{\Lambda_3^2}{64},
\end{aligned} \tag{2.2}$$

For a massive scalar boson field ψ around a BH, it obeys the wave equation

$$\nabla^a \nabla_a \psi = \mu^2 \psi \,, \tag{3.1}$$

with $\mu = \mathcal{M}G/\hbar c$ for a particle of mass $\mathcal{M}$. Equation (3.1) is also separable in the Kerr geometry. When we assume

$$\psi = e^{-i\omega t + im\phi} S(\theta) R(r), \tag{3.2}$$

the separate equations are similar as before. For the angular part, we obtain:

$$\frac{1}{\sin\theta}\frac{d}{d\theta}\left[\sin\theta \frac{dS}{d\theta}\right] + \left[\alpha^2(\omega^2 - \mu^2)\cos^2\theta - \frac{m^2}{\sin^2\theta} + {}_sA_{\ell m}\right] S = 0 \,, \tag{3.3}$$

and for the radial part:

$$\Delta \frac{d}{dr}\left[\Delta \frac{dR}{dr}\right] + \left[\omega^2(r^2+\alpha^2)^2 - 4aMrm\omega + \alpha^2 m^2 - \Delta(\mu^2 r^2 + \alpha^2\omega^2 + {}_sA_{\ell m})\right] R = 0 \,. \tag{3.4}$$

Or equivalently

$$\Delta(r)R''(r) + \Delta'(r)R'(r) + \left(V_T(r) - \mu^2 r^2\right) R(r)|_{s=0} = 0, \tag{3.5}$$

where we set the spin $s = 0$ because we focus only on the scalar field here. The

Comparing the potential of the wave equation in the gauge theory side, we obtain the dictionary for the massive scalar field. For the radial part, we find

$$\begin{aligned}
\Lambda_3 &= -16\mathrm{i}\sqrt{\omega^2-\mu^2}\sqrt{M^2-\alpha^2}, \\
E &= -{}_0A_{\ell m} - (2M^2-\alpha^2)\mu^2 + (8M^2-\alpha^2)\omega^2 - \frac{1}{4}, \\
m_1 &= -2\mathrm{i}M\omega, \qquad m_3 = -\frac{\mathrm{i}M(2\omega^2-\mu^2)}{\sqrt{\omega^2-\mu^2}}, \\
m_2 &= \frac{\mathrm{i}(-2M^2\omega+\alpha m)}{\sqrt{M^2-\alpha^2}}.
\end{aligned} \tag{3.7}$$

For the angular part, we have the same dictionary as the case of the massless scalar field (2.20) with $c = \alpha\sqrt{\omega^2-\mu^2}$. As in the previous section, the angular eigenvalue ${}_0A_{\ell m}$ can be expanded in c as

$${}_0A_{\ell m} = \ell(\ell+1) + \sum_{k=1}^{\infty} f_k c^{2k}, \tag{3.8}$$

and we employ up to the c^6 order in our numerical calculations. Note that if we take $\mu = 0$, the dictionary straightforwardly reduces to the identifications in the massless scalar case.

To compute the complex eigenfrequencies for the radial part of Teukolsky equation, we need to impose the boundary conditions at the horizon and spatial infinity. In general, we obtain the following asymptotic behaviors of the field at the horizon and spatial infinity:

$$R(r \to r_+) \sim (r - r_+)^{\pm i\sigma}, \tag{4.1}$$

$$R(r \to \infty) \sim r^{-1} r^{M(\mu^2 - 2\omega^2)/q} e^{qr}, \tag{4.2}$$

where

$$\sigma = \frac{2Mr_+\omega - \alpha m}{r_+ - r_-}, \quad q = \pm\sqrt{\mu^2 - \omega^2}. \tag{4.3}$$

The sign of the exponent in (4.1) corresponds to an outgoing and ingoing wave near the horizon. Also, the sign of the real part of q in (4.2) determines the asymptotic

In terms of the field $y(z)$ solving the radial equation in Schrödinger form, the above boundary conditions are rewritten as

$$y(z \to 1) \sim (z-1)^{\frac{1}{2} \pm i\sigma}, \tag{4.4}$$

$$y(z \to \infty) \sim (\Lambda_3 z)^{\mp m_3} \, e^{\mp \frac{\Lambda_3 z}{8}}. \tag{4.5}$$

Note that the asymptotic behavior at spatial infinity is written in terms of the quantities in the gauge theory. According to the connection formula [17], asymptotic expansions at different boundaries are related each other due to crossing symmetry. Now if we impose the ingoing wave boundary condition at the horizon, $y(z \to 1) \sim (z-1)^{\frac{1}{2} - i\sigma}$, and use the connection formula studied in [13], we can derive the asymptotic behavior at spatial infinity as

$$y(z \to \infty) \sim C_1(\Lambda_3, a, \mathbf{m}) \, (\Lambda_3 z)^{+m_3} \, e^{+\frac{\Lambda_3 z}{8}} + C_2(\Lambda_3, a, \mathbf{m}) \, (\Lambda_3 z)^{-m_3} \, e^{-\frac{\Lambda_3 z}{8}}, \tag{4.6}$$

which is written as the linear combination of the asymptotic behaviors in (4.5).

The full SU(2) Nekrasov-Shatashvili free energy $\mathcal{F}^{(N_f)}(a;\mathbf{m};\Lambda_{N_f},\hbar)$ [11] has contributions from its classical, one-loop and instanton components, with this relation given explicitly as [8]

$$\begin{aligned}\partial_a\mathcal{F}^{(N_f)}(a;\mathbf{m};\Lambda_{N_f},\hbar) &= -2\,a(4-N_f)\log\left[\frac{\Lambda_{N_f}2^{-\frac{1}{(2-N_f/2)}}}{\hbar}\right]-\pi\hbar\\ &-2\,\mathrm{i}\,\hbar\log\left[\frac{\Gamma(1+\frac{2\mathrm{i}a}{\hbar})}{\Gamma(1-\frac{2\mathrm{i}a}{\hbar})}\right]-\mathrm{i}\,\hbar\sum_{j=1}^{N_f}\log\left[\frac{\Gamma(\frac{1}{2}+\frac{m_j-\mathrm{i}a}{\hbar})}{\Gamma(\frac{1}{2}+\frac{m_j+\mathrm{i}a}{\hbar})}\right]+\frac{\partial\mathcal{F}^{(N_f)}_{\mathrm{inst}}(a;\mathbf{m};\Lambda_{N_f},\hbar)}{\partial a}.\end{aligned}\tag{4.9}$$

The SU(2) instanton part $\mathcal{F}^{(N_f)}_{\mathrm{inst}}(a;\mathbf{m};\Lambda_{N_f},\hbar)$ can be obtained by removing the U(1) contribution in the U(2) instanton part $F^{(N_f)}_{\mathrm{inst}}(a;\mathbf{m};\Lambda_{N_f},\hbar)$, which is defined by

$$F^{(N_f)}_{\mathrm{inst}}(a;\mathbf{m};\Lambda_{N_f},\hbar)=-\hbar\lim_{\epsilon_2\to0}\epsilon_2\log Z^{(N_f)}(\mathrm{i}a,\mathbf{m},\hbar,\epsilon_2).\tag{4.10}$$

The Nekrasov partition function $Z^{(N_f)}(\mathrm{i}a,\mathbf{m},\epsilon_1,\epsilon_2)$ is exact in ϵ_i, and can be written explicitly in terms of Λ_{N_f} instanton expansion [16], as a convergent series.

边界条件

B Quantization condition for quasi-bound states

Following [14] we derive the quantization condition for the calculations of quasi-bound state frequencies. By imposing the ingoing boundary condition at the horizon, the field $y(z)$ for the radial part is written as

$$y(z\to\infty)\sim C_1(\Lambda,a,\mathbf{m})\,(\Lambda z)^{+m_3}\,e^{+\frac{\Lambda z}{2}}+C_2(\Lambda,a,\mathbf{m})\,(\Lambda z)^{-m_3}\,e^{-\frac{\Lambda z}{2}}, \tag{B.1}$$

where we follow the convention in [14] and Λ relates to our convention via $\Lambda=\Lambda_3/4$. Additionally, we have to change $a\to -ia$ to match our convention, which gives a different U(1) factor and a sign difference in the definition of the free energy $\mathcal{F}$. The coefficients $C_{1,2}$ are explicitly given by

$$\begin{aligned}C_1(\Lambda,a,\mathbf{m}) &= \Lambda^a M_{\alpha_{2+},\alpha_+}\mathcal{A}_{\alpha_+ m_{0+}}\frac{\langle\Delta_{\alpha+},\Lambda_0,m_{0+}|V_{\alpha_2}(1)|\Delta_{\alpha_1}\rangle}{\langle\Delta_{\alpha},\Lambda_0,m_0|V_{\alpha_{2+}}(1)|\Delta_{\alpha_1}\rangle}\\ &\quad+\Lambda^{-a}M_{\alpha_{2+},\alpha_-}\mathcal{A}_{\alpha_- m_{0+}}\frac{\langle\Delta_{\alpha-},\Lambda_0,m_{0+}|V_{\alpha_2}(1)|\Delta_{\alpha_1}\rangle}{\langle\Delta_{\alpha},\Lambda_0,m_0|V_{\alpha_{2+}}(1)|\Delta_{\alpha_1}\rangle},\end{aligned} \tag{B.2}$$

$$\begin{aligned}C_2(\Lambda,a,\mathbf{m}) &= \Lambda^a M_{\alpha_{2+},\alpha_+}\mathcal{A}_{\alpha_+ m_{0-}}\frac{\langle\Delta_{\alpha+},\Lambda_0,m_{0-}|V_{\alpha_2}(1)|\Delta_{\alpha_1}\rangle}{\langle\Delta_{\alpha},\Lambda_0,m_0|V_{\alpha_{2+}}(1)|\Delta_{\alpha_1}\rangle}\\ &\quad+\Lambda^{-a}M_{\alpha_{2+},\alpha_-}\mathcal{A}_{\alpha_- m_{0-}}\frac{\langle\Delta_{\alpha-},\Lambda_0,m_{0-}|V_{\alpha_2}(1)|\Delta_{\alpha_1}\rangle}{\langle\Delta_{\alpha},\Lambda_0,m_0|V_{\alpha_{2+}}(1)|\Delta_{\alpha_1}\rangle}.\end{aligned} \tag{B.3}$$

Here, we omit to write down the definitions of each factor because we use the same convention as in [14]. The condition of $C_1=0$ reads

$$1+\Lambda^{-2a}\frac{M_{\alpha_{2+},\alpha_-}\mathcal{A}_{\alpha_- m_{0+}}\,\langle\Delta_{\alpha-},\Lambda_0,m_{0+}|V_{\alpha_2}(1)|\Delta_{\alpha_1}\rangle}{M_{\alpha_{2+},\alpha_+}\mathcal{A}_{\alpha_+ m_{0+}}\,\langle\Delta_{\alpha+},\Lambda_0,m_{0+}|V_{\alpha_2}(1)|\Delta_{\alpha_1}\rangle}=0. \tag{B.4}$$

In the Nekrasov-Shatashvili limit,

$$\begin{aligned}&\frac{\langle\Delta_{\alpha-},\Lambda_0,m_{0+}|V_{\alpha_2}(1)|\Delta_{\alpha_1}\rangle}{\langle\Delta_{\alpha+},\Lambda_0,m_{0+}|V_{\alpha_2}(1)|\Delta_{\alpha_1}\rangle}=\frac{Z^{(3)}\left(\Lambda,a+\frac{\epsilon_2}{2},m_1,m_2,m_3+\frac{\epsilon_2}{2}\right)}{Z^{(3)}\left(\Lambda,a-\frac{\epsilon_2}{2},m_1,m_2,m_3+\frac{\epsilon_2}{2}\right)}\\ &=\exp\frac{1}{\epsilon_1\epsilon_2}\left[\mathcal{F}^{(3)}_{\text{inst}}\left(\Lambda,a+\frac{\epsilon_2}{2},m_1,m_2,m_3+\frac{\epsilon_2}{2}\right)-\mathcal{F}^{(3)}_{\text{inst}}\left(\Lambda,a-\frac{\epsilon_2}{2},m_1,m_2,m_3+\frac{\epsilon_2}{2}\right)\right]\\ &\to\exp\frac{\partial_a\mathcal{F}^{(3)}_{\text{inst}}(\Lambda,a,m_1,m_2,m_3)}{\epsilon_1},\end{aligned} \tag{B.5}$$

边界条件

and

$$\begin{aligned}\frac{M_{\alpha_{2+},\alpha_-}\mathcal{A}_{\alpha_- m_{0+}}}{M_{\alpha_{2+},\alpha_+}\mathcal{A}_{\alpha_+ m_{0+}}} &= \frac{\Gamma\left(\frac{2a}{\epsilon_1}\right)\Gamma\left(1+\frac{2a}{\epsilon_1}\right)\Gamma\left(\frac{1}{2}+\frac{a_2+a_1-a}{\epsilon_1}\right)\Gamma\left(\frac{1}{2}+\frac{a_2-a_1-a}{\epsilon_1}\right)\Gamma\left(\frac{1}{2}+\frac{m_3-a}{\epsilon_1}\right)}{\Gamma\left(-\frac{2a}{\epsilon_1}\right)\Gamma\left(1-\frac{2a}{\epsilon_1}\right)\Gamma\left(\frac{1}{2}+\frac{a_2+a_1+a}{\epsilon_1}\right)\Gamma\left(\frac{1}{2}+\frac{a_2-a_1+a}{\epsilon_1}\right)\Gamma\left(\frac{1}{2}+\frac{m_3+a}{\epsilon_1}\right)} \\ &= \frac{\Gamma\left(\frac{2a}{\epsilon_1}\right)\Gamma\left(1+\frac{2a}{\epsilon_1}\right)}{\Gamma\left(-\frac{2a}{\epsilon_1}\right)\Gamma\left(1-\frac{2a}{\epsilon_1}\right)}\prod_{i=1}^{3}\frac{\Gamma\left(\frac{1}{2}+\frac{m_i-a}{\epsilon_1}\right)}{\Gamma\left(\frac{1}{2}+\frac{m_i+a}{\epsilon_1}\right)} \\ &= e^{-i\pi}\left(\frac{\Gamma\left(1+\frac{2a}{\epsilon_1}\right)}{\Gamma\left(1-\frac{2a}{\epsilon_1}\right)}\right)^2\prod_{i=1}^{3}\frac{\Gamma\left(\frac{1}{2}+\frac{m_i-a}{\epsilon_1}\right)}{\Gamma\left(\frac{1}{2}+\frac{m_i+a}{\epsilon_1}\right)} \\ &= \exp\left[-i\pi+2\log\frac{\Gamma\left(1+\frac{2a}{\epsilon_1}\right)}{\Gamma\left(1-\frac{2a}{\epsilon_1}\right)}+\sum_{i=1}^{3}\log\frac{\Gamma\left(\frac{1}{2}+\frac{m_i-a}{\epsilon_1}\right)}{\Gamma\left(\frac{1}{2}+\frac{m_i+a}{\epsilon_1}\right)}\right], \end{aligned} \tag{B.6}$$

where we use the relations of parameters between CFT and gauge theory

$$m_1 = a_1 + a_2, \quad m_2 = -a_1 + a_2. \tag{B.7}$$

Setting $\epsilon_1 = 1$, the second term of (B.4) becomes

$$\begin{aligned}\exp\left[-2a\log\Lambda - i\pi + 2\log\frac{\Gamma\left(1+\frac{2a}{\epsilon_1}\right)}{\Gamma\left(1-\frac{2a}{\epsilon_1}\right)}+\sum_{i=1}^{3}\log\frac{\Gamma\left(\frac{1}{2}+\frac{m_i-a}{\epsilon_1}\right)}{\Gamma\left(\frac{1}{2}+\frac{m_i+a}{\epsilon_1}\right)}+\partial_a\mathcal{F}^{(3)}_{\text{inst}}\right] \\ = \exp\left[\partial_a\mathcal{F}^{(3)}(\Lambda, a, \mathbf{m}, \hbar=1)\right].\end{aligned} \tag{B.8}$$

Therefore, we obtain the quantization condition for the QNM:

$$\partial_a\mathcal{F}^{(3)}(\Lambda, a, \mathbf{m}, 1) = i(2n+1)\pi, \tag{B.9}$$

where n is an integer.

超辐射

Table 1. The complex frequencies $2\omega_n$ of the QNM in the Schwarzschild geometry.

	Numerical	SW-QNM
$n = 0,\ s = l = 0$	$0.22091\ -0.209791i$	$0.235216\ -0.205777i$
$n = 0,\ s = l = 1$	$0.496527\ -0.184975i$	$0.495127\ -0.18661i$
$n = 1,\ s = l = 1$	$0.429031\ -0.587335i$	$0.428845\ -0.588262i$
$n = 0,\ s = l = 2$	$0.747343\ -0.177925i$	$0.743992\ -0.0175352i$
$n = 1,\ s = l = 2$	$0.693422\ -0.54783i$	$0.690244\ -0.542829i$
$n = 2,\ s = l = 2$	$0.602107\ -0.956554i$	$0.602514\ -0.959309i$

Table 2. The complex frequencies ω_n of the QNM in the Kerr geometry.

	Numerical	SW-QNM
$n = 0,\ s = l = m = 0,\ \alpha/M = 0.1$	$0.110533\ -0.104802i$	$0.117687\ -0.102787i$
$n = 0,\ s = l = m = 0,\ \alpha/M \approx 1$	$0.110245\ -0.089433i$	$0.117755\ -0.0883568i$

超辐射

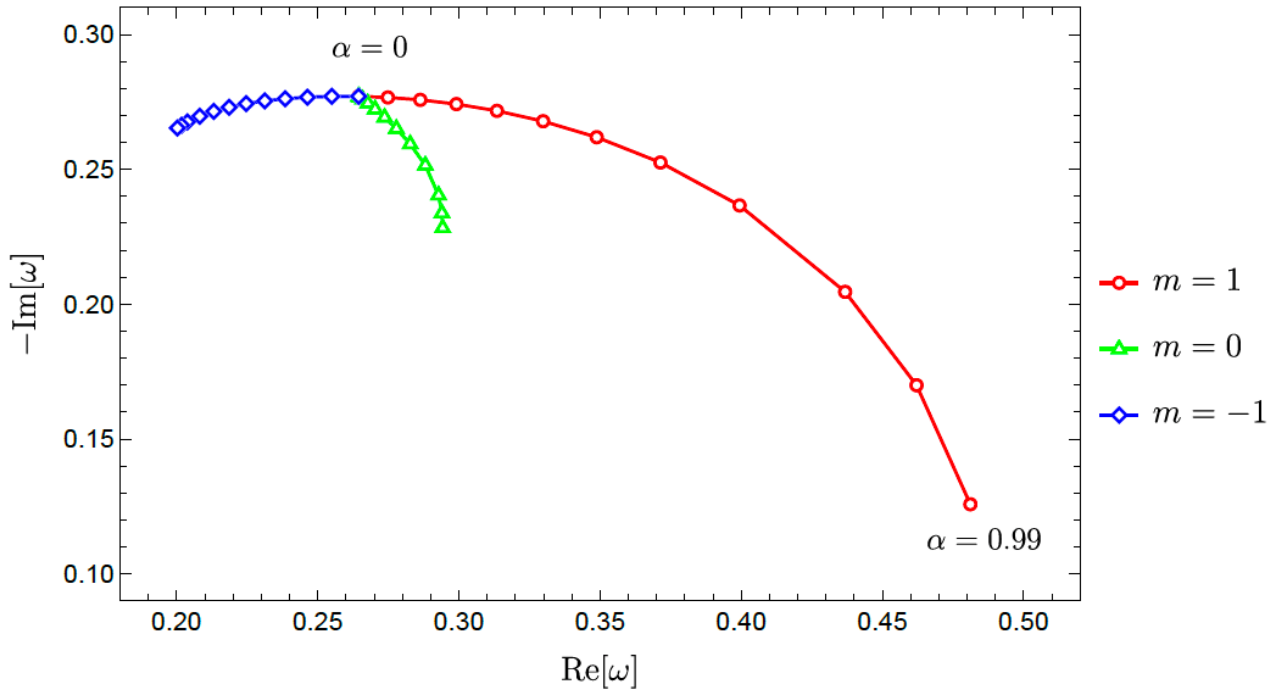

Figure 1. The QNM with $l = 1$, $m = 0, \pm 1$, and $\mu = 0.3$ as a function of the rotating parameter α in the complex frequency plane. The points denote each plot for from $\alpha = 0$ to $\alpha = 0.99$.

超辐射

Table 3. The complex frequencies ω/μ of the quasi-bound state for $\alpha = 0.99$ and several values of $M\mu$ near the superradiant regime. The values of Continued fraction method are obtained following [37].

$M\mu$	Continued fraction method	SW-QNM
0.400	$0.976311 + 3.31172 \times 10^{-7}i$	$1.15754 + 2.12772 \times 10^{-5}i$
0.421	$0.973191 + 3.57332 \times 10^{-7}i$	$1.10408 + 2.01818 \times 10^{-5}i$
0.450	$0.968326 - 9.69046 \times 10^{-8}i$	$1.03881 + 1.83035 \times 10^{-5}i$
0.500	$0.957896 - 3.93289 \times 10^{-5}i$	$0.942834 - 8.93944 \times 10^{-4}i$
0.520	$0.952658 - 1.73567 \times 10^{-4}i$	$0.910458 - 6.81511 \times 10^{-4}i$

2 Proca fields in Schwarzschild geometry

Following the description in [24], we consider the Schwarzschild BH geometry

$$\mathrm{d}s^2 = -f(r)\mathrm{d}t^2 + f^{-1}(r)\mathrm{d}r^2 + r^2\left(\mathrm{d}\theta^2 + \sin^2\theta\mathrm{d}\varphi^2\right), \tag{2.1}$$

with

$$f(r) = 1 - \frac{2M}{r}. \tag{2.2}$$

Considering the vector fields coupled to the gravitational fields, the Proca equation is given as

$$\nabla_\nu F^{\mu\nu} - \mu^2 A^\mu = 0, \tag{2.3}$$

where $F^{\mu\nu} = \partial_\mu A_\nu - \partial_\nu A_\mu$ is the field strength and μ is the mass of the vector field. Since $\nabla_\mu\nabla_\nu F^{\mu\nu} = 0$, the Lorentz condition $\nabla_\mu A^\mu = 0$ is derived from the field equations. This

Proca fields in Schwarzschild geometry

Table 1. The lower frequencies of the QNM in the numerical calculations and SW curve method. We choose $M\mu = 0.01$, $M\mu = 0.10$, and $M\mu = 0.25$ as the vector field mass.

n	$M\mu$	Numerical results	SW curve
0	0.01	$0.110523 - 0.104649i$	$0.113683 - 0.097919i$
	0.10	$0.121577 - 0.079112i$	$0.128517 - 0.072731i$
	0.25	$0.222081 - 0.012994i$	$0.225000 - 0.014527i$
1	0.01	$0.086079 - 0.348013i$	$0.086755 - 0.350993i$
	0.10	$0.082277 - 0.344140i$	$0.082957 - 0.347425i$
	0.25	$0.062605 - 0.325191i$	$0.061854 - 0.316085i$

Proca fields in Schwarzschild geometry

Table 2. The lowest frequencies of the QNM in the numerical calculations and SW curve method with $n = 0$. We choose $M\mu = 0.01$, $M\mu = 0.10$, and $M\mu = 0.25$ as the vector field mass.

l	$M\mu$	Numerical results	SW curve
1	0.01	$0.221028 - 0.098658i$	$0.247620 - 0.093267i$
	0.10	$0.225895 - 0.094428i$	$0.253229 - 0.089493i$
	0.25	$0.251250 - 0.070101i$	$0.283507 - 0.068436i$
2	0.01	$0.443745 - 0.096846i$	$0.436065 - 0.085560i$
	0.10	$0.447099 - 0.095583i$	$0.439503 - 0.084390i$
	0.25	$0.465036 - 0.088755i$	$0.457766 - 0.077829i$

Table 3. The lowest frequencies of the quasi-bound state for the monopole mode and odd sector mode in the numerical calculations and SW curve method with $n = 0$. We choose $M\mu = 0.40$, $M\mu = 0.50$, and $M\mu = 0.60$ as the vector field mass.

mode	$M\mu$	Numerical results	SW curve
Monopole	0.40	$0.389603 - 0.004629i$	$0.369759 - 0.003110i$
$(n = 0)$	0.50	$0.483253 - 0.012616i$	$0.418001 - 0.012913i$
	0.60	$0.577496 - 0.024107i$	$0.553471 - 0.025139i$
Odd	0.40	$0.395322 - 0.000561i$	$0.389260 - 0.000781i$
$(n = 0, l = 1)$	0.50	$0.478042 - 0.009056i$	$0.429927 - 0.007097i$
	0.60	$0.567624 - 0.022672i$	$0.553683 - 0.024132i$

Proca fields in Schwarzschild geometry

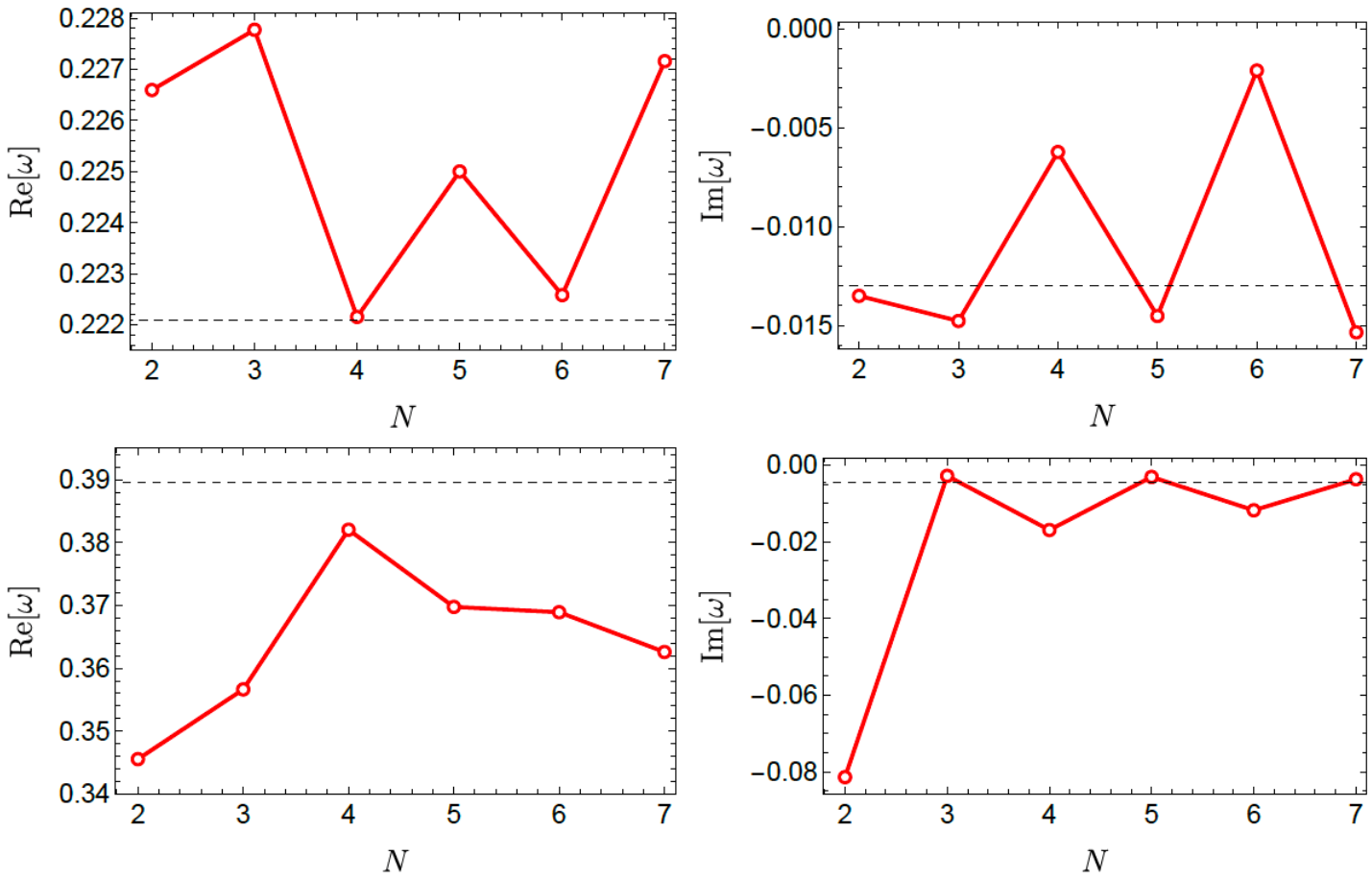

Figure 2. The real (left) and imaginary (right) parts of the lowest-frequency ($n = 0$) of the QNMs (upper) and quasi-bound states (lower) for the monopole mode, plotted as functions of the Nth order in the instanton series expansion. We choose $M\mu = 0.25$ for the QNMs and $M\mu = 0.40$ for the quasi-bound states. The black dashed lines denote the numerical results with the continued fraction method.

演示页

Strings, Gravity, and Gravitational Waves

15th - 18th August 2025@Rizhao City

Rizhao（日照）
means Sunshine

Blue Sky,
Green Sea,
and Golden Beach

演示页

Introduction

In 2002, Nekrsov performed a technique called Ω deformation in the reduction from 6D $\mathcal{N}=1$ gauge theory to 4D $\mathcal{N}=2$ gauge theory, and implied its connection with 2D conformal theory.

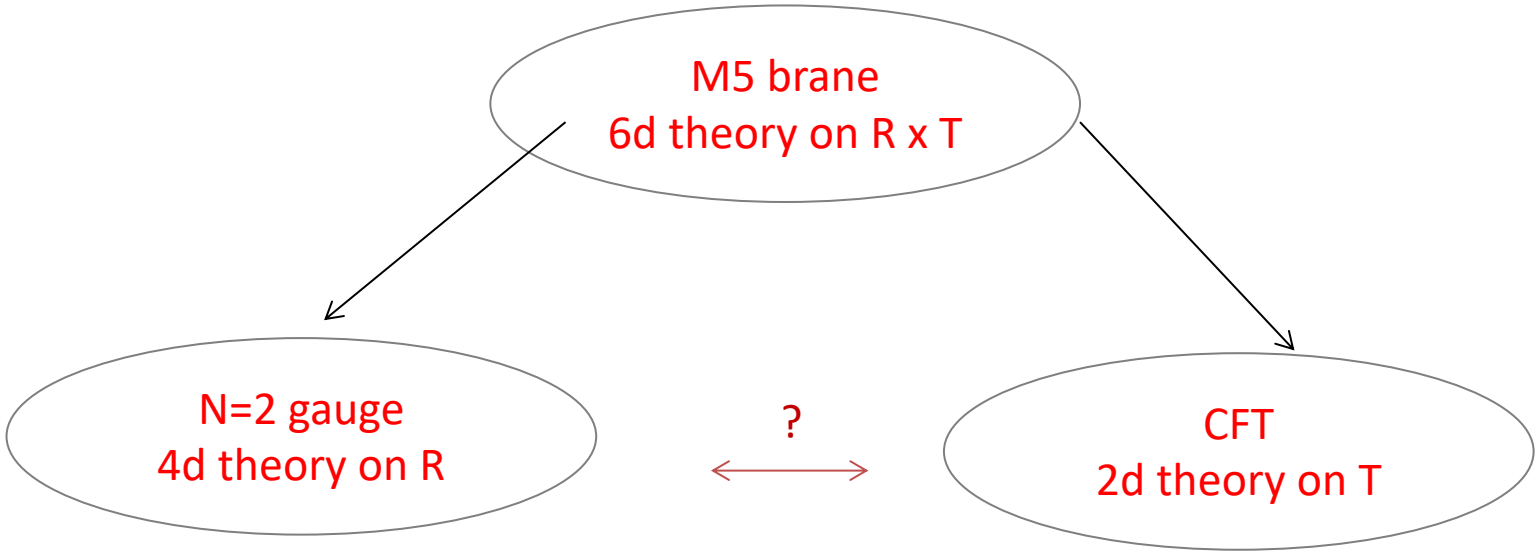

He found exact formulae of the partition function (Nekrasov partition function) of the $\mathcal{N}=2$ gauge theory, and showed that it reproduces the prepotential as determined by the Seiberg–Witten curve.

Introduction

AGT conjecture

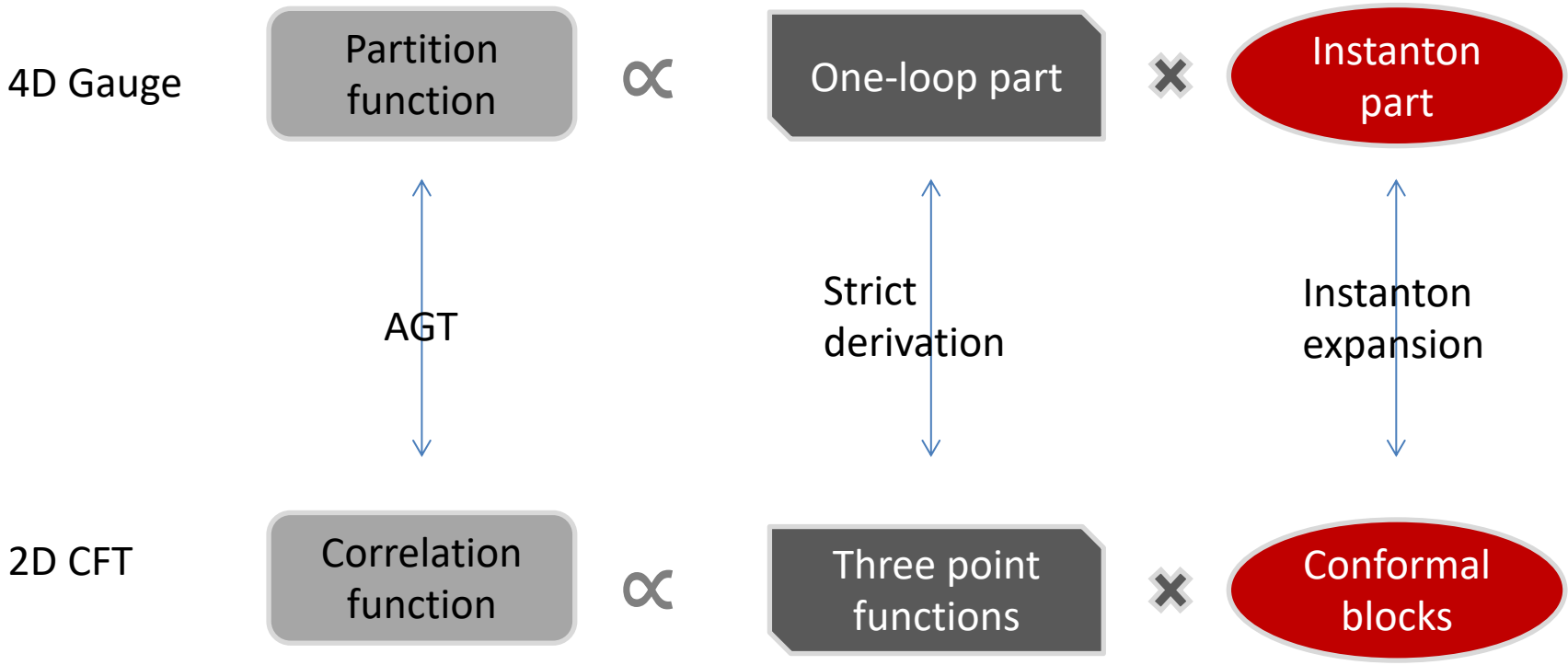

SU(2) [Alday-Gaiotto-Tachikawa '09]

SU(N) [Wyllard '09]

Introduction

We have been working on the proof of AGT conjecture through two different ways.

Direct approach

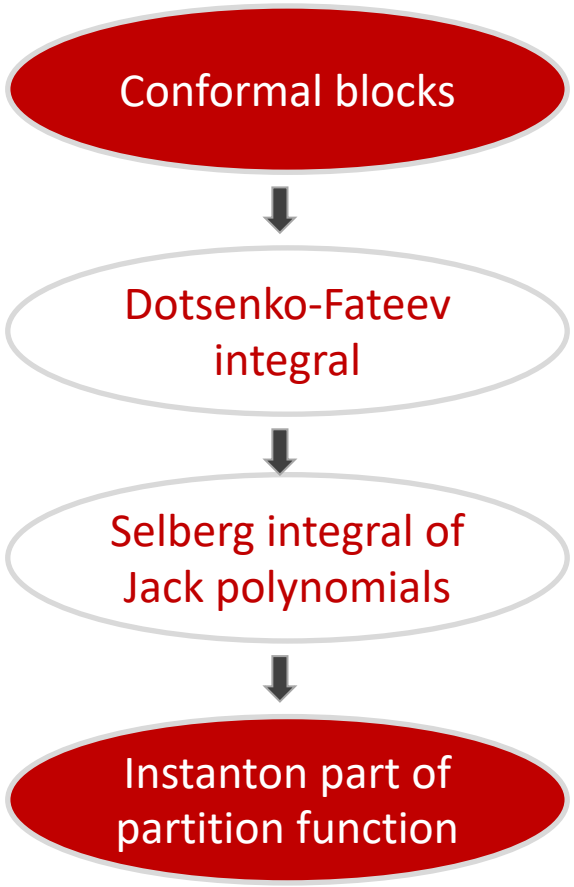

We calculated the conformal block in the form of Dotsenko–Fateev integral and reduce it in the form of Selberg integral of N Jack polynomials.

We found a formula for such Selberg average which satisfies some nontrivial consistency conditions and showed that it reproduces the SU(N) version of AGT conjecture.

$\beta = 1$ SU(2) [A. Mironov et. al. '10]

$\beta = 1$ SU(N) [Zhang Matsuo '11]

Introduction

Recursive approach

2D CFT

4D Gauge

Conformal blocks

AGT conjecture

$$\langle\langle \vec{Y}|V|\vec{W}\rangle\rangle = Z$$

Partition function

Satisfy Ward identity

trivial

nontrivial

Constrained by a recursion Relation

$$\sum \hat{\mathcal{O}} \langle\langle \vec{Y}|V|\vec{W}\rangle\rangle = 0$$

$$\sum \hat{\mathcal{O}} Z = 0$$

$\beta = 1$ SU(N) [Kanno-Matsuo-Zhang '12]

arbitrary β SU(N) [Kanno-Matsuo-Zhang '13]

A brief review of AGT conjecture and Nekrasov formula

Nekrasov partition function

Consider lifting the $\mathcal{N}=2$ four dimensional theory to $\mathcal{N}=(1,0)$ six dimensional theory, and then compactify the six dimensional $\mathcal{N}=1$ SUSY gauge theory on the manifold with the topology **T2** $\times$ ***R4*** with the metric :

$$ds^2 = r^2 dz d\bar{z} + g_{\mu\nu}\left(dx^\mu + V^\mu dz + \bar{V}^\mu d\bar{z}\right)\left(dx^\nu + V^\nu dz + \bar{V}^\nu d\bar{z}\right)$$

where $V^\mu = \Omega^\mu_\nu x^\nu,\ \bar{V}^\mu = \bar{\Omega}^\mu_\nu x^\nu,$ and

$$\Omega^{\mu\nu} = \begin{pmatrix} 0 & \epsilon_1 & 0 & 0 \\ -\epsilon_1 & 0 & 0 & 0 \\ 0 & 0 & 0 & \epsilon_2 \\ 0 & 0 & -\epsilon_2 & 0 \end{pmatrix}, \quad \bar{\Omega}^{\mu\nu} = \begin{pmatrix} 0 & \bar{\epsilon}_1 & 0 & 0 \\ -\bar{\epsilon}_1 & 0 & 0 & 0 \\ 0 & 0 & 0 & \bar{\epsilon}_2 \\ 0 & 0 & -\bar{\epsilon}_2 & 0 \end{pmatrix}$$

The action of the four dimensional theory in the limit *$r \to 0$ is not that of the pure supersymmetric Yang–Mills* theory on *R4*. Rather, it is a deformation of the latter by the Ω–dependent terms. It is called an $\mathcal{N}=2$ *theory in the Ω-background*.

$$\beta = -\epsilon_1/\epsilon_2$$

Nekrasov partition function

With his idea of the Ω-background, Nekrasov calculated the following partition function

$$Z(\tau, a, m, \epsilon) = \int_{\phi(\infty)=a} D\Phi DAD\lambda \ldots e^{-S(\Omega)}$$

Y

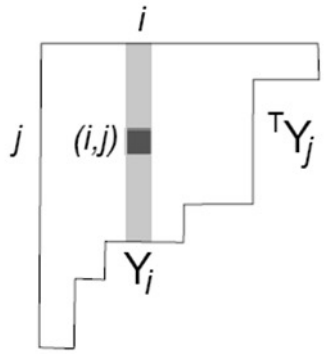

It has the important property that it gives the prepotential of the Seiberg-Witten theory in the limit $\epsilon_1 = -\epsilon_2 = \hbar \to 0$

$$F(\tau, a, m) = \lim_{\hbar \to 0} \hbar^2 \log Z_{\text{full}}(\tau, a, m; \hbar, -\hbar)$$

$$Z_{\text{full}}(q; a, m; \epsilon) = Z_{\text{tree}} Z_{\text{1loop}} Z_{\text{inst}}, \quad Z_{\text{inst}}(q; a, m; \epsilon) = \sum_{\mathbf{Y}} \mathbf{q}^{\mathbf{Y}} z(\mathbf{Y}, a, m)$$

where the instanton is labeled by a N-tuple of Young diagrams: $\mathbf{Y} := (\vec{Y}^{(1)}, \cdots, \vec{Y}^{(n)})$, (Fig. 1). The parameter a (resp. m) represents the diagonalized VEV of vector multiplets (resp. mass of hypermultiplets) whereas $q_i = e^{\pi i \tau_i}$ is the instanton expansion parameter for ith gauge group $SU(N_i)$, $\mathbf{q}^{\mathbf{Y}} := \prod_{i=1}^{n} q_i^{|\vec{Y}^{(i)}|}$. The total partition function is decomposed into a product of the contributions of the perturbative parts Z_{tree}, $Z_{1-\text{loop}}$ and non-perturbative instanton correction Z_{inst}. The latter is further decomposed into a sum of sets of Young diagrams. $\vec{Y}^{(i)} = (Y_1^{(i)}, \cdots, Y_{N_i}^{(i)})$ is a collection of N_i Young diagram which parameterizes the fixed points of instanton moduli space for i th gauge group $U(N_i)$.

Nekrasov partition function

Single gauge group case

$$Z_{\rm full}(q;a,\mu;\epsilon) = Z_{\rm tree} Z_{\rm 1loop} Z_{\rm inst}, \quad Z_{\rm inst}(q;a,m;\epsilon) = \sum_{\vec{Y}} q^{|\vec{Y}|} N^{\rm inst}_{\vec{Y}}(a,\mu),$$

$$N^{\rm inst}_{\vec{Y}}(a,\mu) = z_{\rm vect}(\vec{Y},a) \prod_{i=1}^{2N} z_{\rm fund}(\vec{Y},\mu_i) = \frac{\prod_{s=1}^{N}\prod_{k=1}^{2N} f_{Y_s}(\mu_k + a_s)}{\prod_{t,s=1}^{N} g_{Y_t,Y_s}(a_t - a_s)},$$

linear quiver gauge case

with gauge group $SU(N_1)\times\cdots\times SU(N_n)$.

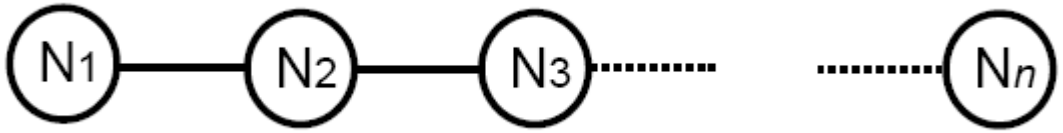

$$Z^{\rm Nek} = \sum_{\vec{Y}(1),\cdots,\vec{Y}(n)} q_i^{|\vec{Y}(i)|} \bar{V}_{\vec{Y}(1)} \cdot Z_{\vec{Y}(1)\vec{Y}(2)} \cdots Z_{\vec{Y}(n-1)\vec{Y}(n)} \cdot V_{\vec{Y}(n)}$$

$$\begin{aligned} Z_{\vec{Y}(i)\vec{Y}(i+1)} &= Z(\vec{a}^{(i)},\vec{Y}^{(i)};\vec{a}^{(i+1)},\vec{Y}^{(i+1)};\mu^{(i)}), \\ \bar{V}_{\vec{Y}(1)} &= Z(\vec{\lambda},\vec{\emptyset};\vec{a}^{(1)},\vec{Y}^{(1)};\mu^{(0)}), \\ V_{\vec{Y}(n)} &= Z(\vec{a}^{(n)},\vec{Y}^{(n)};\vec{\lambda}',\vec{\emptyset};\mu^{(n)}), \end{aligned}$$

AGT conjecture

For a Liouville theory on a sphere, the four-point correlation function of *V at* positions *∞, 1, q, 0 is*

$$\langle V_{\beta_0}(\infty)V_{m_0}(1)V_{m_1}(q)V_{\beta_1}(0)\rangle = \int \frac{d\beta}{2\pi} C(\beta_0^*, m_0, \beta)C(\beta^*, m_1, \beta_1)\left|q^{\Delta_\beta-\Delta_{m_1}-\Delta_{\beta_1}}\mathcal{F}_{\beta_0}{}^{m_0}{}_{\beta}{}^{m_1}{}_{\beta_1}(q)\right|^2$$

$$\propto \int a^2 da \left|Z_{\beta_0}{}^{m_0}{}_{\beta}{}^{m_1}{}_{\beta_1}(q)\right|^2$$

Where C(β 1, β 2, β 3) is the three point function given by the DOZZ formula.

The function *F* carries the coordinate (*q*) dependence and reflects the contributions of the conformal descendants. It is called conformal block.

$$Z_{\text{inst}}^{U(2),N_f=4}(a, m_0, \tilde{m}_0, m_1, \tilde{m}_1) = (1-q)^{2m_0(Q-m_1)}\mathcal{F}_{\beta_0}{}^{m_0}{}_{\beta}{}^{m_1}{}_{\beta_1}(q)$$

it is Checked $\mathcal{F}_{\beta_0}{}^{m_0}{}_{\beta}{}^{m_1}{}_{\beta_1}(q)$ is the conformal block of a virasoro algebra with central charge c = 1 + 6Q2 at position ∞, 1, q, 0,

Up to order q11

AGT conjecture

SU(N) generalization

$$\langle V_{\alpha_4}(\infty) V_{\alpha_3}(1) V_{\alpha_2}(q) V_{\alpha_1}(0) \rangle$$

The conformal block of this
correlation function is written in the form,

$$\mathcal{F}_{\alpha_4,\alpha_3,\alpha_2,\alpha_1}(q) = \sum_{\vec{Y}} q^{|\vec{Y}|} N^{\mathrm{Toda}}_{\vec{Y}}(\alpha_1, \alpha_2, \alpha_3, \alpha_4)$$

Correlation functions of Toda theory and Selberg Formula

SU(N) Toda

Bosons $\phi(z) = (\phi_1(z), \cdots, \phi_N(z))$

$$\phi_i(z)\phi_j(0) \sim \delta_{ij} \ln(z)$$

Symmetry: W_N algebra

$$R_N =: \prod_{m=1}^{N} \left(Q\frac{d}{dz} - i(h_m, \partial_z \varphi) \right) : = \sum_k W^{(k)}(z) \left(Q\frac{d}{dz} \right)^{N-k}$$

$$c = (N-1)(1 + N(N+1)Q^2)$$

$W^{(k)}$ satisfies W_N algebra (a nonlinear algebra) with central charge

$$V_{\vec{\alpha}}(z) =: e^{(\alpha, \phi(z))} :$$

$$Q_j^{(\pm)} = \int \frac{dz}{2\pi i} V_j^{(\pm)}(z) = \int \frac{dz}{2\pi i} : e^{\alpha_\pm (e_j, \phi(z))} :$$

Dotsenko-Fateev integral

$$Z_{\rm DF}(q) = \left\langle\!\!\left\langle : e^{(\tilde{\alpha_1},\phi(0))} :: e^{(\tilde{\alpha_2},\phi(q))} :: e^{(\tilde{\alpha_3},\phi(1))} :: e^{(\tilde{\alpha_4},\phi(\infty))} : \prod_{a=1}^{N-1} \left(\int_0^q : e^{b(e_a,\phi(z))} : dz \right)^{N_a} \left(\int_1^\infty : e^{b(e_a,\phi(z))} : dz \right)^{\tilde{N}_a} \right\rangle\!\!\right\rangle$$

We apply *Wick's theorem* to evaluate the correlator

$$\left\langle\!\!\left\langle : e^{(\tilde{\alpha}_1,\phi(z_1))} : \ \ldots \ : e^{(\tilde{\alpha}_n,\phi(z_n))} : \right\rangle\!\!\right\rangle = \prod_{1\le i<j\le n} (z_j - z_i)^{(\tilde{\alpha}_i,\tilde{\alpha}_j)}$$

$$Z_{\rm DF}(q) = q^{(\alpha_1,\alpha_2)/\beta}(1-q)^{(\alpha_2,\alpha_3)/\beta} \prod_{a=1}^{N-1} \prod_{I=1}^{N_a} \int_0^q dz_I^{(a)} \prod_{J=N_a+1}^{N_a+\tilde{N}_a} \int_1^\infty dz_J^{(a)} \prod_{i<j}^{N_a+\tilde{N}_a} (z_j^{(a)} - z_i^{(a)})^{2\beta} \ \times$$

$$\times \prod_{i}^{N_a+\tilde{N}_a} (z_i^{(a)})^{(\alpha_1,e_a)} (z_i^{(a)} - q)^{(\alpha_2,e_a)} (z_i^{(a)} - 1)^{(\alpha_3,e_a)} \prod_{a=1}^{N-2} \prod_{i}^{N_a+\tilde{N}_a} \prod_{j}^{N_{a+1}+\tilde{N}_{a+1}} (z_j^{(a+1)} - z_i^{(a)})^{-\beta} \ .$$

Selberg integral

$$\int_{[0,1]^k} |\Delta(x)|^{2\gamma} \prod_{i=1}^{k} x_i^{\alpha-1}(1-x_i)^{\beta-1}\,\mathrm{d}x = \prod_{i=1}^{k} \frac{\Gamma(\alpha+(i-1)\gamma)\Gamma(\beta+(i-1)\gamma)\Gamma(i\gamma+1)}{\Gamma(\alpha+\beta+(i+k-2)\gamma)\Gamma(\gamma+1)}$$

When $k = 1$ the Selberg integral simplifies to the Euler beta integral

$$\int_0^1 x^{\alpha-1}(1-x)^{\beta-1}\,\mathrm{d}x = \frac{\Gamma(\alpha)\Gamma(\beta)}{\Gamma(\alpha+\beta)}, \qquad \Re(\alpha) > 0,\ \Re(\beta) > 0,$$

Here we consider its *AN*−1 extension (*AN*−1 Selberg integral):

$$S_{\vec{u},\vec{v},\beta} = \int dx \prod_{a=1}^{N-1} \left[\left|\Delta\left(x^{(a)}\right)\right|^{2\beta} \prod_{i=1}^{N_a} \left(x_i^{(a)}\right)^{u_a} \left(1-x_i^{(a)}\right)^{v_a} \right] \prod_{a=1}^{N-2} \left|\Delta\left(x^{(a)}, x^{(a+1)}\right)\right|^{-\beta}$$

Selberg integral

$$I^{A_n}_{N_1,\dots,N_n}(\mathcal{O};u_1,\dots,u_n,v;\beta)$$
$$\equiv \int_{C_\beta^{N_1,\dots,N_n}[0,1]} \mathcal{O}(x^{(1)},\dots,x^{(n)}) \prod_{r=1}^{n}\prod_{i=1}^{N_r} (x_i^{(r)})^{u_r}(1-x_i^{(r)})^{v_r}$$
$$\times \prod_{r=1}^{n} |\Delta(x^{(r)})|^{2\beta} \prod_{r=1}^{n-1} |\Delta(x^{(r)},x^{(r+1)})|^{-\beta}\,\mathrm{d}x^{(1)}\cdots\mathrm{d}x^{(n)}$$

Seamus P. Albion, Eric M. Rains, and S. Ole Warnaar, 2021

For β = 1

$$C^{N_1,\dots,N_n} = C_1^{N_1}\times\cdots\times C_n^{N_n}, \quad \text{where} \quad C_r^{N_r} = \underbrace{C_r\times\cdots\times C_r}_{N_r \text{ times}}.$$

$$I^{A_n}_{N_1,\dots,N_n}(\mathscr{O};u_1,\dots,u_n,v)$$
$$\equiv \frac{1}{(2\pi\mathrm{i})^{N_1+\cdots+N_n}} \int_{C^{N_1,\dots,N_n}} \mathscr{O}(x^{(1)},\dots,x^{(n)}) \prod_{r=1}^{n}\prod_{i=1}^{N_r} (x_i^{(r)})^{u_r}(x_i^{(r)}-1)^{v_r}$$
$$\times \prod_{r=1}^{n} \Delta^2(x^{(r)}) \prod_{r=1}^{n-1} \Delta^{-1}(x^{(r)},x^{(r+1)})\,\mathrm{d}x^{(1)}\cdots\mathrm{d}x^{(n)}$$

Reduction to Selberg integral

$$Z_{DF}(q) = \sum_{\vec{Y}} q^{|\vec{Y}|} \left\langle \prod_{a=1}^{N} j_{Y_a}^{(\beta)}(-r_k^{(a)} - \frac{v'_{a+}}{\beta}) \right\rangle_+ \left\langle \prod_{a=1}^{N} j_{Y_a}^{(\beta)}(\tilde{r}_k^{(a)} + \frac{v'_{a-}}{\beta}) \right\rangle_-$$

$j_{Y_a}^{(\beta)}$: Jack polynomials

$\langle \cdots \rangle_\pm$: Selberg average

$$p_k^{(a)} := \sum_i (x_i^{(a)})^k$$

Cauchy–Stanley identity

$$\exp(\beta \sum_{k=1}^{\infty} \frac{1}{k} p_k p'_k) = \sum_R j_R^{(\beta)}(p) j_R^{(\beta)}(p')$$

Jack polynomials

Jack polynomials are characterized by the fact that they are the eigenfunctions of Calogero-Sutherland Hamiltonian written in the form,

$$\mathcal{H} = \sum_{i=1}^{M} D_i^2 + \beta \sum_{i<h} \frac{z_i + z_j}{z_i - z_j}(D_i - D_j), \quad D_i := z_i \frac{\partial}{\partial z_i} .$$

The explicit form of low level ones are listed below;

$$J^{(\beta)}_{[1]}(p_k) = p_1 \ ,$$

$$J^{(\beta)}_{[2]}(p_k) = \frac{p_2 + \beta p_1^2}{\beta + 1}, \quad J^{(\beta)}_{[11]}(p_k) = \frac{1}{2}(p_1^2 - p_2) \ ,$$

$$J^{(\beta)}_{[3]}(p_k) = \frac{2p_3 + 3\beta p_1 p_2 + \beta^2 p_1^3}{(\beta+1)(\beta+2)}, \ J^{(\beta)}_{[21]}(p_k) = \frac{(1-\beta)p_1 p_2 - p_3 + \beta p_1^3}{(\beta+1)(\beta+2)}, \ J^{(\beta)}_{[111]}(p_k) = \frac{1}{6}p_1^3 - \frac{1}{2}p_1 p_2 + \frac{1}{3}p_3 \ .$$

Selberg integral

Schur functions,

$$\chi_\lambda(x) = \frac{\det_{1\leqslant i,j\leqslant n}\left(x_i^{\lambda_j+n-j}\right)}{\Delta(x)}$$

Seamus P. Albion, Eric M. Rains, and S. Ole Warnaar, 2021

$$\left\langle \prod_{r=1}^{n+1} \chi_{Y^{(r)}}\left[x^{(r)}-x^{(r-1)}\right] \right\rangle_{u_1,\ldots,u_n,v}^{N_1,\ldots,N_n}$$
$$= \prod_{r=1}^{n+1} \prod_{1\leqslant i<j\leqslant \ell_r} \frac{Y_i^{(r)} - Y_j^{(r)} + j - i}{j-i} \prod_{r,s=1}^{n+1} \prod_{i=1}^{\ell_r} \frac{(A_{r,s} - N_{s-1} + N_s - i + 1)_{Y_i^{(r)}}}{(A_{r,s} + \ell_s - i + 1)_{Y_i^{(r)}}}$$
$$\times \prod_{1\leqslant r<s\leqslant n+1} \prod_{i=1}^{\ell_r} \prod_{j=1}^{\ell_s} \frac{Y_i^{(r)} - Y_j^{(s)} + A_{r,s} + j - i}{A_{r,s} + j - i},$$

AGT conjecture from Selberg integral

Reduction to Selberg integral

Before we go to the details conclusion first

$$Z_{\rm inst}(q) = Z_{\rm DF}(q)$$

$$N_{\vec{Y}}^{\rm inst} = N_{\vec{Y}}^{\rm Toda}$$

$$N_{\vec{Y}}^{\rm inst} \equiv N_{\vec{Y}+}^{\rm inst} N_{\vec{Y}-}^{\rm inst}, \quad N_{\vec{Y}}^{\rm Toda} \equiv N_{\vec{Y}+}^{\rm Toda} N_{\vec{Y}-}^{\rm Toda},$$

$$N_{\vec{Y}+}^{\rm inst} \equiv \frac{\prod_{s=1}^{n+1}\prod_{k=1}^{n+1} f_{Y_s}(\mu_k + a_s)}{\prod_{t,s=1}^{n+1} G_{Y_t,Y_s}(a_t - a_s)} \prod_{s=1}^{n+1} \left\{ (-1)^{|Y_s|} \sqrt{\frac{G_{Y_s,Y_s}(0)}{G_{Y_s,Y_s}(1-\beta)}} \right\},$$

$$N_{\vec{Y}\pm}^{\rm Toda} \equiv \left\langle \prod_{a=1}^{n+1} j_{Y_a}^{(\beta)}(-r_k^{(a)} - \frac{v'_{a\pm}}{\beta}) \right\rangle_{\pm} = \prod_{a=1}^{n+1} \sqrt{\frac{G_{Y_a,Y_a}(0)}{G_{Y_a,Y_a}(1-\beta)}} \left\langle \prod_{a=1}^{n+1} J_{Y_a}^{(\beta)}(-r_k^{(a)} - \frac{v'_{a\pm}}{\beta}) \right\rangle_{\pm}$$

Known results on Selberg average

SU(2) **case:** The relevant Selberg averages for one and two Jack polynomials were obtained by Kadell.

$$\left\langle J_Y^{(\beta)}(p)\right\rangle_{u,v,\beta}^{SU(2)} \qquad \left\langle J_A^{(\beta)}(p+w)J_B^{(\beta)}(p)\right\rangle^{SU(2)}$$

SU(*n*+1) **case:**

The one-Jack Selberg integral for *SU*(*n*+1) could be calculated by the formula offered by Warnaar.

$$\left\langle J_B^{(\beta)}(p_k^{(n)})\right\rangle_{\vec{u},\vec{v},\beta}^{SU(n+1)}$$

He also gives A_2 two Jack integral $\left\langle J_R^{(\beta)}(p_k^{(1)})J_B^{(\beta)}(p_k^{(2)})\right\rangle_{u,v,\beta}^{SU(3)}$

A conjecture on Selberg average

To evaluate we need Selberg average of (n + 1) Jack polynomials. While we do not perform the integration so far, we find a formula for β = 1 which reproduces known results and satisfies consistency conditions.

The Jack polynomial for β = 1 is called Schur polynomial. $J_Y^{(\beta)}|_{\beta=1} = \chi_Y$.

Conjecture : *We propose the following formula of Selberg average for n + 1 Schur polynomials,*

$$\left\langle \chi_{Y_1}(-p_k^{(1)} - v_1') \cdots \chi_{Y_r}(p_k^{(r-1)} - p_k^{(r)} - v_r') \cdots \chi_{Y_{n+1}}(p_k^{(n)}) \right\rangle_{\vec{u},\vec{v},\beta=1}^{SU(n+1)}$$

$$= \prod_{s=1}^{n} \left\{ (-1)^{|Y_s|} \times \frac{[v_s + N_s - N_{s-1}]_{Y_s'}}{[N_s + N_{s-1}]_{Y_s'}} \times \prod_{1 \le i < j \le N_{s-1}+N_s} \frac{(j-i+1)_{Y_{si}'-Y_{sj}'}}{(j-i)_{Y_{si}'-Y_{sj}'}} \right\} \times \prod_{1 \le i < j \le N_n} \frac{(j-i+1)_{Y_{(n+1)i}-Y_{(n+1)j}}}{(j-i)_{Y_{(n+1)i}-Y_{(n+1)j}}}$$

$$\times \prod_{1 \le t < s \le n+1} \left\{ \frac{[v_t + u_t + \cdots + u_{s-1} + N_t - N_{t-1}]_{Y_t'}}{[v_t - v_s + u_t + \cdots + u_{s-1} + N_t - N_{t-1} - N_s]_{Y_t'}} \times \frac{[-v_s + u_t + \cdots + u_{s-1} - N_s + N_{s-1}]_{Y_s}}{[v_t - v_s + u_t + \cdots + u_{s-1} - N_{t-1} - N_s + N_{s-1}]_{Y_s}} \right.$$

$$\left. \times \prod_{i=1}^{N_t} \prod_{j=1}^{N_{s-1}} \frac{v_t - v_s + u_t + \cdots + u_{s-1} + N_t - N_{t-1} - N_s + N_{s-1} + 1 - (i+j)}{v_t - v_s + u_t + \cdots + u_{s-1} + N_t - N_{t-1} - N_s + N_{s-1} + 1 + Y_{ti}' + Y_{sj} - (i+j)} \right\},$$

Proof

$$\left\langle \prod_{r=1}^{n+1} \chi_{Y^{(r)}} \left[x^{(r-1)} - x^{(r)} \right] \right\rangle_{+} = \left. \frac{\prod_{s=1}^{n+1} (-1)^{|Y^{(s)}|} \prod_{r=1}^{n+1} \prod_{s=1}^{n+1} f_{Y^{(s)}}(\mu_r + a_s)}{\prod_{r,s=1}^{n+1} G_{Y^{(r)},Y^{(s)}}(a_r - a_s)} \right|_{\beta=1},$$

and the second part,

$$\left\langle \prod_{r=1}^{n+1} \chi_{Y^{(r)}} \left[y^{(r)} - y^{(r-1)} \right] \right\rangle_{-} = \left. \frac{\prod_{s=1}^{n+1} (-1)^{|Y^{(s)}|} \prod_{r=n+2}^{2n+2} \prod_{s=1}^{n+1} f_{Y^{(s)}}(\mu_r + a_s)}{\prod_{r,s=1}^{n+1} G_{Y^{(r)},Y^{(s)}}(a_r - a_s)} \right|_{\beta=1}.$$

Proof

Lemma 1

$$\prod_{1\leqslant i<j\leqslant l_Y} \frac{(Y_i - Y_j + \beta(j-i))_\beta}{(\beta(j-i))_\beta} \prod_{i=1}^{l_Y} \frac{1}{(\beta(l_Y - i + 1))_{Y_i}} = \frac{1}{G_{Y,Y}(0)}$$

Lemma 2

$$\prod_{i=1}^{l_Y} (-z - \beta i + \beta)_{Y_i} = (-1)^{|Y|} f_Y(z)$$

Lemma 3

$$\prod_{i=1}^{l_Y} \prod_{j=1}^{l_W} \frac{Y_i - W_j - x + j - i}{-x + j - i} \prod_{i=1}^{l_Y} \frac{1}{(-x + l_W - i + 1)_{Y_i}} \prod_{i=1}^{l_W} \frac{1}{(x + l_Y - i + 1)_{W_i}}$$
$$= \frac{(-1)^{|Y|+|W|}}{G_{Y,W}(x) G_{W,Y}(-x)} \bigg|_{\beta=1}.$$

Proof

Lemma 1

$$\prod_{1\leqslant i<j\leqslant l_Y} \frac{(Y_i - Y_j + \beta(j-i))_\beta}{(\beta(j-i))_\beta} \prod_{i=1}^{l_Y} \frac{1}{(\beta(l_Y - i + 1))_{Y_i}} = \frac{1}{G_{Y,Y}(0)}$$

Lemma 2

$$\prod_{i=1}^{l_Y} (-z - \beta i + \beta)_{Y_i} = (-1)^{|Y|} f_Y(z)$$

Lemma 3

$$\prod_{i=1}^{l_Y} \prod_{j=1}^{l_W} \frac{Y_i - W_j - x + j - i}{-x + j - i} \prod_{i=1}^{l_Y} \frac{1}{(-x + l_W - i + 1)_{Y_i}} \prod_{i=1}^{l_W} \frac{1}{(x + l_Y - i + 1)_{W_i}}$$
$$= \frac{(-1)^{|Y|+|W|}}{G_{Y,W}(x) G_{W,Y}(-x)} \bigg|_{\beta=1}.$$

演示页

5D

$$Z_{\rm inst}(\mathfrak{q}) = \sum_{\vec{Y}} \mathfrak{q}^{|\vec{Y}|} N_{5d}^{\rm inst}(\vec{a},\mu),$$

$$N_{5d}^{\rm inst} = \prod_{r,s=1}^{n+1} \frac{\mathbb{F}_{Y^{(s)}}(\mu_r + a_s, q^{-1})\mathbb{F}_{Y^{(s)}}(\mu_{n+1+r} + a_s, q)}{\mathbb{G}_{Y^{(r)},Y^{(s)}}(a_r - a_s, q)\mathbb{G}_{Y^{(s)},Y^{(r)}}(a_s - a_r + 1 - \beta, q^{-1})},$$

$$\mathbb{F}_Y(z,q) = \prod_{(i,j)\in Y} (1 - q^{z+\beta(i-1)-(j-1)}),$$

$$\mathbb{G}_{Y,W}(x,q) = \prod_{(i,j)\in Y} (1 - q^{x+\beta(Y'_j-i)+(W_i-j)+\beta}).$$

5D

$$[n]_q \equiv \frac{1-q^n}{1-q}.$$

$$[n_1]_q[n_2]_q \neq [m_1]_q[m_2]_q$$

q-deformed Selberg integral

$$
\begin{aligned}
&I^{A_n}_{N_1,\dots,N_n}(\mathcal{O};u_1,\dots,u_n,v;\beta)\\
=&\frac{1}{N_1!\cdots N_n!(2\pi\mathrm{i})^{N_1+\cdots+N_n}}\int\limits_{\mathbb{T}^{N_1+\cdots+N_n}}\mathcal{O}\big(x^{(1)},\dots,x^{(n)}\big)\prod_{i=1}^{N_n}\frac{(q^{a_n}/x_i^{(n)},q^{1-a_n}x_i^{(n)};q)_\infty}{(q^{v+1}/x_i^{(n)},x_i^{(n)};q)_\infty}\prod_{r=1}^{n-1}\prod_{i=1}^{N_r}(x_i^{(r)})^{a_r}\\
\times&\prod_{r=1}^{n}\prod_{1\leqslant i<j\leqslant N_r}\frac{(x_i^{(r)}/x_j^{(r)},x_j^{(r)}/x_i^{(r)};q)_\infty}{(tx_i^{(r)}/x_j^{(r)},tx_j^{(r)}/x_i^{(r)};q)_\infty}\prod_{r=1}^{n-1}\prod_{i=1}^{N_r}\prod_{j=1}^{N_{r+1}}\frac{((qt)^{1/2}x_j^{(r+1)}/x_i^{(r)};q)_\infty}{((q/t)^{1/2}x_j^{(r+1)}/x_i^{(r)};q)_\infty}\frac{\mathrm{d}x^{(1)}}{x^{(1)}}\cdots\frac{\mathrm{d}x^{(n)}}{x^{(n)}},
\end{aligned}
$$

In [11] the Selberg integral formula for $n+1$ Schur polynomials is proposed. We now find a new q-deformed Selberg integral average formula, containing a product of $n+1$ Schur functions:

$$
\begin{aligned}
&\Big\langle\prod_{r=1}^{n+1}\chi_{Y^{(r)}}\big[x^{(r)}-x^{(r-1)}\big]\Big\rangle^{N_1,\dots,N_n}_{u_1,\dots,u_n,v}\\
=&\prod_{r=1}^{n+1}\prod_{(i,j)\in Y^{(r)}}\frac{1-q^{-N_r+N_{r-1}+i-j}}{1-q^{-Y_i^{(r)}-Y_j'^{(r)}+i+j-1}}\prod_{1\leq r<s\leq n+1}\prod_{i=1}^{L_{Y^{(r)}}}\prod_{j=1}^{L_{Y^{(s)}}}\frac{1-q^{-Y_i^{(r)}+Y_j^{(s)}-A_{r,s}-j+i}}{1-q^{-A_{r,s}-j+i}}\\
\times&\prod_{1\leq r<s\leq n+1}\prod_{(i,j)\in Y^{(r)}}\frac{1-q^{-A_{r,s}+N_{s-1}-N_s+i-j}}{1-q^{-A_{r,s}-L_{Y^{(s)}}+i-j}}\prod_{(i,j)\in Y^{(s)}}\frac{1-q^{-A_{r,s}+N_r-N_{r-1}-i+j}}{1-q^{-A_{r,s}+L_{Y^{(r)}}-i+j}}.
\end{aligned}
$$

q-deformed conformal blocks

$$\left\langle\!\!\left\langle \prod_{r=1}^{n} \left\{ \prod_{i=1}^{N_r} (\mathfrak{q} x_i^{(r)}; q)_{v_{r-}} \prod_{j=1}^{\tilde{N}_r} (\mathfrak{q} y_i^{(r)}; q)_{v_{r+}} \right\} \prod_{r,s=1}^{n} \prod_{i=1}^{N_r} \prod_{j=1}^{\tilde{N}_s} \left(\mathfrak{q} x_i^{(r)} y_j^{(s)}; q \right)_{\beta}^{C_{rs}} \right\rangle_{+} \right\rangle_{-}$$

$$\sum_{\vec{Y}} \mathfrak{q}^{|\vec{Y}|} \left\langle \prod_{r=1}^{n+1} \chi_{Y^{(r)}} \left[x^{(r-1)} - x^{(r)} \right] \right\rangle_{+} \left\langle \prod_{r=1}^{n+1} \chi_{Y^{(r)}} \left[y^{(r)} - y^{(r-1)} \right] \right\rangle_{-}$$

$$\left\langle \prod_{r=1}^{n+1} \chi_{Y^{(r)}} \left[x^{(r-1)} - x^{(r)} \right] \right\rangle_{+} \left\langle \prod_{r=1}^{n+1} \chi_{Y^{(r)}} \left[y^{(r)} - y^{(r-1)} \right] \right\rangle_{-}$$

$$= \prod_{r,s=1}^{n+1} \frac{\mathbb{F}_{Y^{(s)}}(\mu_r + a_s, q)\mathbb{F}_{Y^{(s)}}(\mu_{n+1+r} + a_s, q^{-1})}{\mathbb{G}_{Y^{(r)},Y^{(s)}}(a_r - a_s, q)\mathbb{G}_{Y^{(s)},Y^{(r)}}(a_s - a_r + 1 - \beta, q^{-1})}.$$

Lemma

$$\prod_{i=1}^{L_Y} \prod_{j=1}^{L_W} \frac{1 - q^{x+Y_i-W_j+j-i}}{1 - q^{x+j-i}} \prod_{(i,j)\in Y} \frac{1}{1 - q^{x+L_W-i+j}} \prod_{(i,j)\in W} \frac{1}{1 - q^{x-L_Y+i-j}}$$

$$= \frac{1}{\mathbb{G}_{Y,W}(-x, q^{-1})\mathbb{G}_{W,Y}(x, q)}\bigg|_{\beta=1}.$$

Conclusions

演示页